



HELSINKI UNIVERSITY OF TECHNOLOGY  
Institute of Digital Communications  
Radio Laboratory

Ville-Hermanni Kilpiä

## Experimental frequency converter for a DVB-T transmitter

Thesis submitted in partial fulfillment of the requirements for the  
degree of Master of Science in Engineering  
Espoo, September 4, 2003

Supervisor

Professor Pekka Eskelinen

Instructor

Markku Nieminen, M.Sc.(Tech.)

**Author:** Ville-Hermanni Kilpiä**Name of the thesis:** Experimental frequency converter for a DVB-T transmitter**Date:** September 4, 2003**Number of pages:** 114**Department:** Department of Electrical and Communications Engineering**Professorship:** Radio Engineering (S-26)**Supervisor:** Professor Pekka Eskelinen**Instructor:** Markku Nieminen, M.Sc.(Tech.)

In the recent years, motivation towards receiving a digital television broadcast with a mobile terminal has grown a lot. During the finalization of the European digital television broadcasting standard DVB-T, an ad-hoc group DVB-X was formed to specify a standard that would allow mobile reception. Nowadays, the growing trend towards wireless communication, especially in local area networks, has motivated regulatory authorities to allocate a number of frequency bands in the microwave frequencies for the recent high-performance wireless LAN standard HiperLAN/2. Since the DVB-T and the HiperLAN/2 standard use the same kind of transmission technique, the OFDM, these two different applications of radio communication can be utilized in a construction of a DVB-T frequency converter.

In this Master's Thesis, the background study of the DVB-T technology is presented to aid the design of an experimental frequency converter. Also, the critical parts of a DVB-T transmitter are pointed out and possible design solutions are discussed. For the converter an output power requirement of 10 W EIRP was determined after a link budget calculation, based on the reception area study and the review of recent published articles on microwave propagation and antenna technology. The required EIRP can be achieved with a 1 W power amplifier, since the transmit antenna will have high gain of 20 dB. Since the DVB-T broadcast requires a highly linear transmitter, and a substantially overrated power amplifier can be used in the design, the used amount of backoff is about 10 dB. A practical frequency converter design for the 5.8 GHz ISM band is presented and the block level components are evaluated from the commercially off-the-shelf available component listings.

Also, other methods to linearize a power amplifier are reviewed in order to assert the use of backoff. To aid in a decision concerning what kind of frequency converter should be constructed, various methods to verify the performance of a DVB-T transmitter are discussed, and the results of a small measurement campaign are also presented.

**Keywords:** DVB-T, OFDM, experimental, frequency converter, microwave, transmitter



## TEKNILLINEN KORKEAKOULU      Diplomityön tiivistelmä

**Tekijä:** Ville-Hermanni Kilpiä

**Työn nimi:** Kokeellinen taajuusmuunnin DVB-T -lähettimeen

**Päivämäärä:** 4.9.2002

**Sivumäärä:** 114

**Osasto:** Sähkö- ja tietoliikennetekniikan osasto

**Professuuri:** Radiotekniikka (S-26)

**Työn valvoja:** Professori Pekka Eskelinen

**Työn ohjaaja:** DI Markku Nieminen

Kiinnostus digitaalisen televisiolähetteen vastaanottamiseen matkaviestimillä on lisääntynyt viime vuosina. Euroopalaista DVB-T -digitaaliteleviostandardia viimeistellessä perustettiin ad-hoc ryhmä DVB-X tutkimaan, miten standardia voitaisiin muuttaa, jotta liikkuva vastaanotto olisi mahdollista. Samaan aikaan langattomien lähiverkkojen käyttö on lisääntynyt huomattavasti, joten viestintäviranomaiset ovat varanneet uusia taajuuskaistoja mikroaaltotaajuuksilta näiden käyttöön. Koska uuden sukupolven langattomien lähiverkkojen standardi HiperLAN/2 ja digitaaliteleviostandardi DVB-T käyttävät samankaltaista OFDM-lähetystekniikkaa, yhdistämällä lähiverkkojen kaupalliset RF osat ja DVB-T lähete on mahdollista toteuttaa mikroaaltotaajuuksilla toimiva digitaaliteleviolähetin.

Diplomityössä esitetään ratkaisu, jossa UHF-taajuuksinen digitaaliteleviolähetenostetaan taajuusmuuntimella 5,8 GHz ISM-kaistalle. Jotta muuntimen kriittisten osien sekä taajuusmuunnoksen ongelmat voitaisiin ratkoa, työssä esitetään lyhyt kertaus DVB-T -tekniikan tärkeimpiin alueisiin. Läpikäymällä viimeaikaisia radioaaltojen etenemismallien mittauskampanjoita alan kirjallisuudesta sekä vastaanottoalueen kartoistus, todetaan linkkibudjettilaskelmalla, että tarvittava lähetysteho on noin 10 W EIRP. Koska vastaanottoalue on kapea, lähetinantenni vahvistaa signaalia 20 dB. Tällöin DVB-T -lähettimen vaatimuksiin kuuluva lineaarinen vahvistin toteutetaan käyttämällä ylimitoitettua 1 W tehovahvistinta 10 dB alle sen maksimitehon.

Työssä käsitellään myös muita tapoja linearisoida tehovahvistin, jotta backoff:n käyttö voidaan perustella. Jotta rakennetun taajuusmuuntimen suorituskykyä voitaisiin arvioida, diplomityön loppupuolella esitellään eri mittausten menetelmiä sekä VTT:n Otadigi-lähettimen signaalin voimakkuuden mittauksen tulokset. Mittaustuloksien avulla voidaan myös arvioida, millainen taajuusmuunnin on järkevä toteuttaa.

**Avainsanat:** DVB-T, OFDM, kokeellinen, taajuusmuunnin, mikroaalto, lähetin

# Preface

I would like to express my gratitude to Professor Pekka Eskelinen and M.Sc. Markku Nieminen for their creative comments, sound advices and thorough reviews during the completion of this thesis. Also, the practical skills and knowledge, which they shared on various other projects that I participated while working here at IDC, are gratefully acknowledged.

A warm thanks goes to the staff of IDC, Ulla and Sanna, for their aid in every-day problems that usually were quite more complicated than fundamentals of radio engineering. Hanna, Risto and Tero; thanks for all those coffee breaks that sometimes prolonged to hours of imaginative conversation — and what has become of lunch hours is another story...

To Mommy and Daddy, the sincerest thanks for all support and encouragement during these twenty years that I managed to stay on the school bench.

Last — but not least by number, all the friends and fellows whom I met while participating in the activities of the Guild of Electrical Engineering, ORC, and in numerous homework sessions and laboratory exercises here at HUT, one small word:

Cheers!

*Espoo, September 4, 2003*

A handwritten signature in black ink, appearing to read 'VK' followed by a stylized flourish.

*Ville-Hermanni Kilpiä*

# Contents

Abstract	2
Tiivistelmä	3
Preface	4
Nomenclature	7
1 Introduction	12
2 Digital Terrestrial Television Broadcasting	13
2.1 Terrestrial Digital Video Broadcasting in Europe . . . . .	14
2.1.1 Channel Coding and Modulation Method in the DVB-T . . . . .	14
2.1.2 Orthogonal Frequency Division Multiplexing . . . . .	15
2.1.3 Parameters Chosen for the Terrestrial Broadcasting . . . . .	17
2.2 Digital Television Broadcasting in the U.S. . . . .	19
2.3 Digital Broadcasting in Japan . . . . .	20
2.4 A Transmitter for DVB-T Broadcasting . . . . .	23
2.5 Technical Requirements for a DVB-T transmitter . . . . .	24
2.5.1 Frequency Requirements . . . . .	24
2.5.2 Frequency Translation Requirements . . . . .	26
2.5.3 Linearity Requirements . . . . .	26
3 RF Amplifier Linearization	28
3.1 Basic RF Amplifier Types . . . . .	28
3.2 Amplifier Linearization Techniques . . . . .	29
3.2.1 Feedback . . . . .	30
3.2.2 Feedforward . . . . .	30
3.2.3 Predistortion . . . . .	31
3.3 Linearization of the Frequency Converter . . . . .	33
4 Radio Wave Propagation	35
4.1 Free Space Propagation . . . . .	36
4.2 Reflection . . . . .	36
4.3 Ground Reflection . . . . .	37
4.4 Diffraction . . . . .	39
4.5 Scattering . . . . .	41
4.6 Okumura Model . . . . .	42



4.7	Log-distance Path Loss Model . . . . .	42
4.8	Radio Wave Propagation Measurements . . . . .	44
4.8.1	The United States . . . . .	45
4.8.2	Europe . . . . .	45
4.8.3	Japan . . . . .	45
4.9	Estimating Propagation Losses . . . . .	46
<b>5</b>	<b>The System Environment</b>	<b>48</b>
5.1	The OtaDigi Project . . . . .	48
5.2	Area of Reception . . . . .	50
5.3	Transmit Frequency . . . . .	52
5.4	The Test Receiver . . . . .	53
5.5	Link Budget . . . . .	55
5.6	Speculation about the Location of ‘Ostadigi’ Transmitter . . . . .	58
<b>6</b>	<b>Experimental Frequency Converter</b>	<b>60</b>
6.1	System Configuration . . . . .	60
6.2	Alternative Configuration . . . . .	62
6.3	Block Level Components . . . . .	63
6.3.1	Mixer . . . . .	64
6.3.2	Up-conversion Operation Specialities in Mixers . . . . .	65
6.3.3	5.8 GHz ISM band filters and transmission lines . . . . .	66
6.3.4	Power Amplifier . . . . .	68
6.3.5	UHF block . . . . .	70
6.3.6	Antenna . . . . .	71
6.3.7	Local Oscillator . . . . .	74
<b>7</b>	<b>Measuring the Performance of a DVB-T System</b>	<b>77</b>
7.1	Linearity Measurements . . . . .	77
7.2	Phase Noise Measurements . . . . .	80
7.3	System Level Measurements . . . . .	81
<b>8</b>	<b>Ostadigi Reception Measurement</b>	<b>82</b>
<b>9</b>	<b>Conclusions</b>	<b>87</b>
	<b>Bibliography</b>	<b>88</b>
	<b>Appendices</b>	<b>95</b>

# Nomenclature

## Symbols

$a$	Aperture dimension of a horn antenna in H-plane
$a_0$	Inner dimension of a waveguide in H-plane
$a(h_r)$	Antenna correction factor
$A_{mu}$	Median attenuation relative to the free space (attenuation)
$A_R$	Radar cross section (RCS)
$b$	Aperture dimension of a horn antenna in E-plane
$b_0$	Inner dimension of a waveguide in E-plane
$B_1$	Bandwidth of the multi-tone signal
$B_2$	Bandwidth of the adjacent channel
$B_n$	Noise bandwidth
$C$	Coupling factor of a directional coupler
$D$	Largest physical dimension of an antenna
$d$	Distance, usually measured along the ground
$d_0$	Reference distance, in the log-distance path loss model
$d_1$	Distance from a transmitter to a blocking object
$d_2$	Distance from a blocking object to a receiver
$d_c$	Distance from the transmit antenna to a ground incidence point of the center of the antenna beam
$d_d$	Line-of-sight distance between a transmitter and a receiver
$d_f$	Distance to the far-field, the Fraunhofer, region
$d_g$	Distance between the Otaniemi water tower and a ground incidence point of the center of the antenna beam
$d_i$	Distance between a transmitter and a receiver, travelled along the ground-reflected path
$d_r$	Distance between a receiver and a scatterer
$d_t$	Distance between a transmitter and a scatterer
$d_\Delta$	Excess path length in a diffraction
$F$	Noise figure
$f_1$	Carrier signal used in the two-tone test
$f_2$	Second carrier signal used in the two-tone test
$f_c$	Center frequency, of the signal channel or a filter
$f_o$	Offset of the center of adjacent channel bandwidth $B_2$ from the center of the signal channel $f_c$

## Symbols (cont.)

$f_s$	Carrier spacing, in the OFDM
$F(v)$	Knife-edge diffraction gain
$G$	Gain
$G_{area}$	Environmental gain
$G(h_t)$	Transmitter antenna gain as a function of height
$G(h_r)$	Receiver antenna gain as a function of height
$G_m$	Gain of the $m$ th component in a cascade connection
$G_r$	Gain of a receiver antenna
$G_t$	Gain of a transmitter antenna
$h$	Height of an object
$h_c$	Critical height of surface protuberances
$h_r$	Height of a receiver
$h_s$	Effective road height due to e.g. vehicles and pedestrians
$h_t$	Height of a transmitter
$I_0$	Modified Bessel function of the first kind and of the zeroth order
$j$	Imaginary unit
$k$	Wave number of an RF wave
$k_B$	Boltzmann constant ( $k_B = 1.381 \cdot 10^{-23}$ J/K)
$L$	Attenuation coefficient of a component
$L_{50}$	Median path loss
$l_e$	Slant length of the flare in the E-plane
$L_{fsp}$	Free space path loss
$l_h$	Slant length of the flare in the H-plane
$m$	Integer, index number
$n$	Path-loss exponent in the log-distance path loss model
$P_{1dB}$	1 dB compression point
$P_{1dB,IN}$	Input port 1 dB compression point
$PG$	Path gain, usually a negative value
$P_{in}$	Input power
$\overline{PL}$	Average of all possible path losses at the given distance $d$
$P_{LO}$	Local oscillator output power (requirement)
$P_{max}$	Maximum power level
$P_n$	Noise power
$P_{out}$	Output power, in general
$P_r$	Signal power received by a receiver
$P_{rel}$	Power level relative to the maximum signal power
$P_t$	Output power of a transmitter
$R$	Code rate of a convolutional coder
$R_{bp}$	Breakpoint distance
$r_m$	Radius of the $m$ th Fresnel zone
$s$	Maximum phase deviation in wavelengths, in the E-plane
$S_{11}$	Complex input port scattering parameter (i.e. reflection coefficient)



## Symbols (cont.)

$S_{12}$	Complex reverse direction scattering parameter (e.g. isolation)
$S_{21}$	Complex forward direction scattering parameter (e.g. gain or attenuation)
$S_{22}$	Complex output port scattering parameter (i.e. reflection coefficient)
$T$	Noise temperature
$t$	Maximum phase deviation in wavelengths, in the H-plane
$T_0$	Standard noise temperature ( $T_0 = 290$ K)
$T_A$	Antenna temperature
$T_G$	Guard interval
$T_m$	Noise temperature of the $m$ th component in a cascade connection
$T_{phys}$	Physical temperature of a component
$T_R$	Receiver noise temperature at the input of a receiver
$T_S$	Receiver system temperature
$T_{SYM}$	Duration of a transmitted symbol
$T_U$	Usable signal duration
$w$	Width of the reception area
$v$	Fresnel-Kirchoff diffraction parameter
$X_\sigma$	Log-normal shadowing parameter for a given environment
$2\psi_e$	Total flare angle, in the E-field plane
$\Gamma$	Complex reflection coefficient
$\Gamma_{rough}$	Complex reflection coefficient for rough surfaces
$\Gamma_{\parallel}$	Complex reflection coefficient for a vertically polarized RF field
$\Gamma_{\perp}$	Complex reflection coefficient for a horizontally polarized RF field
$\epsilon_0$	Permittivity of a vacuum
$\epsilon_1$	Permittivity of a medium
$\epsilon_2$	Permittivity of a different medium
$\epsilon_r$	Relative permittivity of a medium
$\theta_E$	Vertical beam width of an antenna
$\theta_H$	Horizontal beam width of an antenna
$\Theta_i$	Angle of incidence between a propagating radio wave and the normal of the boundary between two media
$\lambda$	Wave length of a radio wave
$\mu_1$	Permeability of a media
$\mu_2$	Permeability of a different media
$\rho_1$	Length of an antenna along the center line of the waveguide
$\rho_s$	Scattering loss factor
$\sigma$	Standard deviation
$\sigma_h$	Standard deviation for surface height about the mean surface height
$\varphi$	Auxiliary variable used to derive the antenna beam widths
$\varphi_i$	Angle of incidence between a reflecting ray and the ground
$\phi$	Phase difference of Excess path length $d_\Delta$

## Abbreviations

16QAM	16-state Quadrature Amplitude Modulation
64QAM	64-state Quadrature Amplitude Modulation
8-VSB	Trellis Coded 8-Level Vestigial Sideband, the American digital television standard
802.11	High-performance Wireless LAN protocol, in the U.S. (IEEE standard)
AC-3	Dolby Digital Sound Format, used in the American digital television broadcasting standard
AAC	Advanced Audio Coding, sound coding method used in the ISDB-T, devised by the Fraunhofer Institute in German
ACPR	Adjacent Channel Power Ratio, a measurement concept
AFC	Automatic Frequency Control
AGC	Automatic Gain Control
BER	Bit Error Rate
BPSK	Binary Phase Shift Keying
BROCOM	Interactive Services and Technologies for Mixed Broadcasting, Navigation and Communication in the Mobile Society
C/N	Carrier-to-noise ratio
COST	European Cooperation in Scientific and Technical Research
CW	Carrier Wave
DQPSK	Differential Quadrature Phase Shift Keying
DSP	Digital Signal Processing
DVB	Digital Video Broadcasting, European standard
DVB-T	Terrestrial Digital Video Broadcasting; European standard
DVB-X	Ad-hoc DVB standard for Mobile Terminals, based on DVB-T
EIRP	Equivalent Isotropically Radiated Power
ETSI	European Telecommunications Standards Institute
FEC	Forward Error Correction
FFT	Fast Fourier Transformation
GPS	Global Positioning System
GSM	Global System for Mobile Communication
HDTV	High-Definition Television
HF	High Frequency, an RF frequency band of 3–30 MHz
HiperLAN/2	High-performance Wireless LAN standard, in Europe
HUT	Helsinki University of Technology
IC	Integrated Circuit
IDC	Institute of Digital Communications
IEEE	Institute of Electrical & Electronics Engineers
IF	Intermediate Frequency
IFFT	Inverse Fast Fourier Transformation
IL	Insertion Loss
IMD	Intermodulation Distortion
IP <sub>3</sub>	Third Order Intermodulation Intercept Point (see also TOI)

## Abbreviations (cont.)

IRC	Institute of Radio Communications
ISDB-T	Terrestrial Integrated Services Digital Broadcasting, Japanese standard
ISM	Industrial, Scientific and Medical
IT	Information Technology
LAN	Local Area Network
LO	Local Oscillator
LOS	Line of Sight
LNA	Low Noise Amplifier
MEG	Mean Effective Gain
M-IMR	Multitone InterModulation Ratio, a measurement concept
MPEG-2	Transport stream standard devised by the Motion Picture Expert Group
MUX	Multiplexer
NICAM	Near Instantaneous Companding Audio Multiplexed
NLOS	Non-Line of Sight
NPR	Noise Power Ratio, a measurement concept
NTSC	National Television System Committee
OFDM	Orthogonal Frequency Division Multiplexing
PLL	Phase Locked Loop
PRBS	Pseudo-Random Binary Sequence
QPSK	Quadrature Phase Shift Keying, 2 bits per symbol
RS	Reed-Solomon coding, a data coding method
RCS	Radar Cross Section
RF	Radio Frequency
SDTV	Standard Definition Television
SFN	Single-Frequency Network
TE <sub>10</sub>	the lowest mode of an electro-magnetic field distribution in a waveguide, the preferred mode also.
TOI	Third Order Intermodulation Intercept Point, a measure of the linearity of a device
TV	Television
UHF	Ultra High Frequency, an RF frequency band of 300–3000 MHz
U-NII	Unlicensed National Information Infrastructure, high-performance Wireless LAN allocations in the U.S.
WWW	World Wide Web
VCO	Voltage Controlled Oscillator
VHF	Very High Frequency, an RF frequency band of 30–300 MHz
VNA	Vector Network Analyzer
VSF	Vestigial Sideband Modulation
VSWR	Voltage Standing Wave Ratio
VTT	Technical Research Centre of Finland
XO	Crystal Oscillator



# Chapter 1

## Introduction

The chosen standard for European terrestrial digital television broadcasting DVB-T [1], due to the used modulation, has a ability to cope with effects of multi-path propagation. Thus, it is possible to receive the DVB-T signal with a mobile terminal. In recent years there has been a lot of interest in the mobile DVB-T reception; even an ad-hoc group for a mobile DVB standard, DVB-X, was created [2].

One problem in receiving the RF signal in UHF, or in GSM band, is the lack of possibilities to produce a good antenna array for the handset. The wavelength of RF signal is so long that a design for a good, or even reasonably good, and small antenna array is complicated.

A few years ago European and U.S. regulatory authorities allocated frequencies near 5.8 GHz to Wireless LAN use, designated as the U-NII, or 802.11a [3], in the U.S. and the HiperLAN/2 [4] in Europe. This has caused numerous companies to start designing RF components for that frequency range. Also, a number of propagation studies in the outdoor environment have already been completed [5], [6].

This gives a good basis for studying the mobile reception of the DVB-T signal within bands near 5.8 GHz, where the ISM frequencies in Finland are located. Also, the design of advanced mobile handset antennas, particularly small arrays, is much easier at the frequency of 5.8 GHz due to the shorter wavelength.

In this thesis a review of the DVB-T technology is presented. The critical parts of the design are pointed out and possible solutions are discussed. Also, a short introduction to amplifier linearization is given. After a practical formula to model the radio wave propagation is presented, the link budget for the given broadcasting environment is calculated. Thus the design specifications for the frequency converter can be derived. A block level implementation of the frequency converter is then presented. Finally, a short discussion about the verification of the performance of the frequency converter is made, and a small campaign to measure the 'Ostadigi' [7] DVB-T broadcast is completed.

This study is done within the Interactive Services and Technologies for Mixed Broadcasting, Navigation and Communication in the Mobile Society (BROCOM) project under the Institute of Digital Communications (IDC) at Helsinki University of Technology (HUT), Finland.

A paper [8] composed from this thesis, will be presented in the European Conference on Wireless Technology held during the European Microwave Week 6-10 October 2003.

## Chapter 2

# Digital Terrestrial Television Broadcasting

After the introduction of the color television in 1967, the digital aspect of the analog television broadcasting started to develop. Much of this was due to the increase in additional services transmitted along the analog signal (e.g. the teletext system, the Video Programme System and the NICAM sound).

In Europe, the end of the analog television technology development was reached in September 1993, when the European Commission ended support for the European high definition television (HDTV) standard, designated HD-MAC. The reasons were many. Arguments about the financial profitability were made, but also a technological aspect was brought forth: the analog technology, which was already superseded, can not be supported any longer. The new goal was to make a standard, if possible a world-wide standard, for digital television [9].

The development of digital television broadcasting technology started already in 1991 in form of various research projects. Major part of this work was done under various national broadcasting companies and research institutes. These projects were finally harmonized and concentrated in 1993 to produce European digital video broadcasting (DVB) standard (to cover terrestrial, cable and satellite transmission), and also to develop strategies for the introduction of the DVB in various transportation media. This work towards the integration of numerous European projects reached its first goal in December 1995, when the first specification for the terrestrial digital video broadcasting (DVB-T) was adopted [9].

In this chapter, the main subject of discussion is the DVB-T standard, its performance and its technical requirements. Also, a brief look on the chosen standards in the United States and Japan is taken, and a comparison is conducted between these terrestrial broadcasting standards and the DVB-T. Finally, technical requirements for a DVB-T transmitter are pointed out and discussed. These requirements are used as design guidelines for the experimental frequency converter.



## 2.1 Terrestrial Digital Video Broadcasting in Europe

The digital television standard development in Europe was aimed to produce a standard that could be transmitted using the existing analog television system.

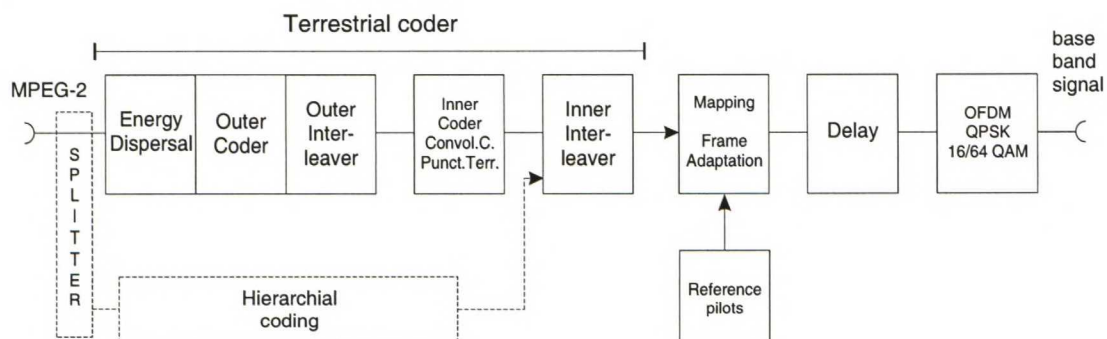
The technology used in the terrestrial digital video broadcasting (DVB-T) can be divided to two parts. The first part deals with audio and video encoding and the use of the MPEG-2 (a standard devised by Motion Picture Expert Group) transport stream. This part is common to all transmission techniques: cable, satellite and terrestrial.

The second part, the terrestrial transmission system, describes framing structure, channel coding and modulation method used in the DVB-T. To be able to adapt to different transmission channel characteristics, the DVB-T standard uses a multi-carrier modulation method, called the orthogonal frequency division multiplexing (OFDM), which is combined with a powerful error-correction coding. The terrestrial transmission system for digital video broadcasting is standardized in European Telecommunications Standards Institute (ETSI) standard EN 300 744, the current version is 1.4.1 and is dated January, 2001 [1].

In the following sections the DVB-T transmission system is described. The interest is in channel coding and modulation methods used, while the input data (the MPEG-2 stream) is considered as a general bit stream. Also, the principles of a DVB-T transmitter are described, and in the end, the technical requirements for the DVB-T transmitter are discussed.

### 2.1.1 Channel Coding and Modulation Method in the DVB-T

The channel coding in the DVB-T standard is carried out in five steps, after which the data is mapped and modulated into the baseband. These parts are illustrated in Figure 2.1.



**Figure 2.1:** Block diagram of the DVB-T coder and the OFDM modulator. The DVB-T standard provides a possibility for a hierarchial transmission. (edited from [9],[1])

First, the energy dispersal of the input data stream is carried out by using a pseudo-random binary sequence (PRBS) with predetermined generator polynomial. This process is necessary in order to avoid a long constant-value bit stream in transmission, which would degrade the usage of the transmission channel spectrum and the clock recovery in



the receiver. The randomization process is even carried out when there is no input stream (missing or non-compliant) in order to avoid an unmodulated data carrier.

The randomized stream is then coded using Reed-Solomon coding RS(204,188,t=8), which is a shortened code based on the RS(255,239,t=8). The 188 bytes of input data are coded into a word of 204 bytes, from which up to 8 random erroneous bytes can be corrected in the receiver. The Reed-Solomon coding is efficient in channels having a high probability for multiple errors.

Following the outer coder, the data stream is subjected to convolutional interleaving. The RS-coded packets of 204 bytes are divided into 17 blocks of 12 bytes each, and are then cyclically interleaved. The benefit of this interleaving is the improved error correction against a burst and spark-like interference by temporally spreading consecutive bits further away from each other.

In the inner coder, the data stream goes through a convolutional coder with puncturing. The code rate can be chosen according to the requirements of the transmission system and the broadcast, and the possible code rates  $R$  are  $7/8$ ,  $5/6$ ,  $3/4$ ,  $2/3$  and  $1/2$ , from which the last is the strongest code (i.e. only half of the output bits are payload, rest is for the error correction).

The benefit from using two separate and nested coders is that the outcome is better than by only extending the code length of a one coder.

After the inner coder, inner interleaving is performed. It consists of bit-wise interleaving chosen according to the used modulation method, and symbol interleaving which depends on the number of carriers in the OFDM. In the inner interleaver, the data stream is scrambled in a manner that the data is spread out in the frequency domain when it is modulated. This makes the transmission more robust against spurious signals and other bandwidth-limited interference.

A remark shall be made that the outer coder and interleaver are common to all DVB standards (satellite, cable and terrestrial), also the inner coder is the same as in satellite broadcasting. The inner coder is unique to the terrestrial transmitters.

In the DVB-T standard, there is a possibility to transfer data using a hierarchical coding. This is illustrated in Figure 2.1 by the dashed section. By using the hierarchical coding, it is possible to transmit a multiplexed service in two independent channels that are protected differently in order to optimally match channel requirements.

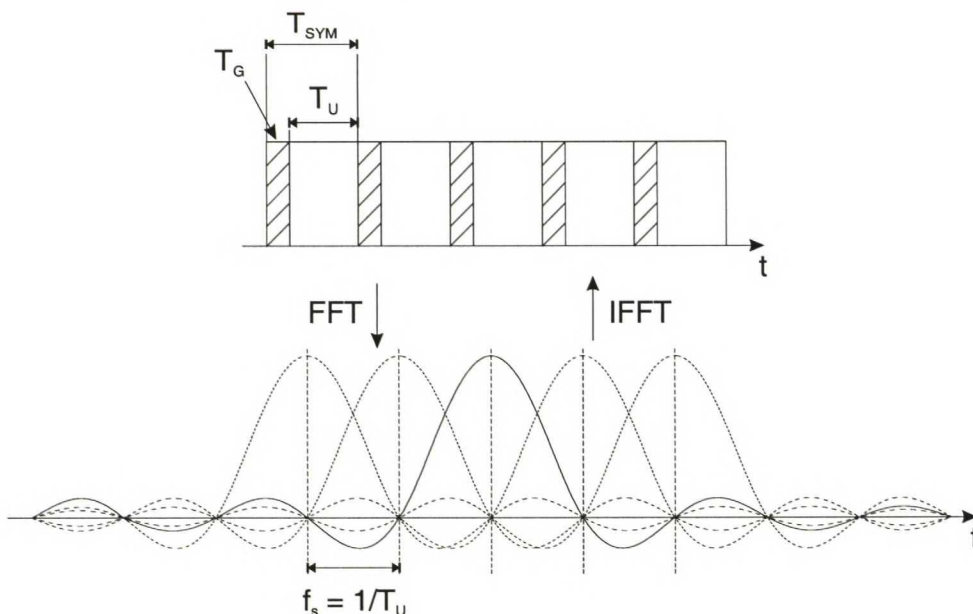
After the terrestrial coder, the data stream is bit-mapped according to the used modulation scheme. Also, reference pilots, for coherent demodulation, and transmission parameter signalling pilots are incorporated into the OFDM frame structure. Before sent into the modulator, the signal is delayed in order to provide a bit-synchronous transmission in a single frequency network (SFN).

### 2.1.2 Orthogonal Frequency Division Multiplexing

The DVB-T system uses the orthogonal frequency division multiplex (OFDM) transmission. In the OFDM, the transmission channel is divided into a number of sub-carriers. Also, the signal is organized into periods of duration  $T_{SYM}$ . The carrier spacing  $f_s$  and the usable signal duration  $T_U$  have a relation  $f_s = 1/T_U$ , which ensures that carriers are orthogonal to each other. The element specified by duration  $T_{SYM}$  and of bandwidth  $f_s$

transmits one modulation symbol, and all elements in one time slot of  $T_{SYM}$  compose one OFDM symbol (and 68 symbols compose one OFDM frame). This is illustrated in Figure 2.2.

In the DVB-T standard the number of sub-carriers depend on the length of the fast fourier transformation (FFT) available in the modulator. The number of sub-carriers defined in the DVB-T standard is either 1705 (a 2k samples long FFT, the 2k mode) or 6817 (the 8k mode). The 2k mode can be used in systems that cannot afford the more complex hardware required by the 8k FFT (e.g. the mobile terminals).



**Figure 2.2:** *The OFDM signal in time and frequency domains. The baseband time domain signal is created by the use of inverse fast fourier transformation (IFFT) in the modulator. (edited from [9])*

The gross bit rate is modulated into these sub-carriers within the allocated TV channel of 8 MHz. Depending on the chosen modulation of QPSK, 16QAM or 64QAM, each sub-carrier transmits either 2, 4 or 6 bits per symbol. Symbols are coded by using the Gray mapping (i.e. there is only a one-bit change between adjacent symbols). Also, there is a possibility to use a non-uniform constellation in the 16QAM and 64QAM.

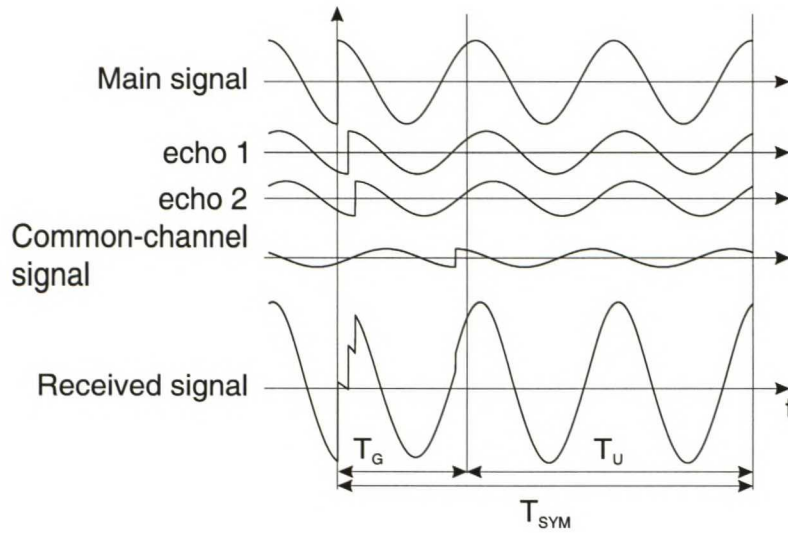
These choices are the advantage of the OFDM compared to the single-carrier methods. The low bit rate per carrier makes the long duration of one symbol  $T_{SYM}$  possible, thus it is possible to insert a guard interval  $T_G$  in the beginning of every symbol. During this guard interval the receiver does not interpret the value of the symbol, which makes the OFDM reception highly immune to echoes occurring in the multi-path propagation environment. In the transmitter the guard interval is produced by repeating some proportion of the symbol, and in the DVB-T standard designated values for the guard interval  $T_G$  are  $1/4$ ,  $1/8$ ,  $1/16$  and  $1/32$  parts of the useful symbol duration  $T_U$ . The guard interval  $T_G$  is chosen by estimating multi-path propagation delays in the broadcasting environment.



The use of the guard interval also provides the possibility to implement a single frequency network (SFN), where all transmitters use the same broadcasting frequency. Transmit frequencies are locked together, and transmissions are timed by using a designated clock signal (e.g. the GPS signal).

The effect of guard interval usage in the radio-channel recovery is demonstrated in Figure 2.3. The signal is simplified to a cosine signal, and in the reception two echoes and one other transmitter distort the signal. After the duration of guard interval  $T_G$ , the symbol is in a steady state. The adaptation to different multi-path propagation environments can be carried out by using reference pilot signals incorporated in the data stream.

A remark shall be made that it is also possible to scale parameters of the DVB-T standard to enable transmission in a 6 MHz or 7 MHz TV channel [1].



**Figure 2.3:** *Recovery of the OFDM symbol after the duration of the guard interval  $T_G$ . The  $T_G$  is chosen according known multi-path delays in the propagation channel. (edited from [9])*

### 2.1.3 Parameters Chosen for the Terrestrial Broadcasting

As seen from previous sections, the DVB-T standard allows a wide variety of transmission parameters to be chosen according to the needs of a broadcaster and the transmission environment. In Table 2.1, transmission parameters defined in the DVB-T standard are summarized, and the chosen parameters for the national broadcasting in Finland [10] are respectively highlighted.

Even though the DVB-T standard was not designed to support mobile reception, it has been noticed that the mobile reception is possible — and recently there has been a lot of research in this field. The numerous choices the broadcaster has over the parameters of a DVB-T transmission allow the data rate and error correction to be modified to cope with reception difficulties when using a mobile receiver. By examining the published literature



(e.g. [9],[11]), a viable parameter range for the mobile DVB-T reception is presented in Table 2.2.

A remark shall be made that in published articles and literature, the term ‘mobile reception’ has a broad meaning, e.g. the receiver might travel at speeds up to 120 km/h [11]. In general, mobile measurements were made using an automobile, or in a tram, that travelled at speed of about 50 to 100 km/h [10],[12],[13]. So, when reviewing the results in published articles the environment, in which the reception is made should be carefully examined.

In this thesis, the receiver is thought to be in a hand of a human, so an estimate for the speed of the receiver should be about 5 km/h. The slow speed could be beneficial for the reception of a DVB-T signal, comparing to a case of a moving vehicle where high speeds will cause problems in the reception. In both cases, the transmitter will provide the antenna diversity and frequency hopping to ensure the highest possible quality in the radio link.

This could lead to better reception conditions and allow higher data rates to be used than estimated in Table 2.2. Even data rates as high as in the standard DVB-T, in Table

**Table 2.1:** *Transmission parameters according to the DVB-T standard [1]. The DVB-T broadcasting parameters used in Finland are highlighted [10].*

Parameter		the DVB-T standard	
FFT length (the OFDM mode)		2k	<b>8k</b>
Number of sub-carriers		1705	<b>6817</b>
Sub-carrier spacing		4.464 kHz	<b>1.116 kHz</b>
Channel width		7.61 MHz	
Modulation		QPSK, 16QAM, <b>64QAM</b>	
Code rate $R$		1/2, <b>2/3</b> , 3/4, 5/6, 7/8	
Guard interval $T_G$	1/4	56 $\mu$ s	224 $\mu$ s
	<b>1/8</b>	28 $\mu$ s	<b>112 <math>\mu</math>s</b>
	1/16	14 $\mu$ s	56 $\mu$ s
	1/32	7 $\mu$ s	28 $\mu$ s
Net data rate		4.98 – 31.67 Mbit/s ( <b>22.12 Mbit/s</b> )	

**Table 2.2:** *Transmission parameters considered suitable for mobile DVB-T reception*

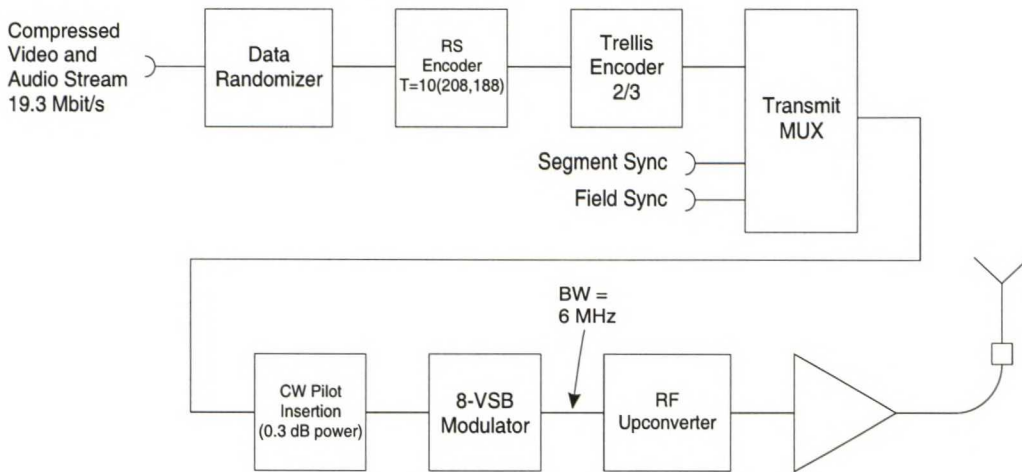
Parameter	Mobile DVB-T reception
FFT length	2k, 8k
Modulation	QPSK, 16QAM
Code rate $R$	1/2, 2/3
Guard interval $T_G$	1/4, 1/8
Data rate	5 – 13.3 Mbit/s

2.1, are considered possible [10].

## 2.2 Digital Television Broadcasting in the U.S.

The United States was in the vanguard of the development of digital terrestrial television broadcasting. Comparing to the European choice of more channels with a standard television quality, the U.S. chose to achieve a high-definition television (HDTV) picture quality while keeping the number of available channels same.

The work started in early 1990s and in 1995 a standard developed by Advanced Television Systems Committee was finished. The approved standard was called Trellis Coded 8-Level Vestigial Side-Band (8-VSB). The basic structure of the 8-VSB system specification is shown in Figure 2.4, and parameters for the terrestrial broadcasting are given in Table 2.3. The structure of the 8-VSB system can be described as follows.



**Figure 2.4:** Basic schematic of the 8-VSB television system. The 8-level vestigial side-band modulation is coherently demodulated using the inserted pilot carrier. (edited from [9])

The picture layer provides picture sizes of  $1280 \times 720$  and  $1920 \times 1080$  pixels and a number of refresh rates using either a progressive or an interlaced scanning. In the 8-VSB system, the compression layer is based on the MPEG-2 video (19.4 Mbit/s) and the Dolby AC-3 audio (384 kbit/s) coding, and the transport layer has a packet format according to the MPEG-2 standard and ensures flexibility for TV and audio broadcasting and data services.

The transmission layer of the 8-VSB systems uses a single carrier frequency technology with a vestigial sideband (VSB) modulation. The serial bit stream is modulated into a signal that can be transmitted over a 6 MHz television channel.

The data is transmitted using a Trellis-code with 8 discrete levels of signal amplitude. A pilot tone is provided to ensure a rapid acquisition of the signal by the receiver, and to make a coherent demodulation possible. By using complex coding techniques and



adaptive equalization, the reception is made more robust to multi-path propagation, noise and interference. The 8-VSB system has a transmit data rate of about 19.3 Mbit/s [14].

Recent articles and published literature suggest that the 8-VSB has a larger coverage area, causes less interference with analog TV signals, and has a greater robustness in the digital signal than the DVB-T [9]. Also, it has higher spectrum efficiency, a lower peak-to-average ratio, and is more robust to impulse noise (from household appliances) and phase noise [11].

On the downside, apparently the 8-VSB has some serious problems with in-house reception due to inefficient techniques to counteract multi-path propagation [14]. This maybe the consequence of the design of the 8-VSB standard, as it was devised for multi-frequency network use. It seems that it might be possible to negate some of the effects of multi-path propagation by using a better receiver with a longer ghost-cancelling range [14].

This would also indicate that mobile reception using the 8-VSB is not possible, or at least is very difficult.

**Table 2.3:** *Parameters for the 8-VSB terrestrial transmission [15]*

Parameter	Terrestrial 8-VSB transmission
Channel bandwidth	6 MHz
Excess bandwidth	11.5%
Symbol rate	10.76 Msymbols/s
Bits per symbol	3
Trellis FEC	2/3
Segment length	832 symbols
Segment sync	4 symbols per segment
Frame sync	1 per 313 segments
Payload data rate	19.28 Mbit/s
NTSC co-channel rejection	NTSC rejection filter in receiver
Pilot power contribution	0.3 dB
C/N threshold	14.9 dB

## 2.3 Digital Broadcasting in Japan

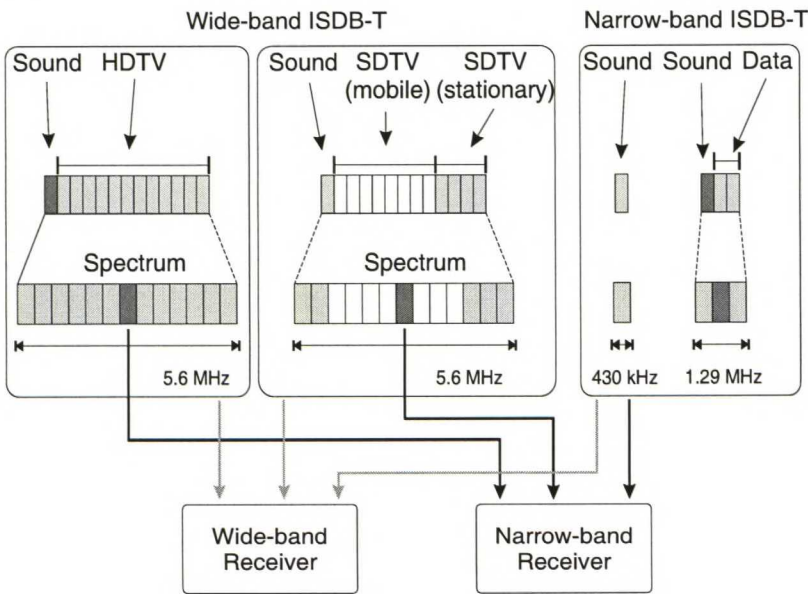
The standard for digital terrestrial broadcasting in Japan was developed by Japanese Association of Radio Industries and Business in 1990s. Comparing to the other standards, the Japanese digital broadcasting standard covered television, sound broadcasting and data services as a whole. The broadcasting standard, called Terrestrial Integrated Services Digital Broadcasting (ISDB-T), is able to transmit all these three types of service separately in a large number of combinations.

As in other digital television standards, the Japanese also chose the MPEG-2 for the source coding method, but the sound coding is done using the AAC (advanced audio



coding) from Fraunhofer Institute in Germany [16]. The RF transmission uses OFDM, and the transmission bandwidth is 5.6 MHz [17], so the signal can be transmitted in the existing 6 MHz analog television channel.

While the ISDB-T is similar to the DVB-T in many ways, there are many improvements and additional features included in the standard. By using the hierarchial transmission technique, up to three different services with different transmission parameters can be provided simultaneously in a transmission channel. This generally addresses various types of receivers (illustrated in Figure 2.5), thus a 6 MHz channel provides different services with the same infrastructure.



**Figure 2.5:** *Partial (hierarchial) reception used in the ISDB-T system, where a transmission, consisting of independent segments, can be received by an appropriate receiver. (edited from [18])*

In the ISDB-T, partial reception of the broadcasting spectrum is possible since the OFDM spectrum is divided into 13 segments (Figure 2.5). If the transmission parameters influence only a one OFDM segment, this segment can be received independently of the other 12 segments. So a complete signal can be received by evaluating this one segment. If suitable transmission parameters are chosen, this one segment can be designed to be nearly immune to interference, thus it is possible to design services (mobile video download etc.) that specially address the mobile devices.

Channel coding in the ISDB-T is provided by three identical paths, which also provide the hierarchial coding for different services. The functional design of the channel coding system is illustrated in Figure 2.6.

Every transport stream packet is coded using the Reed-Solomon coding. Then the stream is split into three hierarchial layers. To each of these hierarchial layers, a dispersion of energy is committed using a pseudo-random binary sequence (PRBS).

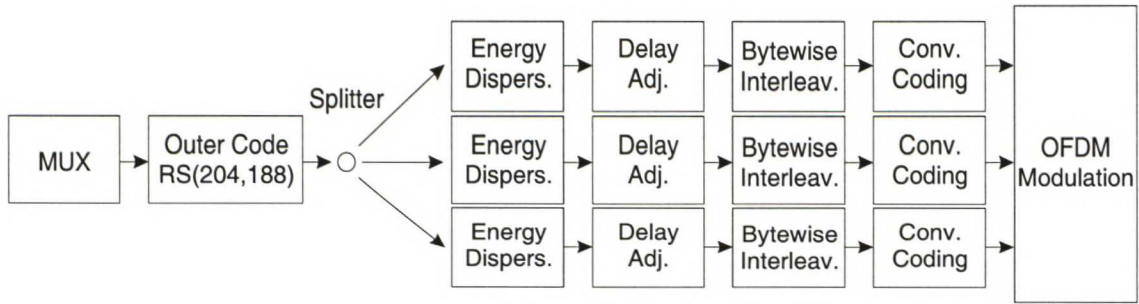
Depending on the modulation and code-rate parameters of the transmission, data streams are delayed to minimize the receiver delay. Also, subsequent delay differences are

compensated here in advance.

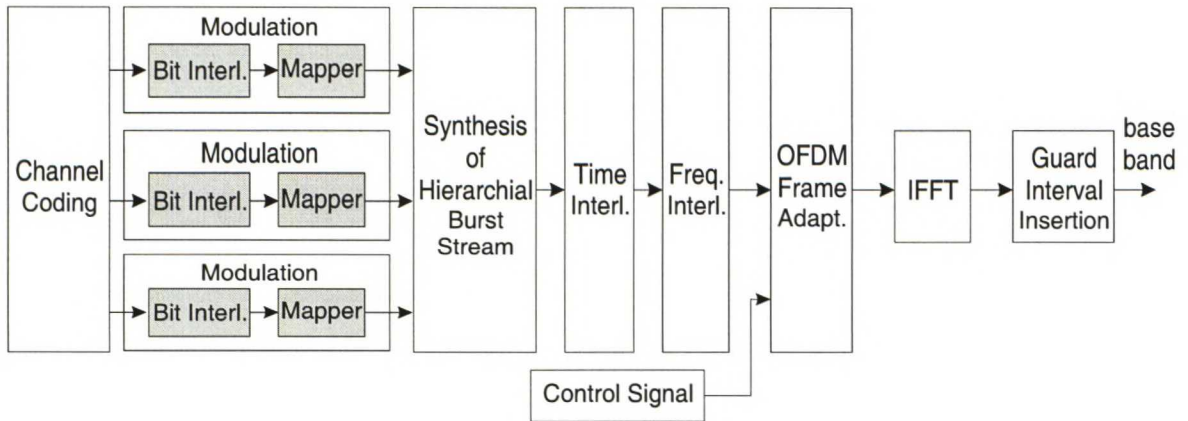
Then, data streams are byte-wise interleaved to counter the burst-like interference in the transmission channel. During the de-interleaving, burst errors occurred in the transmission channel are sorted into single bit errors that the Reed-Solomon decoder can correct. The convolutional coder adds further redundancy to the data stream in order to permit error correction in the receiver. The code rate can be selected according to the required transmission characteristics of the system.

The modulation block, illustrated in Figure 2.7, first performs the modulation of the three separate channel coded streams. Modulation includes automatic bitwise interleaving with delay adjustment, and then the streams are mapped to a constellation depending on required transmission characteristics. Possible constellations are QPSK, DQPSK, 16QAM and 64QAM.

After the modulation, the hierarchical data stream is synthesized by appending three data streams end-to-end to form a single serial stream. Further symbol-by-symbol time interleaving is performed, the depth of the interleaving can be chosen separately for different layers of hierarchy.



**Figure 2.6:** The ISDB-T channel coding system. Three identical paths provide the hierarchical coding for different services. (edited from [17])



**Figure 2.7:** Schematic of the ISDB-T modulation block. The hierarchical data streams from channel coder are modulated and synthesized into a single serial stream that is transformed into a time-domain base band signal. (edited from [17])



The data stream is then scrambled within the OFDM symbol. The OFDM frames are then constructed from 204 symbols by adding pilot carriers, various control carriers, as well as auxiliary channel carriers to different positions in the data stream.

Then, the generated data is transformed into the time domain using the inverse fourier transformation (IFFT). The length of the IFFT is chosen according to the ISDB-T mode. Last, the OFDM symbol is protected against multi-path propagation errors in the reception by inserting a guard interval. Transmission parameters for the three defined transmission modes are given in Table 2.4

The used techniques strengthen the ISDB-T, compared to the European DVB-T, especially in the mobile reception, in a possible narrow-band reception where only a part of the transmitted data is evaluated, and on the hierarchial transmission when adapting to different reception conditions.

Currently, field tests are taking place, and ISDB-T operations should start in Tokyo, Nagoya and Osaka between 2003 and 2005. The nation-wide coverage should be deployed by 2006, and the analog broadcasting ought to be discontinued in 2010 [17].

**Table 2.4:** *Transmission parameters for the ISDB-T [17]*

	Mode 1	Mode 2	Mode 3
Number of segments	13		
Bandwidth	5.575 MHz	5.573 MHz	5.572 MHz
Carrier offset	3.968 kHz	1.984 kHz	0.992 kHz
Number of carriers	1405	2809	5617
Carrier modulation	QPSK, DQPSK, 16 QAM, 64 QAM		
Symbols per frame	204		
Symbol duration	252 $\mu s$	504 $\mu s$	1008 $\mu s$
IFFT length	2k	4k	8k
Guard interval	1/4, 1/8, 1/16, 1/32		
Inner code	Convolutional code (1/2, 2/3, 3/4, 5/6, 7/8)		
Outer code	Reed-Solomon (204,188)		

## 2.4 A Transmitter for DVB-T Broadcasting

In Section 2.1.1, the digital signal was channel coded and modulated into baseband. To be able to broadcast it soundly, it shall be fed to an RF transmitter that will up-convert it to a VHF/UHF channel used in the DVB-T transmission. Also, the transmitter must amplify the signal to a level that is required for good reception in the border of the reception area. In this section, the DVB-T transmitter is described. Basic schematic for the transmitter is in Figure 2.8.

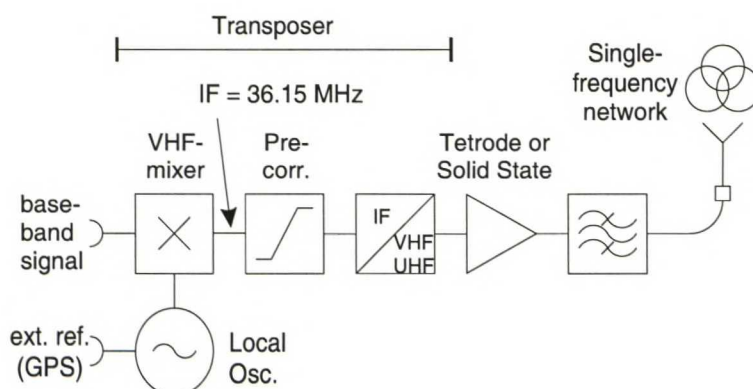
The baseband signal fed by the channel coder and modulator system, is converted into an intermediate (IF) frequency of 36.15 MHz by a VHF mixer. The VHF mixer is fed



by a local oscillator that is locked to an external reference signal (e.g. the GPS signal) so that the transmitting frequency in a single frequency network is constant.

The pre-correction of non-linearities in the transmitter, especially non-linearities in the high power amplifier block, is carried out at the IF frequency. The pre-corrected signal is then up-converted into an allocated broadcast channel at VHF/UHF band.

Before fed to a transmitter antenna, the signal is amplified in a tetrode or solid state high power amplifier. Out-of-band emissions produced during the amplification are suppressed in a channel filter.



**Figure 2.8:** Basic schematic of a DVB-T transmitter used in a synchronous single frequency network. Constant transmit frequency, throughout the system, is achieved by locking into an external common reference, e.g. the GPS. (edited from [9])

## 2.5 Technical Requirements for a DVB-T transmitter

A number of technical requirements are imposed on a DVB-T transmitter. These requirements are drawn from the fact that the transmission (of an OFDM symbol) in a single frequency network shall be made precisely at the same frequency, same time and symbols of one time slot shall not interfere with each other.

In this section a discussion about the importance of local oscillator (LO) specification and design is made. The primary concern, due to the nature of the experimental frequency converter, is nonetheless with the linearity requirements of the power amplifier. Also, to some extent, linearity requirements of filters are discussed.

### 2.5.1 Frequency Requirements

The first requirement of the congruent transmission frequency can be fulfilled by using an external reference frequency. The usage of the GPS signal for synchronization is one viable choice. The GPS signal is available world wide and has a high accuracy. The problem is that the GPS system is controlled by an outside operator, the U.S. government, so the accuracy of the GPS signal can be altered as they see fit. Another choice for frequency synchronization is to lock the transmitting frequency to a frequency recovered from the

transport stream data clock, but the result is dependent on the quality of radio link and clock recovery system. Also, the usage of a frequency standard (e.g. rubidium oscillator) would be possible, but it might be expensive and the standard must be calibrated annually [9]. On the contrary, it might be quite easy, and cheap, to apply rubidium standards to a DVB-T system, since rubidium clocks are used to provide a common time reference in modern analog broadcasting systems.

In the DVB-T specification [1] or implementation guidelines [19], the frequency stability requirement is not discussed. But, on a technical report about a microwave frequency DVB-T [20], it is mentioned that a commercial DVB-T receiver has typical automatic frequency control (AFC) range of  $\pm 70$  kHz, but most of this control range is required to compensate internal inaccuracies of the receiver.

The bit-synchronous transmission requirement can be fulfilled by using an external clock pulse. Again, the GPS is the prime candidate. Delays in radio links and in transmitter systems must also be taken into account. This requires a careful calculation of link geometry and measurement of transmitter systems. The fact that the reception range from a transmitter is finite will ease this task a bit.

In addition to the requirement of the oscillator to be frequency-stable, there is requirement that local oscillator (LO) shall have a low phase noise. This requirement arises from the fact that the OFDM has numerous close-spaced sub-carriers that are required to be orthogonal to each other. If the LO is too noisy, then when the frequency of an OFDM signal is converted, the phase noise of the LO will deteriorate the signal quality. Also, if too much attention is put to lower the phase noise near LO frequency, there is a possibility that the far frequency phase noise will deteriorate the signal quality as the total phase noise power will rise.

The use of a microwave frequency DVB-T transmitter is discussed in [20], and the following phase noise values in Table 2.5 are given as a ‘rough guide’ — these values were used in a number of different research projects. It seems that these values are not that difficult to achieve by using available microwave components when building the phase-locked voltage-controlled oscillator.

**Table 2.5:** *Recommended phase noise values for the LO in a microwave DVB-T system*

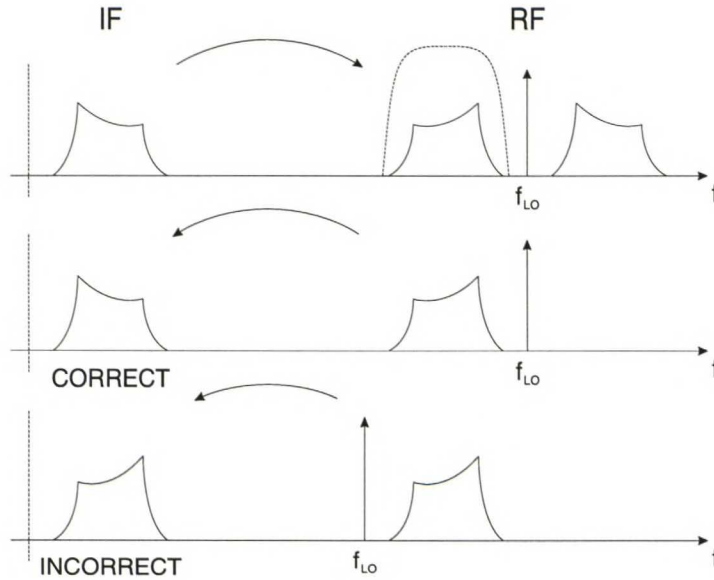
Frequency offset	Phase noise level
1 kHz	-65 dBc/Hz
10 kHz	-68 dBc/Hz
100 kHz	-86 dBc/Hz
1 MHz	-105 dBc/Hz

For the experimental frequency converter specified in this thesis, the frequency stability requirement is of a few orders of magnitude less severe than in a single frequency network. Therefore it can be achieved by using a phase-locked VCO as the local oscillator. But, an effort shall be made to keep the phase noise characteristic of the LO in the specifications, or even lower.



### 2.5.2 Frequency Translation Requirements

The frequency translation of an OFDM signal must be done using the same mixing sideband for both translations. A single translation causes the inversion of the signal handedness and the imaginary axis of the signal. If the translation process is repeated in the same manner, the resulting signal will comply with the original [20]. The proper frequency translation procedure, and incorrect, are demonstrated in Figure 2.9.



**Figure 2.9:** Illustration of proper up-conversion – down-conversion technique. Use of same mixing sideband is required in order to preserve correct handedness and complexity of the OFDM signal.

### 2.5.3 Linearity Requirements

Linearity of components, in particular of amplifiers, used in a DVB-T transmitter is of great importance. Noticing the fact that there are up to 6817 sub-carriers close to each other in one DVB-T channel, the intermodulation distortion (IMD) produced by non-linearities in the amplifier will lead to a degradation of the signal and will make the demodulation of the signal much more difficult.

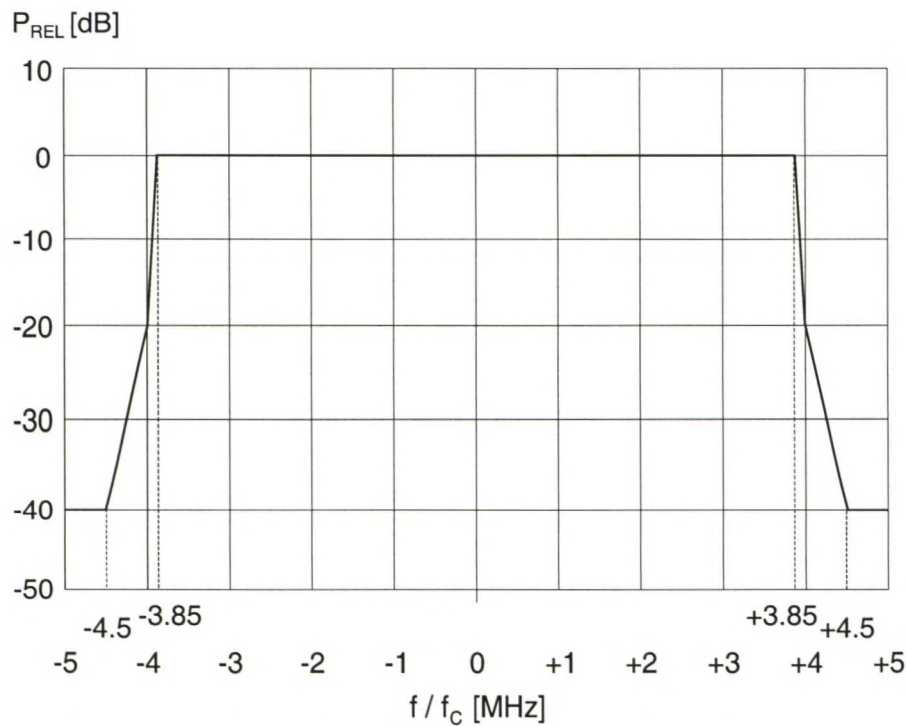
Also, harmonic and out-of-band signals produced in non-linear components, may interfere other transmissions. This is a problem especially in the beginning of the transition from the analog broadcasting to the digital, when the DVB-T signal is transmitted next to the analog TV signal, which is much more sensitive to outside interference than the DVB-T. So, in addition to linearization of the amplifier, the filtering of intermediate and output signals shall be carried out to keep the DVB-T signal within the required spectrum mask shown in Figure 2.10.

For the VHF/UHF band transmissions adjacent to analog television broadcasting, and for special critical cases, additional spectrum masks are given in [1].



There are many different techniques for amplifier linearization, starting from back-off to digital correction, and this subject is discussed more thoroughly in Chapter 3.

In filters, non-linearities occur in sense of a non-constant group delay as a function of frequency. This non-linearity will spread sub-carriers of a single OFDM symbol temporally, which can potentially hinder the interpretation of symbol values. This constant group delay requirement can be fulfilled with much less effort than the high linearity of a power amplifier — a careful selection of the filter design is required.



**Figure 2.10:** *Spectrum mask for spurious signals in a DVB-T broadcast, relative to the maximum signal power and the center frequency of the transmission channel. (edited from [9])*

# Chapter 3

## RF Amplifier Linearization

A long range transmitter requires a lot of power to broadcast the signal far enough. An RF amplifier is this required power source. Its purpose is to amplify the RF signal to a wanted power level. This output power requirement, and the fact that the power budget (the power efficiency) of the transmitter is of much concern in the broadcasting business, forces to drive as much output power as possible from the amplifier.

This high output power point is in more non-linear region of the amplifier. To prevent the non-linear behavior of the amplifier from degrading the quality of an RF signal (e.g. from causing the intermodulation distortion in the OFDM), the linearization of the amplifier shall be carried out by using some technique. In the DVB-T transmission, the linearity of the amplifier is of great importance, since the OFDM signal consists of multiple close spaced sub-carriers that are required to be orthogonal to each other.

In the following sections, a brief examination of some basic amplifier types is made. Then, the linearization techniques are discussed in theory. Finally, a method that could be used to linearize the power amplifier for the frequency converter is described. The most of the text written in this chapter concerning the DVB-T transmission is taken from [9], and the amplifier theory and linearization techniques are taken from [21]. If a more thorough discussion about amplifier linearization is needed, reader is advised to refer [21].

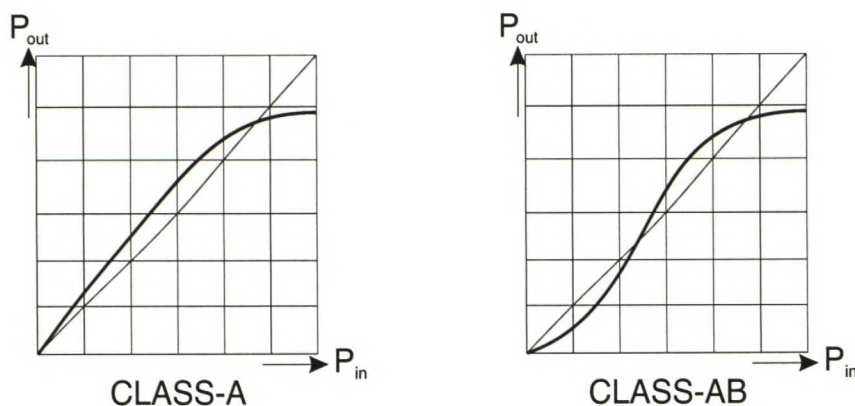
### 3.1 Basic RF Amplifier Types

Basic amplifier types used in the DVB-T broadcasting in the VHF/UHF frequencies are the tetrode amplifier, which is a class-A amplifier, and the solid-state amplifier which is a class-AB amplifier.

The class-A amplifier is the basic type of an amplifier. The operation point of the class-A amplifier is chosen such that the amplifier is in conducting state all the time. This leads to a very low efficiency (theoretical maximum of 50% [21]), but the amplifier has a very high degree of inherent linearity (>90% without correction [9]) and has soft limiting characteristics [9]. The input-output power response of a class-A amplifier is illustrated in Figure 3.1. The inherent linearity of the class-A amplifier can be used for the benefit of linearization, if the output power requirement is not greater issue than the purity of the amplified signal.

In a class-B amplifier, the operation point is chosen to be one or the other extreme of the amplifier operating range. Therefore the amplification takes place for a half a cycle, and the rest of the time the quiescent power is small. This leads to a much higher efficiency compared to a class-A amplifier. A single class-B amplifier would only conduct for half a cycle and therefore would produce significant amount of distortion. A much used configuration is so called push-pull configuration, where two class-B amplifiers are operated in anti-phase (i.e. each conducting for a separate half of the input waveform), for which the theoretical maximum efficiency of 78.5% can be achieved.

The class-AB amplifier is a compromise between the class-A amplifier and the class-B amplifier, the output signal is zero for the less than one-half of the signal period. The amplification response of a class-AB amplifier is illustrated in Figure 3.1. The distortion in a class-AB amplifier is greater than in a class-A amplifier, but the power efficiency is higher. The improvement in the linearity of the amplifier, in compromise of the poorer efficiency because of the biasing currents, is usually worth the sacrifice, so many designers prefer the class-AB amplifier over class-B [9]. As seen from Figure 3.1, the linearity of a class-AB amplifier is much lower than in a class-A. This would require much more elaborate techniques to be used when linearizing the amplifier.



**Figure 3.1:** Typical  $P_{out}(P_{in})$  response curves of a class-A (on left) and a class-AB (on right) RF amplifier. In the lower input power region, the class-A amplifier has an inherent linear behavior. The class-AB has a higher efficiency at the cost of a more nonlinear behaviour. (edited from [9])

Although in this thesis, the frequency converter is designed for a much higher frequency, and much lower output power, the classification of amplifier technologies presented here can be used to describe imperfections also in components of that frequency range and output power.

## 3.2 Amplifier Linearization Techniques

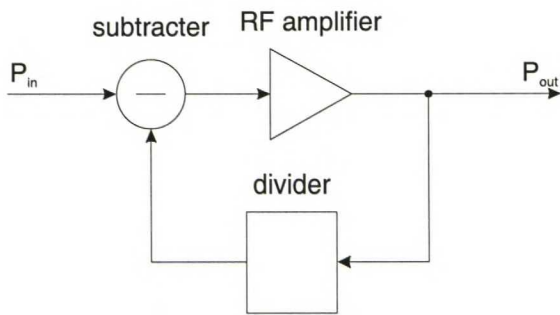
The benefits from linearizing the amplifier are obvious, the amount of distortion in the RF signal is lowered, the interference to other signals is reduced, and the RF amplifiers



output can be driven to a much higher level. So a number of techniques for amplifier linearization are developed. In this section linearization techniques of feedback, feedforward and predistortion are discussed in theory.

### 3.2.1 Feedback

One of the earliest and simplest method to reduce distortion in an amplifier is the feedback circuit, illustrated in Figure 3.2. The feedback circuit, in the simplest case, is a power divider. The subtracter derives an error signal from the input signal and the fed-back output signal. This error signal is then fed to the amplifier. If the amplifier gain is much higher than the feedback gain, the result is an output signal proportional to the gain of the feedback circuit. While the overall gain is lower than of the mere RF amplifier, the resulting system is much more reliable and stable against variations in the gain.



**Figure 3.2:** Schematic of a feedback linearization circuit used in an amplifier. As the result of feedback and subtraction, the output signal is a much more stable and reliable in gain. (edited from [21])

The feedback method was designed to reduce distortion in audio systems. When considering the RF amplification, the linearity requirement is much greater than in an audio system (e.g. 70 dB IMD in an RF system compared to 30–40 dB in the audio [21]). Also, the available gain in RF frequencies and required power levels are much harder to achieve, resulting much less gain benefit while lowering the distortion. Applying feedback to a multi-stage RF amplifier could cause instability, since the cycle times (the period of RF signal) are much shorter than in audio frequencies [21].

### 3.2.2 Feedforward

Feedforward method used in the RF frequencies has brought a number of successful applications in fields of military HF communication, satellite amplifiers and cellular radio systems (in base stations and also in mobile terminals) [21].

The basic operation of the feedforward circuit is illustrated in Figure 3.3, and can easily be described as follows:

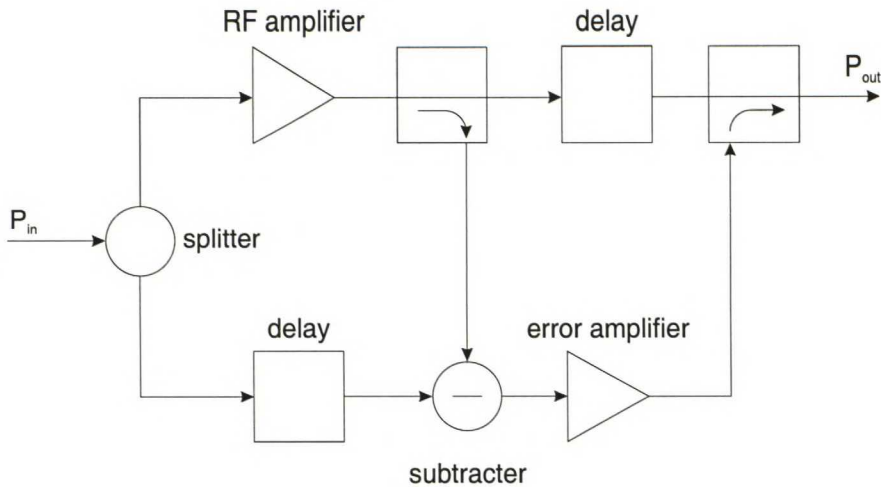
The input signal is split into two identical paths. On the upper path the signal is amplified in the main RF amplifier, and amplification causes distortion to the signal due non-linearities. A sample of the distorted signal is taken with a coupler, and the sample

and the delayed original signal are subtracted to create an error signal, which consists of distortion signals created in the main amplification.

The error signal is linearly amplified in an error amplifier, and is fed to the output coupler anti-phase to the time delayed main signal. This anti-phase summation cancels, reduces in most cases, the distortion in the output signal, while the desired signal is substantially amplified.

Greatest benefit in the feedforward method is that the whole gain of the RF amplifier can be used. Also, the correction is not based on past events, but is applied to the distortion in the current input signal, and it is possible to stack a number of feedforwarding loops to reach even higher level in the distortion correction. The feedforward loop is more fault tolerant (if one amplifier malfunctions, the result is only a degradation in the performance) than the feedback method (which fails totally when the divider malfunctions) [21].

The disadvantages comparing to the feedback method are that the circuit is much more complex, a very high degree of matching between components must be maintained, and the circuit has no compensation against effects of component aging or temperature changes [21].



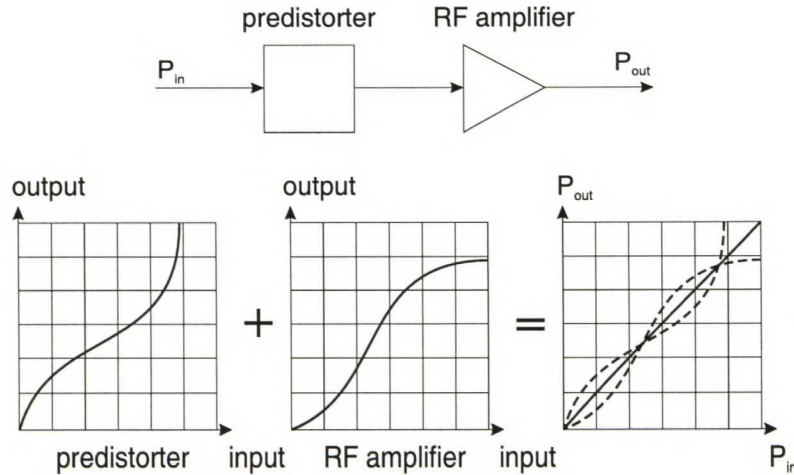
**Figure 3.3:** *Feedforward linearization method used in modern RF systems. As the result of an error signal creation and its anti-phase summation to the amplified signal, the distortion in the output signal is reduced and the gain of the RF amplifier can be fully utilized. (edited from [21])*

### 3.2.3 Predistortion

One possibility to linearize the RF amplifier is to use predistortion. In concept, the use of a predistorter is simple, as seen from Figure 3.4. The response curve of the predistorter is inverse to the RF amplifier response curve. When the two are cascade-connected, the input-output response of the system is linear and no distortion is generated.



As seen from Figure 3.4, the predistortion system does not have any kind of adaptation circuit (i.e. as in the feedback method, and in similar sense, in the feedforward) to adjust the linearization if the characteristics of the RF amplifier do change after installation. In more advanced systems, the adaptation is accomplished by sampling the output signal, and then correcting the predistortion by the use of look-up tables.



**Figure 3.4:** Schematic and response curve of an RF predistortion system. The predistorter is inverse to the RF amplifier response curve. Cascade-connected responses result a linear input to output response. (edited from [21])

Predistortion can be applied in either RF or IF frequencies, or in the baseband frequency. The methods used in RF and IF frequencies are similar, and the advantages and disadvantages are as follows [21]:

Implementation of a predistortion in the RF or IF frequency is simple and requires only a few components. Since the predistortion method does not use any kind of a loop structure, it is unconditionally stable. The technique can be easily applied also on higher frequencies, and the predistortion can be even applied to wide bandwidths (compared to the e.g. the feedforward correction).

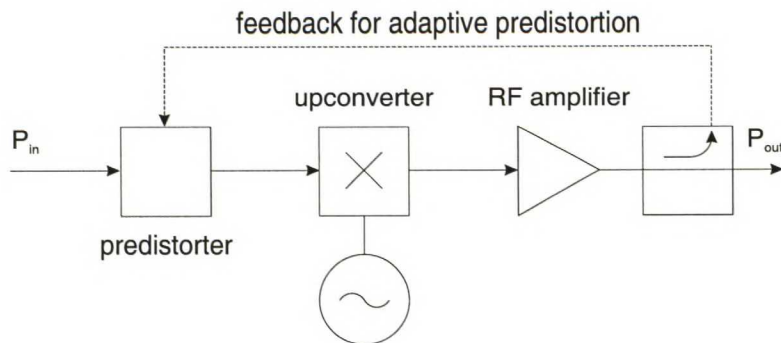
Only a modest improvement in linearization can be gained by using the RF or IF predistortion, comparing to the feedforward or more advanced feedback methods. The RF or IF predistortion has difficulties in reducing the higher orders of distortion. Also, the predistortion has an optimum performance region, so the performance suffers in other power levels.

In baseband frequencies, the possibility to use digital signal processing (DSP) as an engine for the predistortion has opened up new possibilities. The predistortion is applied to the baseband signal, where modelling of the non-linearities is simple to realize.

The lack of adaptation in predistortion circuits is relatively easy to overcome in the DSP, and is widely used in modern transmitters. The DSP can be used to cope with power amplifier and group delay (in output filter) non-linearities, as demonstrated in [22]. The predistortion DSP circuit can be reprogrammed by referencing the sampled output signal to a preprogrammed look-up table. The popularity of using the DSP in a predis-



torter is increasing in this day and age, since DSP processors are becoming progressively smaller, cheaper, and more power efficient. Also, the fact is that the baseband signal in a transmitter system is produced, more or less, in a DSP processor, so the basis for the DSP based predistortion already exists [21].



**Figure 3.5:** Schematic of the baseband predistortion method. The predistortion is applied to signal by using a DSP processor. The predistortion can be reprogrammed by comparing the sampled output signal with a look-up table. (edited from [21])

### 3.3 Linearization of the Frequency Converter

As it can be noted, the linearization of an RF amplifier is not a small task, and easily could be a subject to a study much broader than conducted in this thesis. Also, the linearization techniques described in this chapter are used to correct much more severe form of non-linearities than expected in the power amplifier used in the experimental frequency converter. So, a simple and attainable method to linearize the frequency converter shall be found.

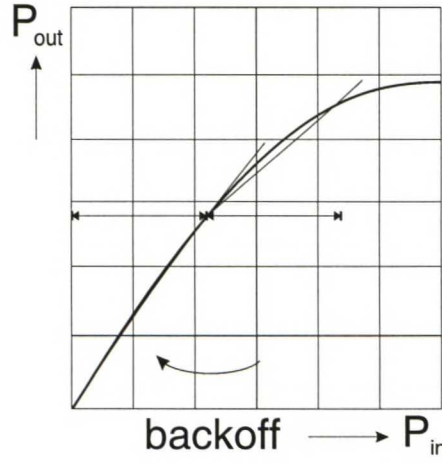
The required amplifier for the frequency converter is estimated to be a medium power range amplifier. Also, one can soundly assume that some antenna gain can be attained from the design. Thus, the requirement for amplifier output power can be further lowered. Since the linearity performance of the medium power amplifier should be similar to the class-A type of amplifiers, the inherit linearity of the power amplifier could be used and further linearity could be obtained through the use of backoff.

The use of backoff, e.g. backing down the input power of the RF amplifier, requires no additional components in the transmitter system if the input power is properly adjusted. In the backoff method, illustrated in Figure 3.6, the input power is translated to a much lower range that is also more linear than the higher power range. This method has been succesfully used in satellite communications to linearize the power amplifier stage. Also, backoff is used as a preliminary linearization for much advanced linearization techniques.

The disadvantage of the use of backoff is that it requires an overrated amplifier to be used, which also means that the system power efficiency will decrease. These disadvantages can be accepted since the frequency converter is implemented to a test environment

and the total power budget, or power costs of the whole system, is of small concern — compared to the distorted output signal which cannot be properly demodulated.

A remark shall be made that despite the discussion in this chapter about only linearizing the gain of an amplifier, the discussion also holds for the phase linearization of the amplifier, which is probably even more harder than the gain linearization. In this thesis, no effort is made to linearize the input power output phase relation. If the phase linearity, of a device, as the function of frequency is constant, the whole OFDM signal should phase-shift equivalently when the input power changes. Therefore, the whole signal diagram will rotate and no apparent distortion will happen.

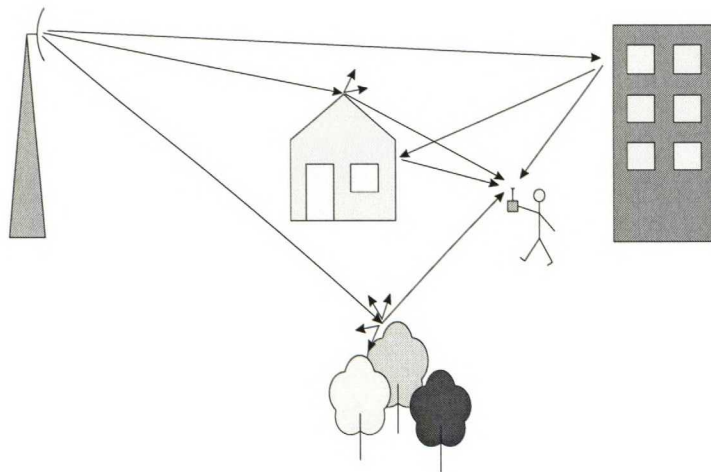


**Figure 3.6:** *The idea of an input power backoff, resulting a more linear region in the amplifier input–output response  $P_{out}(P_{in})$ . The translation of the operation point is carried out earlier in the transmitter system. (edited from [9])*

## Chapter 4

# Radio Wave Propagation

A typical situation when receiving a radio signal is illustrated in Figure 4.1. Most of the time the receiver is not in the line of sight from the transmitter, so the received signal is the sum of reflected, scattered and diffracted copies of the transmitted signal. Therefore it is hard, or even impossible, to model the exact propagation environment. A number of simple situations, e.g. 2-ray ground reflection and knife-edge diffraction, have been successfully modelled. But modelling of a more complex environment, like outdoors, is much more difficult. From experimental data a number of different models to calculate an average path loss are devised to overcome this problem. It is possible to statistically analyze a number of different situations using these experimental models.



**Figure 4.1:** *Illustration of a typical mobile radio propagation environment. Multiple echoes, with variable amplitudes and phases, add up in the receiver, which will result a fast-changing propagation environment.*

In the following sections, a picture of the modelling of radio wave propagation in a modern mobile radio system is given. First we give a short introduction to basic large-scale propagation models: free space propagation, plane-wave reflection, ground reflection, diffraction, and scattering. Using these basic propagation models and a number of field measurements, a widely used computational model for practical path loss calculations is



then introduced. To support this model, a brief review of recent results in propagation measurements near the frequency of 5.8 GHz is made. Finally, conclusions from this chapter are drawn, and an estimate for probable average path loss is presented to aid on defining specifications for the frequency converter.

## 4.1 Free Space Propagation

The free space propagation model can be used in a situation where there is a line-of-sight path between a transmitter and a receiver, and the receiver antenna is in the far-field region of the transmitter antenna. Also the first Fresnel-ellipsoid must be free of obstacles (see Section 4.4). The equation for the received power  $P_r$  is [23]:

$$P_r = G_t G_r \left( \frac{\lambda}{4\pi d} \right)^2 P_t, \quad (4.1)$$

where  $G_t$  is the gain of the transmitter antenna,  $G_r$  the gain of the receiving antenna,  $\lambda$  the wave length of a radio signal,  $d$  the distance between the transmitter antenna and the receiver antenna, and  $P_t$  is the output power of the transmitter.

Equation 4.1 shows that the received power decreases proportionally to the square of distance  $d$ . The radio wave is thought to originate from a point source and then to spread evenly on the spherical surface ( $4\pi d^2$ ). Directivities of antennas are accounted in gain terms  $G_t$  and  $G_r$ .

The far-field region, or the Fraunhofer region, is a distance where the dimensions of the transmitter antenna compared to the wave length of the radio signal are small enough. In other words, the radio wave can be approximated at that region, closely enough as a plane wave. In the literature, the distance for far-field region is given as [24]:

$$d_f = \frac{2D^2}{\lambda},$$

where  $D$  is the largest physical dimension of the transmitter antenna, and  $\lambda$  is the wave length. Additionally, criteria of  $d_f \gg D$  and  $d_f \gg \lambda$  must be satisfied.

## 4.2 Reflection

When a radio wave reaches a boundary between two electrically different media, part of it is reflected from the boundary and the rest propagates through the boundary. Reflections occur from the surface of the earth and from obstacles (e.g. buildings and walls). In most mobile communication cases the first medium is free space ( $\epsilon_1 = \epsilon_0$ ), and the permeabilities of media are equal ( $\mu_1 = \mu_2$ ). Thus, reflection coefficient for vertically  $\Gamma_{\parallel}$ , and horizontally  $\Gamma_{\perp}$ , polarized radio wave can be adapted from [23]:

$$\Gamma_{\parallel} = \frac{\sqrt{\epsilon_r - \sin^2 \Theta_i} - \epsilon_r \cos \Theta_i}{\sqrt{\epsilon_r - \sin^2 \Theta_i} + \epsilon_r \cos \Theta_i}, \quad (4.2)$$

and

$$\Gamma_{\perp} = \frac{\cos \Theta_i - \sqrt{\epsilon_r - \sin^2 \Theta_i}}{\cos \Theta_i + \sqrt{\epsilon_r - \sin^2 \Theta_i}}, \quad (4.3)$$

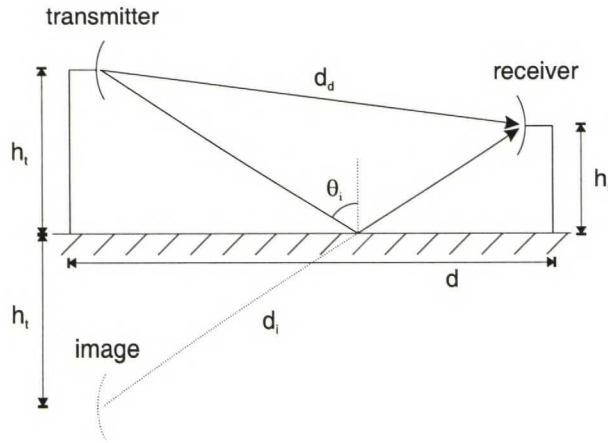
where  $\epsilon_r$  is the relative permittivity of the second medium, and  $\Theta_i$  is the angle of incidence between the incoming radio wave and the normal of the boundary between two media. An elliptically polarized wave can be broken into vertical and horizontal components. Notice that there are differences in literature [23],[24] as to how the angle of incidence  $\Theta_i$  is chosen — apparently it is common to choose different angle in electromagnetics and in telecommunication.

As the angle of incidence  $\Theta_i$  approaches  $90^\circ$ , we can notice from Equations 4.2 and 4.3 that  $\Gamma_{\parallel} \approx 1$  and  $\Gamma_{\perp} \approx -1$  regardless of the relative permittivity  $\epsilon_r$  of the second medium. This illustrates that the ground can be modelled as perfect reflector if the angle of incidence is close to  $90^\circ$  (i.e. a grazing angle).

### 4.3 Ground Reflection

Considering the environment in which mobile devices are used, the free space propagation model (equation 4.1) is in most cases insufficient. The single direct path between the transmitter and the receiver is seldom the only path for propagation.

A 2-ray ground reflection model, illustrated in Figure 4.2, has been shown to be reasonably accurate for predicting large-scale signal strength for mobile systems over distances of a few kilometers, and also in micro-cell channels in an urban environment.



**Figure 4.2:** Geometry in the 2-ray ground reflection model. The transmitter-receiver geometry is simplified by using the image source theory. (edited from [25])

For isotropic antennas, the path gain  $PG$  of the 2-ray model can be given as [25]:

$$PG = \left( \frac{\lambda}{4\pi} \right)^2 \left| \frac{e^{-jk d_d}}{d_d} + \Gamma(\Theta_i) \frac{e^{-jk d_i}}{d_i} \right|^2, \quad (4.4)$$

where  $k$  is the wave number of the radio wave,  $d_d$  the path length travelled along the line of sight,  $d_i$  is the path length travelled by the ground-reflected wave, and  $\Gamma$  is the

reflection coefficient described in Section 4.2. The distances  $d_d$  and  $d_i$  can be calculated as follows [25]:

$$d_{d,i} = \sqrt{d^2 + (h_t \mp h_r)^2}, \quad (4.5)$$

where  $h_t$  is the height of the transmitter antenna,  $h_r$  is the height of the receiver antenna, and the minus sign corresponds to  $d_d$  and the plus sign to  $d_i$ .

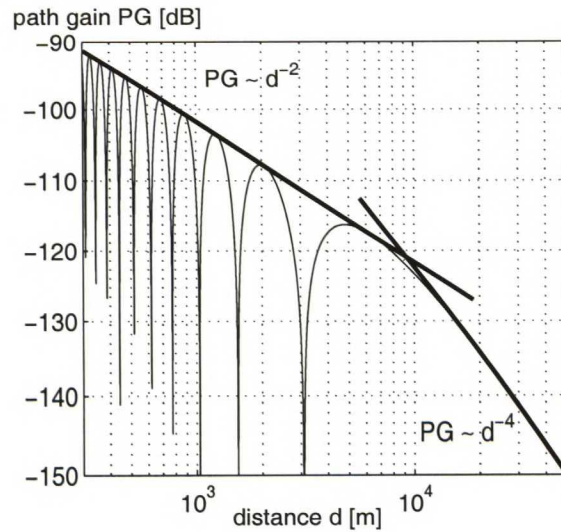
When the receiving antenna is far enough from the transmitting antenna the angle of incidence  $\Theta_i$  is nearly  $90^\circ$  and the reflection coefficients for both polarizations can be approximated as  $|\Gamma_{\parallel}| \approx 1$ ,  $|\Gamma_{\perp}| \approx 1$ . Also, assuming that  $d \gg h_t, h_r$ , the Equation 4.5 can be approximated as [25]:

$$d_{d,i} \approx d + \frac{h_t^2 + h_r^2}{2d} \mp \frac{h_t h_r}{d}$$

and the path-gain Equation 4.4 can be written [25]:

$$PG \approx 4 \left( \frac{\lambda}{4\pi d} \right)^2 \left| \sin \left( 2\pi \frac{h_t h_r}{\lambda d} \right) \right|^2 \quad (4.6)$$

As the distance  $d$  increases, the argument of the sine function decreases. This causes the minima and maxima seen in a typical distance response of the 2-ray model. The response is illustrated in Figure 4.3, for which the wavelength  $\lambda$  of 0.052 m, the transmitter height  $h_t$  of 50 m, and the receiver height  $h_r$  of 1.6 m were used.



**Figure 4.3:** Illustration of the 2-ray ground reflection response. The breakpoint distance  $R_{bp}$  can be easily identified, when the exponent of the path gain changes.

When the argument of the sine function reaches  $\pi/2$  the last maxima occurs, which is considered to be the breakpoint distance  $R_{bp}$  and can be evaluated using a relation [25]:

$$R_{bp} = \frac{4h_t h_r}{\lambda} \quad (4.7)$$



Beyond the breakpoint distance  $R_{bp}$  the argument of sine function can be thought to be small and thereby the sine function can be approximated by its argument. For distances  $d \gg R_{bp}$ , the path gain  $PG$  reduces to [25]:

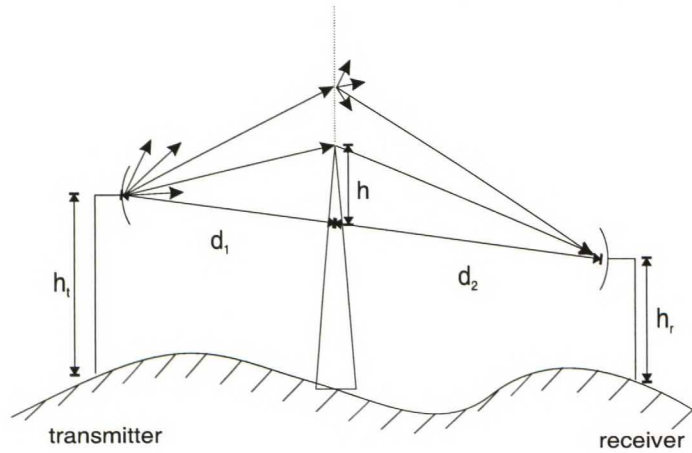
$$PG \approx \frac{h_t^2 h_r^2}{d^4} \quad (4.8)$$

Equation 4.8 indicates that the received power attenuates with distance raised to the fourth power, or 40 dB/decade. This is much faster than the 20 dB/decade in the free space attenuation. Also, at great distances the path attenuation is independent of the frequency of the radio signal.

## 4.4 Diffraction

When a radio wave reaches a sharp edge in a landscape or a round hill, it is possible to detect a faint trace of the signal in the shadow region of the obstacle. The detected signal in the shadowed region behind the edge (or hill) is due to the diffraction. Diffraction is easy to understand using the Huygen's principle. All points of the incident wavefront act as a point of origin for secondary waves. The phenomena of diffraction, the detected wavefront, is the result of the sum of these secondary wavefronts.

Consider the following Figure 4.4 where the free space between a transmitter and a receiver is obstructed by a sharp screen of infinite width. The screen has height  $h$  and is placed at distance  $d_1$  from the transmitter and  $d_2$  from the receiver.



**Figure 4.4:** Illustration of the knife-edge diffraction geometry. Wavefronts diffracted from the top of the obstruction are summed up at the receiver. (edited from [24])

A wave that propagates via the top of the screen has to travel through a longer path than the wave along the line-of-sight path. This difference is called excess path length  $d_\Delta$  and it can be shown that if  $h \ll d_1, d_2$  and  $h \gg \lambda$  [24]:

$$d_\Delta \approx \frac{h^2}{2} \frac{(d_1 + d_2)}{d_1 d_2}$$

The excess path length  $d_\Delta$  can also be measured as a phase difference:

$$\phi = \frac{2\pi d_\Delta}{\lambda} = \frac{2\pi h^2}{\lambda} \frac{(d_1 + d_2)}{2 d_1 d_2} \quad (4.9)$$

For diffraction gain calculations, Equation 4.9 is usually normalized as the Fresnel-Kirchhoff diffraction parameter  $v$ :

$$v = h \sqrt{\frac{2(d_1 + d_2)}{\lambda d_1 d_2}} \quad (4.10)$$

The reason for using this excess path length in diffraction gain (or loss) calculation is the Fresnel zones. These zones define ellipsoids around the transmitter and the receiver where the excess path length compared to direct line-of-sight is  $m \lambda/2$  ( $m$  is an integer). The field that passes through an odd numbered Fresnel zone contributes positively to the total field, and through an even numbered zone the contribution is negative. The approximation for radius of the  $m$ th Fresnel zone is [24] (when  $d_1, d_2 \gg r_m$ ):

$$r_m = \sqrt{\frac{m \lambda d_1 d_2}{d_1 + d_2}},$$

From this radius  $r_m$  it is easy to derive that diffraction gain is, in addition to the frequency, also dependent on the location of the obstacle. Thus, when the radio wave reaches the obstacle in its path, the field strength, or signal power, in the shadow region behind the obstacle can be calculated by summing all the points in Fresnel ellipsoids and by calculating the resulting field.

To estimate the effect of an one obstacle, a simplified model, called the knife-edge diffraction model, was derived. The obstacle is simplified to a horizontally infinite screen that has height  $h$  and an infinitesimal width. The knife-edge diffraction gain can be then calculated by a complex Fresnel integral using the Fresnel-Kirchhoff diffraction parameter  $v$  given in Equation 4.10 [24]:

$$F(v) = \frac{1+j}{2} \int_v^\infty e^{-j\pi t^2/2} dt$$

The above function can be calculated by computer, but is commonly evaluated using approximation formulas, e.g. in [26]:  $F(v) \approx 0.452 [\sqrt{(v-0.1)^2 + 1} - (v-0.1)]$  for  $v > -1$ , or by using set of diagrams and tables.

In the case of multiple knife-edge diffractions, numerous different simplifications have been mentioned in the literature. There are two distinctive ways to approach this problem: try to merge the number of obstacles to one (problem: often gives an over optimistic answer or works only with two obstacles), or find the obstacle that has the largest diffraction loss, use it as a secondary source, calculate the diffraction gains of all secondary links and finally sum them all up (problem: works well if there are a few obstacles and not too close to each other. Also in a situation where there is one dominant obstacle, this method gives a good estimate). The latter method is known as the method of Myyryläinen [26].

Comparing the knife-edge model with a real life situation, one can easily deduce that there are not that many sharp hills or obstacles. The model gives too optimistic values for round hills, but it can still be used as a good estimate.



## 4.5 Scattering

In the mobile radio environment, the received signal is often stronger than the reflection and diffraction models predict. This is due to the scattering of radio waves from surfaces or objects (e.g. trees, cars, or lamp posts) in the vicinity of the receiver. Scattering spreads out (diffuses) the energy of the radio wave in all directions, so even objects further away from the receiver can add to the received signal strength or weaken it depending on the phase difference of signals at the receiver antenna.

Modelling the scattering from a reflective surface is done using so-called Rayleigh criterion which defines whether the surface is rough or smooth [27]:

$$h_c = \frac{\lambda}{8 \cos \Theta_i},$$

where  $h_c$  defines the critical height of surface protuberances for given wave length  $\lambda$ , and  $\Theta_i$  is the angle of incidence as defined in Figure 4.2.

If the protuberance of a reflective surface is greater than  $h_c$ , the surface is rough. Thus, a scattering loss factor  $\rho_s$  shall be included in the calculated reflection coefficient  $\Gamma$  [27]:

$$\Gamma_{\text{rough}} = \rho_s \Gamma$$

$$\rho_s = \exp \left[ -8 \left( \frac{\pi \sigma_h \cos \Theta_i}{\lambda} \right)^2 \right] I_0 \left[ 8 \left( \frac{\pi \sigma_h \cos \Theta_i}{\lambda} \right)^2 \right],$$

where  $\sigma_h$  is the standard deviation for surface height about the mean surface height, and  $I_0$  is modified Bessel function of the first kind and of zero order.

A remark about the equation above: As far as this work is able to deduce, there might be an error in the same formula in [24]. It appears that a simple typing error has occurred. It should read  $\lambda$  instead of  $l$ . Also, while comparing [24] and [27], the use of different incidence angles and trigonometric functions causes a bit of a confusion.

Scattering from an area consisting of a large object (e.g. a row of buildings) or a number of small objects can also be modelled using their radar cross section (RCS). The radar cross section of an object (or an area) is defined as the ratio of power density scattered in the direction of the receiver to power density incident upon the object (or area) from the transmitter. By knowing the RCS of an object, received power at the receiver can be calculated using the bi-static radar equation which can be easily modified from the mono-static counterpart in [28]:

$$P_r = G_r G_t A_R \frac{\lambda^2}{4\pi} \frac{1}{4\pi d_t^2} \frac{1}{4\pi d_r^2} P_t, \quad (4.11)$$

where  $G_r$  and  $G_t$  are the receiver and transmitter antenna gains towards the scatterer,  $A_R$  is the RCS of the scatterer,  $d_r$  and  $d_t$  are the distances from the receiver and the transmitter antenna to the scatterer.



## 4.6 Okumura Model

While, to some extent, it would be possible to calculate the field strength using models described earlier, required computing resources would be enormous even in if a small area would be modelled. So, most of the radio propagation models are derived using empirical methods combined with analytical calculations.

The benefit of empirically derived models is that they take into account all propagation parameters, known and unknown. The problem comes with the fact that models are constrained to measurement conditions: to frequency in use, and to the type of surroundings that the measurements were made in. So a lot of measurements are required to model all conditions and frequencies in which mobile communication systems are used. During past years some classical propagation models have emerged that are nowadays used in mobile communication system design.

One of the most widely used models for predicting signal strength in an urban environment is the Okumura model. The model is based only on extensive measurements made in Japan and does not provide any analytical explanation. It is usable for a frequency range of 150 – 1920 MHz (commonly extrapolated up to 3000 MHz, in belief that the set of diagrams behave smoothly), distances from 1 km to 100 km, and base station antenna heights ranging from 30 m to 1000 m. The model can be expressed as an equation [24]:

$$L_{50}(dB) = L_{fsp} + A_{mu}(f, d) - G(h_t) - G(h_r) - G_{area}, \quad (4.12)$$

where  $L_{50}$  is the median path loss (in dB),  $L_{fsp}$  is the free space path loss (given by Equation 4.1),  $A_{mu}$  is the median attenuation relative to free space,  $G(h_t)$  and  $G(h_r)$  are the transmitter and receiver antenna gains due their height (independent of their radiation patterns), and  $G_{area}$  is the environmental gain.

Parameters  $A_{mu}$  and  $G_{area}$  are given in numerous plots for different types of areas.  $G(h_t)$  and  $G(h_r)$  can be calculated using formulas derived by Okumura. The correctness of the Okumura model was further enhanced by numerous other Okumura curves relating to mixed land-sea parameters, average slope of the terrain etc.

From the Okumura model, an equation called Hata model was derived. The Hata model is valid for a frequency range from 150 MHz to 1500 MHz, and gives good results if the distance between base station and mobile receiver is greater than 1 km. To extend the frequency range a COST-231 (a working committee under European Co-operative for Scientific and Technical research) extension was made for frequencies 1500 – 2000 MHz.

## 4.7 Log-distance Path Loss Model

A much used model, called the log-distance path loss model can be derived from the free space path loss shown in Equation 4.1. Instead of using an exponent of 2 in distance term  $d$ , the log-distance path loss model uses an exponent of  $n$ , which is chosen according to the propagation environment (surrounding terrain) in which the mobile communication device is in. Also, instead of the path loss, an average of all possible path losses  $\overline{PL}$  at the given distance  $d$  is the result obtained from this formula [24]:

$$\overline{PL}(d) \propto \left( \frac{d}{d_0} \right)^n$$

or

$$\overline{PL}(dB) = \overline{PL}(d_0) + 10 n \log \left( \frac{d}{d_0} \right), \quad (4.13)$$

where  $n$  is the path-loss exponent,  $d_0$  is the reference distance for the chosen (measured)  $n$ , and  $d$  is the distance between transmitter and receiver antennas.

The reference distance  $d_0$  is, basically, a free variable — as far as this thesis can deduce there is no standardization completed for  $d_0$ . A number of publications, e.g. [29], seems to suggest that the reference distance  $d_0$  is chosen as follows : 1 km for large cells, 100 m for microcells, and 1 m for indoor channels.

Typical path-loss exponents  $n$  can be obtained from literature and are listed in Table 4.1 [24]. It is uncertain for which frequencies are these values represent.

**Table 4.1:** *Path-loss exponents for different environments*

Environment	Path-loss exponent, $n$
Free space	2
Urban area cellular radio	2.7 – 3.5
Shadowed urban cellular radio	3 – 5
In building line-of-sight	1.6 – 1.8
Obstructed in building	4 – 6
Obstructed in factories	2 – 3

For line-of-sight situations the log-distance path model also includes an another parameter called the breakpoint distance  $R_{bp}$ , which was briefly described in Section 4.3. It defines the distance at which the exponent  $n$  of the log-distance path loss model changes to a larger number due to changes in the propagation geometry. During recent studies measured breakpoint distances were found to be closer than predicted by Equation 4.7. It seemed that pedestrians and vehicles in the street environment caused the ground level (road height) to effectively rise [30]. The revised value for the breakpoint distance  $R_{bp}$  is given by [31]:

$$R_{bp} = 4 \frac{(h_t - h_s)(h_r - h_s)}{\lambda}, \quad (4.14)$$

where  $h_s$  is the effective road height due to e.g. vehicles and pedestrians. A value for  $h_s$  can be acquired from [31]. If  $h_r \leq h_s$  no breakpoint exists.

Various propagation environments at the distance  $d$  from the transmitter can differ from each other. Parameter to cover these different environments, or random shadowing effects, must be added to Equation 4.13. The parameter was named log-normal shadowing parameter  $X_\sigma$ , which is zero-mean Gaussian distributed in decibels with a standard deviation of  $\sigma$ , also in dB. The log-normal shadowing parameter  $X_\sigma$  can be calculated from the measurements, in same the environment and at the same distance, using linear regression. Also this parameter can be used for statistical analysis: a long-time probability that the signal strength is above the wanted level in the coverage area.

Even though in this thesis the indoor propagation of radio waves is not particularly discussed, a brief remark shall be made that according to recent studies, the indoor path



loss seems to obey the log-distance law in Equation 4.13. The effect of the receiver and the transmitter being on different floors can be accounted with an additional floor attenuation factor.

## 4.8 Radio Wave Propagation Measurements

In the recent years most of the research in the field of radio wave propagation has been in frequencies far below 5 GHz due commercial interests. Nowadays the interest has been risen in the field of wireless local area networks and so-called fourth generation mobile devices. A number of studies in this area have surfaced, but there is one problem when comparing them: national allocations of the radio spectrum. Frequencies studied in the United States are near 5.85 GHz, while in Europe the studies are made near 5.3 GHz. In Japan most interest has been frequency bands near 3.35, 8.45 and 15.75 GHz. In this thesis the main area of interest is in outdoor propagation models, and recent studies in that particular area are now examined, and are combined in Table 4.2.

**Table 4.2:** *The measured path-loss exponents  $n$  from different campaigns*

Type of Area	Frequency	Path-loss exponent, $n$	
		LOS	NLOS
residential	5.8 GHz	2.0	3.5
residential	5.85 GHz	— 2.9 —	
urban( $h_t=4$ m)	5.3 GHz	1.3	2.8
urban( $h_t=12$ m)	5.3 GHz	2.5	4.5
urban( $h_t=45$ m)	5.3 GHz	3.5	5.8
suburban	5.3 GHz	2.5	3.4
rural	5.3 GHz	3.3	5.9
urban( $h_r=1.6$ m)	3.35 GHz	3.0	
urban( $h_r=2.7$ m)	3.35 GHz	3.3	
urban( $h_r=1.6$ m)	8.45 GHz	3.4	
urban( $h_r=2.7$ m)	8.45 GHz	2.7	
urban( $h_r=1.6$ m)	15.75 GHz	3.2	
urban( $h_r=2.7$ m)	15.75 GHz	2.1	
urban( $h_t=10$ m)	3.35 GHz	5.3	13.0
urban( $h_t=55$ m)	3.35 GHz	3.4	5.1
urban( $h_t=10$ m)	8.45 GHz	4.3	14.0
urban( $h_t=55$ m)	8.45 GHz	3.3	4.4
urban( $h_t=10$ m)	15.75 GHz	5.2	12.7
urban( $h_t=55$ m)	15.75 GHz	3.1	4.5



### 4.8.1 The United States

In the U.S. a measurement campaign was made by T. Schwengler et al. [32] at a frequency of 5.8 GHz, base station (transmitter) height  $h_t$  of 30 ft. (9.1 m) and within a range of 2 km. Surroundings were a newly built residential area, absent of large trees. A path-loss exponent  $n$  of 2.0 for line-of-sight (LOS) situations and 3.5 for non-line-of-sight (NLOS) situation was calculated.

Also, a campaign was completed by G. Durgin et al. [5]. The used frequency was 5.85 GHz with a transmitter height  $h_t$  of 5.5 m. The measurement range was 150–210 m in a residential area. An outdoor path-loss exponent  $n$  of 2.9 was calculated. Also, a number of shadowing values for trees (11–16 dB) and buildings (15–21 dB) were measured. Apparently the outdoor path-loss exponent  $n$  measured here does not make any distinction between LOS and NLOS situations.

### 4.8.2 Europe

In Finland, an outdoor propagation characteristic measurement campaign was conducted by J. Kivinen et al. in Helsinki University of Technology (HUT) Radio Laboratory in co-operation with Nokia Research Center. Measurements were made using the radio channel sounder developed in Institute of Radio Communications (IRC) under the supervision of professor Pertti Vainikainen in HUT Radio Laboratory. The sounder is described in [33],[34]. The results of the measurement campaign were published in [6], and are now briefly reviewed.

The measurement campaign, at the frequency of 5.3 GHz, consisted three different environments: urban, suburban, and rural in the vicinity of Helsinki. Also three different transmitter heights  $h_t$  were used. The receiver antenna height  $h_r$  was 2.5 m for urban and suburban measurements, and 2 m for rural measurements. The distance covered in measurements were in a range of 30–300 m.

For urban measurements transmitter antenna heights  $h_t$  of 4, 12, and 45 m were used. Calculated path-loss exponents  $n$  were respectively 1.3, 2.5, and 3.5 for LOS situations. For NLOS situations exponents  $n$  were 2.8, 4.5, and 5.8.

In rural environments, a transmitter height  $h_t$  of 55 m was used. Derived path-loss exponents  $n$  were 3.3 for LOS situation and 5.9 for NLOS.

From suburban measurements, path-loss exponents  $n$  of 2.5 (LOS) and 3.4 (NLOS) were calculated. Transmitter antenna height  $h_t$  of 5 m was used in the LOS measurement and  $h_t$  of 12 m were used in the NLOS measurement.

Standard deviations  $\sigma$  of the log-normal shadowing parameter  $X_\sigma$  were in a range of 1.9 to 4.9 dB.

### 4.8.3 Japan

Due to the spectrum allocations, interest in propagation measurements in Japan are on other frequencies than in the U.S. or in Europe. Measurements are mainly made at frequencies of 3.35, 8.45, and 15.75 GHz.

In Tokyo a measurement campaign was devised by H. Masui et al. [30]. Measurements were made in a high-rise (10- to 15-story buildings) urban LOS environment with

a transmitting (base station) antenna height  $h_t$  of 4 meters and receiving antenna heights  $h_r$  of 2.7 m and 1.6 m. The range of measurements was 20 m – 1 km. Resulting path-loss exponents  $n$  calculated for 3.35 GHz were 3.3 ( $h_r = 2.7$  m) and 3.0 ( $h_r = 1.6$  m), for 8.45 GHz 2.7 and 3.4, and for 15.75 GHz 2.1 and 3.2, respectively.

Another campaign was made by K. Sakawa et al. in Yokosuka, Japan [35]. Measurements were made in an urban area, using two different transmitter antenna heights  $h_t$  of 55 m and 10 m, and frequencies mentioned above. The receiver antenna height  $h_r$  was 2.7 meters. The measured distance range was from about 150 m to 800 m, divided to LOS section and NLOS section.

For the LOS situation, the calculated path-loss exponents  $n$  were: for 3.35 GHz 5.3 ( $h_t = 10$  m) and 3.4 ( $h_t = 55$  m), for 8.45 GHz 4.3 and 3.3, and for 15.75 GHz 5.2 and 3.1, respectively.

The NLOS section of measurement started at 600 m and was perpendicular for LOS section. Calculated path-loss exponents  $n$  were 13.0 ( $h_t = 10$  m) and 5.1 ( $h_t = 55$  m) for 3.35 GHz. For 8.45 GHz 14.0 and 4.4, and for 15.75 GHz 12.7 and 4.5.

## 4.9 Estimating Propagation Losses

Using path-loss exponents from previous sections, it is possible to draw a diagram of path-losses for different environments. First, an appropriate reference distance must be chosen. The intended area of reception is from 500 m to 1500 m, so a reference distance  $d_0$  of 100 m seems to be the valid choice, noticing the discussion in Section 4.7. At least, at the distance of 100 m the signal should still be in free space, compared to the choice of 1 km.

The signal will propagate the first 100 meters in free space. After that it will traverse in various surroundings that are covered with the log-distance path loss model and respective path-loss exponents  $n$ . The free-space losses can be calculated using Equation 4.1 and log-distance path losses are calculated from Equation 4.13, with  $d_0 = 100$  m, in the range of 100 – 5000 m. For calculations, the frequency of 6 GHz was used. Therefore, the wave length  $\lambda$  is about 0.05 m.

Since the transmitter antenna is intended to be installed in a water tower, the transmitter has a height  $h_t \approx 50$  m. The mobile handset receiver has an antenna height  $h_r \approx 1$  m. Using the Equation 4.14 and effective road height  $h_s = 0.43$  m [31], a breakpoint distance  $R_{bp}$  of 2260 m can be derived, which is far further than the maximum expected reception distance of 1500 m. Thus, no breakpoint will exist in the path-loss diagram.

The exponents  $n$  are chosen as follows:  $n = 2.5$  is the value for the suburban LOS-environment, which was measured in Finland.  $n = 3.5$  is a good approximation for the suburban NLOS situation, as well as the urban LOS situation in Finland. The values  $n = 4.5$  and  $n = 5.5$  are lower and upper estimates from different urban NLOS measurements in Finland and in Japan. The set of different  $n$  curves are presented in Figure 4.5.

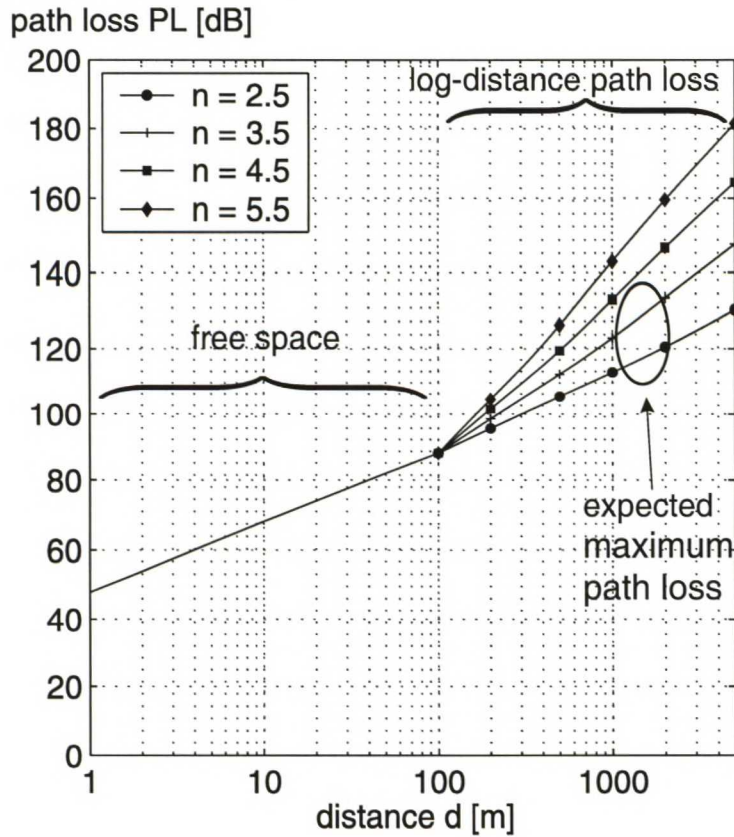
To get an estimate for the path loss in Otaniemi area, the exponent  $n$  in range of 2.5–3.5 seems to be a good starting point for link budget calculation. Buildings in Otaniemi are about 2–5 stories high (opposed to buildings in an urban area that are 5–10 stories high) and the area is not very densely built (e.g. as in mid-town Helsinki). Also, the path-



loss exponent  $n$  decreases considerably (i.e. in order of 2 units in LOS, and 10 units in NLOS situations), when the transmission antenna is raised from 10 meters to 55 meters, as seen from the measurements made in Japan (Section 4.8.3), so a value for exponent  $n$  of 3.5–4.5 seems to be too high.

Thus, from Figure 4.5, a total path-loss of 117–130 dB can be estimated for the link budget calculation.

Considering the radio wave propagation environment in the Otaniemi area, it seems that the signal is mostly received in an NLOS situation, but there are some locations where strong LOS signals are also received. Therefore, the receiver should have a wide dynamic range, when the receiver shifts from an NLOS to a LOS environment. The NLOS propagation environment constrains the type of antennas to be used in the system. The transmitting antenna should be a beam antenna and half-power beam widths should cover the whole Otaniemi area. The receiving antenna on the other hand should be omnidirectional in order to receive as much as possible of all multi-path signals.



**Figure 4.5:** Calculated path losses for exponents  $n = 2.5, 3.5, 4.5$  and  $5.5$ . These exponents represent the different propagation environments, from suburban LOS to high-rise urban city NLOS. Signals propagate the first 100 meters in free space.



## Chapter 5

# The System Environment

One of the fundamental concepts in this thesis was to install the frequency converter as a part of a DVB-T transmitter in operation. This way, the whole implementation process could focus on the frequency converter and could be completed in much shorter time.

In the vicinity of the Helsinki University of the Technology (HUT), the Technical Research Centre of Finland (VTT) had acquired a test permission to broadcast a DVB-T signal in July 2002. This was permitted for studying the digital television broadcasting and the possible use of the DVB-T technology as an aid in education [36]. This research project was named ‘OtaDigi’, and is cooperated with HUT, Otaverkko Oy (an IT company founded by HUT) and the Student Union of HUT [7]. The ‘OtaDigi’ transmitter for its nearby location, and the fact that it is a research project between VTT and HUT, is a good implementation point for the frequency converter proposed in this thesis.

For the intended reception area of the up-converted signal, the campus area of HUT was chosen. This area is the small cape in eastern part of the municipality of Espoo, where VTT and HUT are located. Also, dormitories of the Student Union of HUT are located in this area.

In the following section, the ‘OtaDigi’ project is reviewed. Then, the intended reception area is described, and beam widths for the antenna of the frequency converter are derived. Also, the transmission frequency of the up-converted signal is chosen. For the link budget calculation, and upcoming field-tests, also a test receiver must be devised. Finally, the link budget calculation for the required (minimum) transmission power is completed.

### 5.1 The OtaDigi Project

In July 2002, the Technical Research Centre of Finland (VTT) acquired a permission to broadcast a DVB-T signal in Otaniemi surroundings, in the municipality of Espoo, Finland. This permission was granted to research the use of the DVB-T technology and to develop it as a tool for education. Also, research efforts are directed towards value added services, copyright issues covering the DVB-T broadcasting, and development of production, broadcasting and reception terminals for the DVB-T technology. Research projects are done in cooperation with HUT, Otaverkko Oy (an IT company founded by HUT) and the Student Union of HUT [36]. The cooperative was named the ‘OtaDigi’ [7].

The ‘OtaDigi’ transmitter is located near the VTT Information Technology premises, pointed out in Figure 5.1, in the southern part of Otaniemi. The broadcasting system is a simple rack-setup, where the MPEG-2 coder, the baseband system and the RF transmitter are located in one man-sized cabinet. The RF transmitter and transmit antenna, an omnidirectional dipole, are connected using a semi-rigid cable. The DVB-T and transmission parameters of the ‘OtaDigi’ transmitter are summarized in Table 5.1.

**Table 5.1:** *Transmission parameters used in the ‘OtaDigi’ transmitter [37]*

Parameter	OtaDigi DVB-T transmitter
Location	Otaniemi, Espoo
Coordinates	24E39’31" / 60N10’52"
Channel/frequency	55 / 746 MHz
Channel bandwidth	8 MHz
RF transmitting power	55 W
Power in antenna port	40 W
Transmitter antenna	dipole
Polarization	vertical or horizontal
Modulation	16QAM
FFT length	8k
Guard interval	1/4
Code rate	2/3

The best transmitting location in Otaniemi area, especially for broadcasting purposes, is at the top of the Otaniemi water tower, location indicated in Figure 5.1. The water tower, coordinates ca. 24E49’11.4" / 60N10’52.5", is about 55 meters tall [38] and is located ca. 27 meters above the sea-level [39]. Therefore, it is the ideal place to install the ‘OtaDigi’ transmitter, regarding the fact that the reception area of the ‘OtaDigi’ transmitter is Otaniemi and its surrounding region.

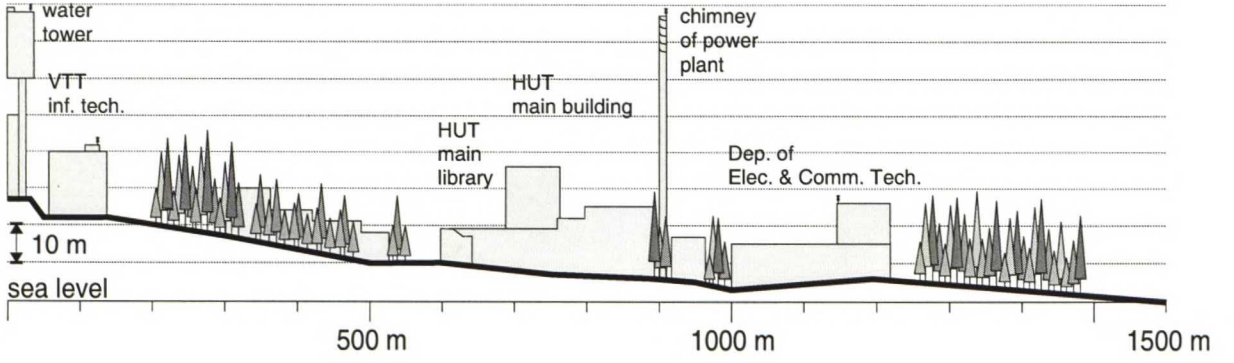
In the beginning of this thesis, this — rather naive — assumption was made about the location of the ‘OtaDigi’ transmitter. It was proven wrong. The actual location of the transmitter is at the top of the VTT Information Technology building. The hindrances of this true location are discussed at the end of this chapter, in Section 5.6.

Regardless of the actual location of the ‘OtaDigi’ transmitter, the experimental frequency converter is designed in the pursue of objective that it will be installed on top of the water tower, since it is the only feasible location for a microwave transmitter that would cover the designated reception area. Also, an alternative configuration is examined, in case the frequency converter can not be installed on the water tower location.

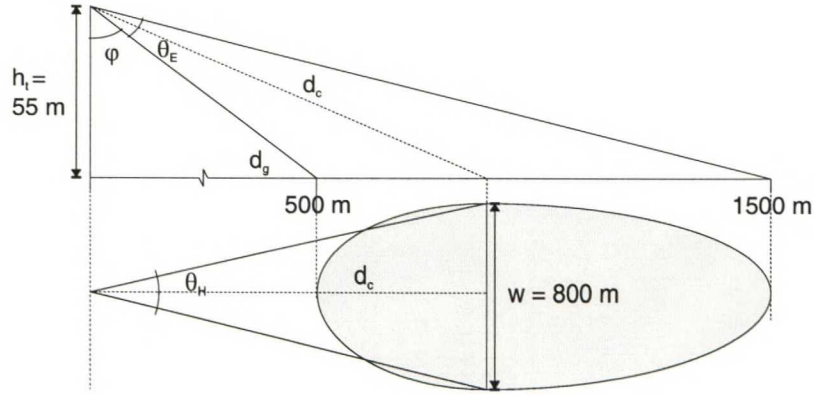








**Figure 5.2:** Illustration of the surface contour in the Otaniemi area. On the left side of the figure, the Otaniemi water tower and the VTT information technology building are located. Also, other feasible locations for the frequency converter are marked with small antennas, these are discussed in Section 5.6.



**Figure 5.3:** Geometry of the reception area. The antenna is located on the top of the Otaniemi water tower ( $h_t = 55$  m). The front edge of the reception area is the library of HUT (the 500 m mark) and the trailing edge is on the tip of the cape of Otaniemi (the 1500 m mark). The width of the reception area (800 m) was estimated from the reception area ellipsoid.

$$\begin{aligned}\varphi &= \arctan\left(\frac{500 \text{ m}}{55 \text{ m}}\right) = 83.7^\circ \\ \varphi + \theta_E &= \arctan\left(\frac{1500 \text{ m}}{55 \text{ m}}\right) = 87.9^\circ \\ \Rightarrow \theta_E &= 87.9^\circ - 83.7^\circ = 4.2^\circ \approx 5^\circ\end{aligned}$$

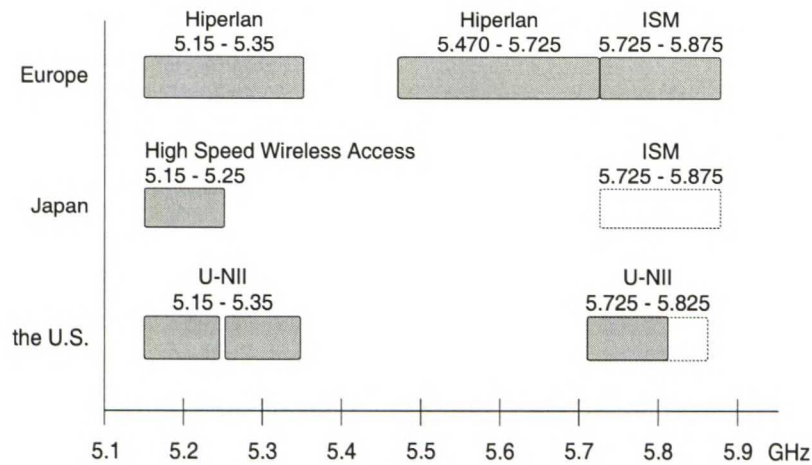
$$\begin{aligned}
d_g &= 55 \text{ m} \cdot \tan(\varphi + \theta_E/2) = 748.9 \text{ m} \\
d_c &= \sqrt{d_g^2 + (55 \text{ m})^2} = 750.9 \text{ m} \\
\Rightarrow \theta_H &= 2 \arctan\left(\frac{800 \text{ m}/2}{d_c}\right) = 56.1^\circ \approx 60^\circ
\end{aligned}$$

From these antenna beam widths  $\theta_E$  and  $\theta_H$ , the antenna gain can be calculated. This gain can be used in the link budget calculation later in this chapter. Also, antenna dimensions can be derived from these beam widths when the design of the frequency converter is underway.

### 5.3 Transmit Frequency

In this thesis, the frequency converter is developed to study the possible use of a mobile handset as a receiver for a digital television broadcast. Also in this day and age, there is movement towards integrating a mobile telephone and a wireless LAN terminal. By selecting a considerably higher frequency compared to modern mobile phone systems, it might be possible to enhance the signal reception. Since this frequency converter should be implemented in relatively short time span, it would seem to be in order to choose the transmit frequency so that commercial off-the-shelf components could be used in the implementation as much as possible.

From these criteria, the selected transmit frequency should be in range of 5 – 6 GHz. As seen from Figure 5.4, a number of allocations for the future high-performance Wireless LAN in the 5–6 GHz band, designated the U-NII or IEEE 802.11a [3] in the U.S. and the HiperLAN/2 [40] in Europe. These standards use the OFDM as their modulation technique, thus commercial RF components with high linearity requirements are going to be introduced, or are already manufactured, for the 5–6 GHz frequency range.



**Figure 5.4:** Frequency allocations in the 5–6 GHz range. If the 5.8 GHz ISM band is chosen as the transmit band, the availability of commercial off-the-shelf components will help the implementation of the experimental frequency converter. (edited from [4])

Parameters for the physical layer of HiperLAN/2 are summarized in Table 5.2. Comparing these against parameters of the DVB-T transmission in Table 2.1, it can be seen that technical requirements for a HiperLAN/2 transmitter are much more lower than for a DVB-T transmitter. The HiperLAN/2 uses OFDM, but also relies on the fact that short symbol duration (wider transmission bandwidth) increases the bit rate. Also, from the specification [40], it can be noticed that the transmit power spectrum is allowed to overlap adjacent channels, and the shoulder attenuation are much more lower than required for the DVB-T. Therefore, linearity of commercial off-the-shelf HiperLAN/2 components might not be as high as in specialized DVB-T components — but is better than nothing, and will cost less.

**Table 5.2:** *Transmission parameters in the HiperLAN/2 standard [40], [41]*

Channel Spacing	20 MHz
FFT size	64
Number of sub-carriers	52 (48 data, 4 pilots)
Sub-carrier spacing	0.3125 MHz (312.5 kHz)
Sub-carrier modulation	BPSK, QPSK, 16QAM (, and 64QAM)
Forward error correction	1/2, (9/16 and 3/4 using code puncturing)
Symbol interval	4.0 $\mu$ s , or 3.6 $\mu$ s
Guard interval	0.8 $\mu$ s (mandatory), 0.4 $\mu$ s (optional)

In the 5–6 GHz range, an Industrial, Scientific and Medical (ISM) band, 5.725–5.875 GHz [42], is allocated for the given group to use as they see fit. The ISM band would also fulfill the requirement of the channel bandwidth for the DVB-T signal, which is 8 MHz as noted in Chapter 2. The only regulation for the use of the ISM band is that the transmit power must be below 25 mW [42]. This rather low requirement might be a hindrance in the frequency converter design, since the far end of the reception area is at considerable distance as seen from the Figure 5.1.

In order to overcome this drawback of low transmit power, re-evaluation the reception area requirement should be considered. Or, an application for a licence to use the frequency converter with a higher transmit power is required.

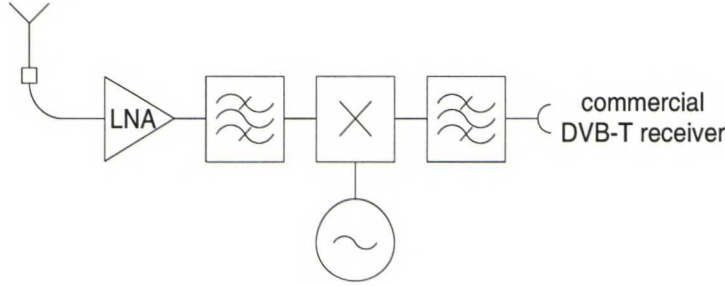
## 5.4 The Test Receiver

Even though the main emphasis on this thesis is in the design and specifications of the frequency converter, also specifications of a test receiver are required. These specifications are required in the link budget calculation for the receiver noise power  $P_n$ , from which an estimate for the required power level at the input of the receiver can be calculated. Also, when verification of the functionality of the frequency converter is carried out in field tests, an exemplar of a feasible receiver systems is necessary.

The design of the test receiver should be from a practical point of view, since it should not take too long to complete and it would only be used in general verification of the



frequency converter. Therefore the following design was concluded, which is illustrated in Figure 5.4.



**Figure 5.5:** Schematic of the test receiver used in the link budget calculation and in general verification of the frequency converter. The 5–6 GHz DVB-T signal from the test receiver is amplified in an LNA and the mixed down to a UHF frequency. The signal is then fed to a commercial DVB-T receiver.

The signal from the frequency converter is at frequency of ca. 5.8 GHz. The antenna of the test receiver is a general omni-directional antenna, so that all of the multi-path signals can be received.

The received signal is amplified in a low noise amplifier (LNA) to ensure that the signal is strong enough when fed to the down-conversion mixer. Then the signal is mixed down to a UHF frequency other than the transmit frequency used in the OtaDigi transmitter, in order to prevent the nearby OtaDigi transmitter from distorting the signal. The signal is filtered to exclude spurious signals and other mixing results from interfering the rest of the receiver system, after which it is fed to a commercial DVB-T receiver.

For the link budget calculations, the noise temperature  $T$  of the receiver system can be derived from the Friis formula [23]:

$$T = T_1 + \frac{T_2}{G_1} + \frac{T_3}{G_1 G_2} \dots, \quad (5.1)$$

where  $T_m$  and  $G_m$  are the noise temperature and gain of the  $m$ th component. The noise temperature  $T_m$  for a component can be calculated for the noise figure  $F$  as follows [23]:

$$T_m = (F - 1)T_0, \quad (5.2)$$

where the  $F$  is the noise figure of a component, and  $T_0$  is the standard noise temperature ( $T_0 = 290$  K). The noise figure  $F$  is commonly given in decibels (dB). For a resistive attenuator, the noise temperature  $T_m$  can be expressed as [23]:

$$T_m = (L - 1)T_{phys}, \quad (5.3)$$

where  $L$  is the attenuation coefficient of the component, and  $T_{phys}$  is the physical temperature of the component.

To estimate the performance of the receiver system, a review of the available components from various commercial manufacturers was performed. For the test receiver the

**Table 5.3:** *List of components for the test receiver*

Component	Manufacturer	Product code	Specifications
LNA	Maxim	MAX2648	$G = 16$ dB, $F = 1.8$ dB
5 GHz ISM filter	Q Microwave	‘5.8 GHz BS’	$L = 1.5$ dB, $T_{phys} = 298$ K
Mixer	Hittite microwave	HMC218MS8	$L = 8$ dB, $F = 8$ dB
UHF filter	Lark Engineering	model 3C	$L = 2.2$ dB, $T_{phys} = 298$ K

following list of components was chosen to reflect the current state in commercial RF components capable of the 5.8 GHz frequency. Component specifications are summarized in Table 5.3.

The Maxim Integrated Products Inc. model MAX2648, a ‘5GHz to 6GHz Low-Noise Amplifier in 6-Pin UCSP’ [43], was chosen for the low noise amplifier (LNA). In the ISM band, the signal is filtered using a ‘5.8 GHz Basestation Filter’ from the Q Microwave, Inc. [44]. The mixer is a Hittite Microwave Corporation model HMC218MS8, a ‘GaAs MMIC Double-Balanced Mixer, 4.5–6 GHz’ [45], and the UHF band pass filter is the Lark Engineering Company model 3C filter with six (6) sections [46].

From these values in Table 5.3, the test receiver noise temperature  $T_R$  can be calculated using Equations 5.1–5.3:

$$\begin{aligned}
 T_R &= (F_1 - 1)T_0 + \frac{(L_2 - 1)T_{phys}}{G_1} + \frac{(F_3 - 1)T_0}{G_1 1/L_2} + \frac{(L_4 - 1)T_{phys}}{G_1 1/(L_2 L_3)} \\
 &= 148.9 \text{ K} + \frac{123 \text{ K}}{39.8} + \frac{1540 \text{ K}}{39.8 \cdot 1/1.4125} + \frac{196.6 \text{ K}}{39.8/(1.4125 \cdot 6.31)} \\
 &\approx 250 \text{ K}
 \end{aligned}$$

For the antenna temperature  $T_A$ , an estimate of 100–150 K can be attained using the sky noise temperature for about 5.8 GHz in the direction of the horizon ( $\Theta_i = 90^\circ$ ) [47].

So, for the whole receiver system noise temperature,  $T_S = T_R + T_A$ , we can make an estimation of  $T_S \approx 400$  K.

## 5.5 Link Budget

To get an estimate for the required transmission power  $P_t$ , a link budget calculation can be made based on the log-distance path loss model discussed in section 4.7. From the free-space model in Equation 4.1 and log-distance path loss model in Equation 4.13, the following formula can be derived:

$$P_r = P_t G_t G_r \left( \frac{\lambda}{4\pi d_0} \right)^2 \left( \frac{d}{d_0} \right)^{-n},$$



which can be expressed in decibels:

$$P_r = \overbrace{P_t + G_t}^{EIRP} + G_r + \overbrace{20 \log \left( \frac{\lambda}{4\pi \cdot 100 \text{ m}} \right) - 10 n \log \left( \frac{d}{100 \text{ m}} \right)}^{\text{total path loss}}, \quad (5.4)$$

if the reference distance  $d_0$  is 100 m as chosen in section 4.9. The transmitter antenna gain  $G_t$  and the transmission power  $P_t$  can be merged as an equivalent isotropically radiated power (EIRP). The total path loss term can be evaluated from the Figure 4.5. The whole link budget calculation is summarized in Table 5.4 and is next described in detail.

The required receiver power  $P_r$  can be evaluated from the carrier-to-noise ratio (C/N) derived from transmission parameters and using the receiver noise power  $P_n$  [23]:

$$P_n = k_B T_S B_n, \quad (5.5)$$

where  $k_B$  is the Boltzmann constant ( $k_B = 1.381 \cdot 10^{-23}$  J/K),  $T_S$  is the receiver system noise temperature derived in section 5.4 ( $T_S \approx 400$  K), and  $B_n$  is the noise bandwidth ( $B_n \approx 8$  MHz).

Various carrier-to-noise ratios C/N are presented in [19] for different transmission parameters. For the ‘OtaDigi’ broadcast, described in Table 5.1, the derived C/N is 14.2 dB, if the propagation channel is presumed to be a Rayleigh channel. The (minimum) receivable signal power can be thus evaluated as:

$$\begin{aligned} P_n &= k_B T_S B_n \\ &= 1.381 \cdot 10^{-23} \text{ J/K} \cdot 400 \text{ K} \cdot 8 \text{ MHz} \\ &= 4.4192 \cdot 10^{-14} \text{ W} \\ &= -103.5 \text{ dBm} \end{aligned}$$

$$\begin{aligned} P_r &= C/N + P_n \text{ in decibels} \\ P_r &= 14.2 \text{ dB} + (-103.5 \text{ dBm}) = -89 \text{ dBm} \end{aligned} \quad (5.6)$$

For the receiver antenna gain  $G_r$ , a value of 0 dB is widely used in system design manuals (e.g. in [48]). By reviewing recent publications, the receiver antenna gain  $G_r$ , more precisely the mean effective gain (MEG), is more likely in order of -3 – -5 dB [49],[50], considering the position of a DVB-T handset receiver in use.

The total path loss can be estimated from Figure 4.5 to be in order of 117 to 130 dB for the intended reception area described in section 5.2 (maximum distance of 1500 m).

To ensure that the signal strength is sufficient in different locations inside the reception area, variations in the signal level must be taken into account. These variations can be estimated using the log-normal shadowing parameter  $X_\sigma$  described in Section 4.7. In Section 4.8, we reviewed a number of recent measurement campaigns. Especially, from the results of suburban measurements in [6], an estimate for the deviation of  $X_\sigma$  can be drawn. The deviation of  $X_\sigma$  for suburban LOS situations can be estimated to be 4.9 dB and for NLOS situations 2.8 dB [6].

A 97.5% coverage of these locations requires that the deviation shall be multiplied 1.96 times [51], since it has a log-normal distribution. Therefore an additional 5.5 dB (NLOS) to 9.6 dB (LOS) must be included in the path losses to ensure adequate signal coverage.



An interesting observation can be drawn from this shadowing. The deviation is much stronger in LOS situations (4.9 dB), which are more likely to occur closer to the transmitter. In the far corners of the reception area, where path-losses are the highest, the NLOS reception occurs more frequently — probably all the time — and the deviation is much lower (2.8 dB). Therefore, in the link budget calculation, the NLOS value should be used as the deviation value.

Also, the 1500 m distance is located at the edge of the 3 dB beam width of the transmission antenna, which adds another -3 dB to the signal level.

Thus, a minimum EIRP of the transmission system is about 40–55 dBm.

**Table 5.4:** *The link budget calculation for the required transmission power  $P_t$*

Receiver system noise temperature	$T_S$	400 K
Receiver system noise bandwidth	$B_n$	8 MHz
the Boltzmann constant	$k_B$	$1.381 \cdot 10^{-23}$ J/K
Receiver noise power	$P_n$	$4.4192 \cdot 10^{-14}$ W
	$P_n$	-103.5 dBm
Carrier-to-noise ratio	C/N	14.2 dB
Minimum receivable signal power	$P_r$	-89 dBm
Receiver antenna gain	$G_r$	-3 – -5 dB
total path loss ( $d = 1500$ m)		117–130 dB
area coverage of 97.5%		5.5 dB
Receiver at the edge of 3 dB antenna beam		-3 dB
EIRP ( $P_t G_t$ )		40–55 dBm
Transmitter antenna gain	$G_t$	20 dB
Minimum transmission power	$P_t$	20–35 dBm
		100 mW – 3.2 W

In Section 5.2, it was derived that the reception area could be covered with antenna of beam widths of  $\theta_E = 5^\circ$  and  $\theta_H = 60^\circ$ . The antenna gain can be derived from these beam widths by the following approximation [52]:

$$G_t \simeq \frac{30000}{\theta_E \theta_H}, \quad (5.7)$$

where  $\theta_E$  and  $\theta_H$  are both in degrees. For the transmitter antenna, this will yield a gain  $G_t$  of 100, or 20 dB.

Therefore the (minimum) transmission power  $P_t$  is in range of 20–35 dBm (100 mW to 3.2 W). This value can be used as a guideline when specifying the components for the frequency converter.

Pointing out the Finnish regulations on the 5.8 GHz ISM band, the maximum EIRP of 25 mW [42], two conclusions can be made:

First, a license for the experimental frequency converter shall be applied: an EIRP of 1 W, transmitting frequency in the 5.8 GHz ISM band, and transmit bandwidth of about 10 MHz.

Second, opt for the unlicensed ISM band and the maximum EIRP of 25 mW (14 dBm). In this case the maximum area of reception is about 150 m, if using Table 5.4 and Figure 4.5 to derive an estimate.

The latter choice is unacceptable, since the distance of 150 m is inadequate for broadcasting purposes, the reception area ends somewhere in the middle of the free space between the Otaniemi water tower and the main library of HUT. Our only choice is then to acquire a license for the frequency converter.

## 5.6 Speculation about the Location of ‘OtaDigi’ Transmitter

In the beginning of this thesis, an assumption was made that the ‘OtaDigi’ transmitter would be located in the Otaniemi water tower, which is in the vicinity of VTT Information Technology premises. As the result of correspondence between the author and Ville Ollikainen, Senior Research Scientist at VTT Information Technology, it has been come to our attention that the ‘OtaDigi’ transmitter is located on top of the VTT Information Technology building. The building is about four stories high (ca. 15–20 m), which is not clearly as tall as the water tower. A view from the antenna installation point towards the Otaniemi cape is shown in Figure 5.6.



**Figure 5.6:** *View from the ‘OtaDigi’ antenna site on top of the Ekono building. The antenna is about 1 meter to right and 1 meter higher than the camera. The HUT main building is shown in the middle of the picture, the Espoo Sähkö power plant chimney on the left. The department of electrical and communications engineering can be seen just on the right side of the HUT main building.*

Since the antenna is located much closer to the tree line and adjacent buildings as illustrated in Figure 5.6, this location is much more susceptible to poorer transmitting and propagation conditions, which will degrade the received signal. At the proposed transmit frequency of the frequency converter of about 5–6 GHz, this lower transmit height would degrade propagation conditions even more, since higher frequencies are even



more susceptible to obstacles and surroundings — even to a level, where the design and output power are inadequate to fulfill transmission requirements.

Therefore it might be required that the design of the frequency converter must be changed to overcome these hindrances. These changes could be implemented as a different transmit location or as a different system configuration.

Feasible alternative locations for the frequency converter are other high buildings or structures close to the HUT campus area. Prime candidates for alternative locations are: on the top of the chimney of the Espoo Sähkö power plant, or on the top of main measurement hall of the High Voltage Institute of Department of Electrical and Communications Engineering HUT. The chimney is 75 meters high [53], which is about in level with the water tower. The top of main measurement hall is at the height of ca. 20 meters. These locations are marked in Figure 5.1 as a triangle and a square, respectively, and are also pointed out in Figure 5.2.

Both alternative locations are much closer to the reception area, which will lower the path loss. The measurement hall height might be a hindrance, since the transmitter should be located much higher than surrounding structures in order to provide good transmitting conditions. For both alternative locations, the transmission antenna gain is much lower than in the primary water tower transmitter configuration, since a more omnidirectional antenna is required. In all, the required transmit power could well be higher than in the primary configuration. Also, a different method to receive the UHF frequency DVB-T signal from the ‘Otadigi’ transmitter must be devised.



# Chapter 6

## Experimental Frequency Converter

The main objective of this thesis is to specify and design a frequency converter for a DVB-T transmitter. The design of the frequency converter is based on requirements introduced in previous chapters, on possible implementation points, and known input and transmit frequencies. Since it seems that installing the frequency converter on the top of the Otaniemi water tower is not possible, an alternative transmitter configuration is presented and reviewed.

Regardless of the problematic, and possibly impossible-to-attain, installation point, the frequency converter design is completed with an assumption that one day the ‘OtaDigi’ transmitter will be installed on top of the Otaniemi water tower.

### 6.1 System Configuration

As described in Chapter 5, the frequency converter is intended to be integrated to the output of a commercial DVB-T transmitter. The ‘OtaDigi’ transmitter is operating at UHF channel 55, an 8 MHz channel with a center frequency of 746 MHz, and has a power amplifier output power of 55 W (47 dBm). The other possible implementation point is the antenna input port, where the signal power is 40 W (46 dBm). This would lead to a different configuration, since the whole frequency converter would be in open air and no long transmission cables would be needed. The components should withstand rough conditions, but the signal would attenuate less while transferring it to the transmitting antenna. The antenna port is designated as the implementation point in the design, since it is more suitable for the implementation than the power amplifier output.

The output power requirement for the power amplifier is 100 mW (20 dBm), as concluded in Section 5.5. The transmit frequency is in the 5.725–5.875 GHz ISM band and the channel width is about 10 MHz. The schematic of the frequency converter is shown in Figure 6.1 and is described next in detail.

A sample of the ‘OtaDigi’ UHF signal is taken by a directional coupler. The directional coupler must withstand an input power of about 40 W. The signal level of the converter system is adjusted with a step attenuator, which is installed in front of the mixer — this position will also improve the matching of the mixer input port.

The sampled signal is up-converted to the 5.8 GHz ISM band. The frequency conversion (up- and down-conversion) can be done either using the lower or upper sideband,

as long as both conversions are done using the same sideband, as observed in Section 2.5.2. Since the IF frequency is 746 MHz and the RF frequency is in the ISM band (5.725–5.875 GHz), the LO frequency is required to be either 4.979–5.129 GHz or 6.471–6.621 GHz.

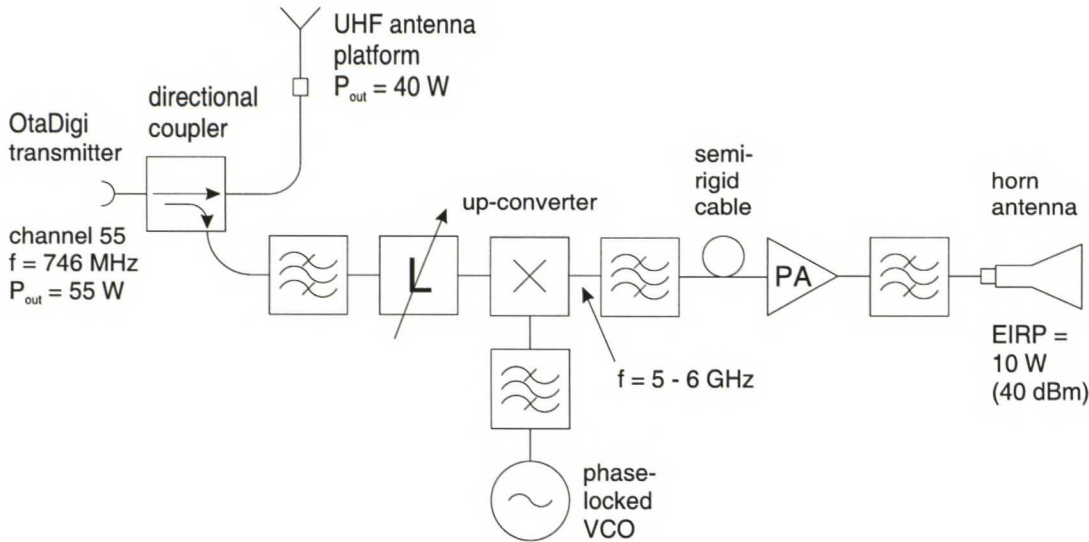
As for the experimental frequency converter, the chosen sideband is not a critical factor, since the harmonics of the LO are at frequencies much higher than the transmitting frequency band and lack of image rejection is not to a hindrance.

The local oscillator signal for the mixer is produced in a phase-locked voltage controlled oscillator (phase-locked VCO), so that a reasonable stable output signal can be provided. The signal is filtered in order to prevent spurious signals from interfering the UHF signal in the up-conversion process.

The up-converted signal is then transferred, using a semi-rigid cable or similar transmission line, to a power amplifier attached to an antenna. This way the power of the amplifier is not lost in the transmission line. Since the installation point of the directional coupler is the UHF antenna input port, no transmission cable is required. At least, the cable has a rather short length and the signal will not attenuate as much as in other cases.

The up-converted signal is then amplified in a power amplifier, up to the required power level, and fed to the antenna. The antenna is a horn antenna with horizontal beam width of 60° and vertical beam width of 5° (resulting a gain of 20 dB) that will cover the whole reception area in 3 dB beam widths. Thus, the EIRP of the converter system is 10 W (40 dBm).

Along the sampling and up-conversion chain, the signal is filtered to prevent spurious responses from degrading the signal quality. Requirements for pass-band bandwidths of the three different filters are derived from specifications earlier in this section. In the block



**Figure 6.1:** Schematic of the experimental frequency converter. A sample of the ‘OtaDigi’ UHF frequency transmission is taken by a directional coupler, then up-converted to the 5.8 GHz ISM band, and amplified just before feeding it to the antenna. The output power level is adjusted with a step attenuator.



level design insertion losses of the filters shall be perceived, in order to derive correct power levels for each component.

For the UHF bandpass filter, the center frequency is 746 MHz and the pass-band bandwidth is 8 MHz (ca. 1.1% relative bandwidth). The LO filter has a center frequency is either 5.054 GHz or 6.546 GHz, and the bandwidth is 150 MHz (2.3–3% relative bandwidth).

Near the 5.8 GHz ISM band, the bandwidth is intended to be 10 MHz, but the actual center frequency depends on the acquired broadcasting license, the relative bandwidth is in any case ca. 0.2%, which is too narrow to be manufactured without a specialized design. The whole ISM band can be covered with a 150 MHz bandpass filter at center frequency of 5.8 GHz. The relative bandwidth is in this case 2.6%. For the ISM band, there exists some commercially manufactured candidates that can attain these requirements.

## 6.2 Alternative Configuration

If the primary location for the frequency converter is not available, an alternative location and configuration shall be chosen. Alternative locations are the chimney of Espoo Sähkö power plant in Otaniemi and on top of the main measurement hall of the High Voltage Institute at Faculty of Electrical and Communications Engineering HUT, as noted in Section 5.2. The frequency converter for these locations shall be more of a relay transmitter type, as illustrated in Figure 6.2.

The UHF frequency DVB-T signal is received from the ‘OtaDigi’ transmitter by an antenna. A problem arises from the choice of the receiver antenna. A narrow-beam antenna would give a better gain and, therefore, a stronger signal would be received. The drawback is that a direct free-space link might not be possible, since the ‘OtaDigi’ transmitter is quite near the tree line.

If no direct link is available, the only choice is to receive a multi-path signal and a wide-beam antenna is the feasible solution. The received signal would be much more deteriorated than in a direct link situation. Also, wider beam would result a lower antenna gain.

Received signal is then amplified in a low noise amplifier (LNA), and the power level of the signal is adjusted in an automatic gain control (AGC) circuit. The rest of the alternative frequency converter is identical to the primary configuration described in Section 6.1.

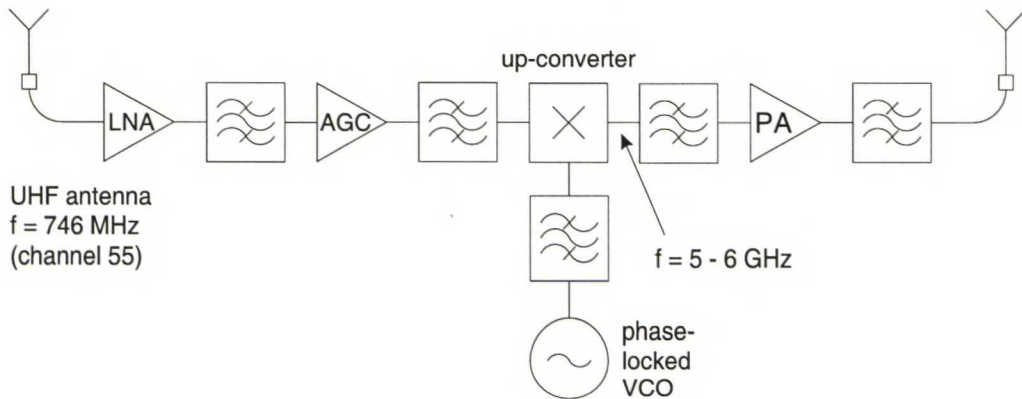
In this design, the AGC circuit is the most critical part, and it is expected that it also requires the most work, even compared to the phase-locked VCO circuit.

The output power  $P_t$  requirement for installations on alternative locations differ from the primary configuration. By using the illustration of the transmitting locations in Figure 5.1, it can be estimated that the maximum reception distance is about 750 m. From Figure 4.5, an estimate for total path loss of 110–120 dB can be roughly derived — this is about 7 dB lower than in the case of the primary location.

The reception area can be covered with an antenna that has a horizontal beam width of 180° (antenna on top of the chimney), or 240° (in case of the measurement hall). Vertical beam widths are about 67° in both cases. Therefore, the antenna gain  $G_t$  is about 3–4 dB,

which is 16–17 dB lower than in the primary configuration.

Given this quick derivation of link budget changes, the output power of the power amplifier should be increased by ca. 10 dB (to a level of 30 dBm, 1 Watt). This requirement might be impossible to satisfy: there simply does not exist a highly linear amplifier with an output power of 30 dBm (1 W). Thus, the decrease in the linearity of amplification process would deteriorate the signal too much.



**Figure 6.2:** *Alternative configuration for the frequency converter. A relay-transmitter approach was used in this design, since the converter would away from the ‘Otadigi’ transmitter. The output power is controlled by the automatic gain control (AGC) circuit.*

## 6.3 Block Level Components

From the system configuration specified earlier in this chapter, a block level design can be composed by choosing possible candidates for different sections of the converter schematic in Figure 6.1.

These candidates were chosen by reviewing WWW home-pages of various RF device manufacturers. An interesting observation is that the quality of manufactured components is evolving at a rather quick speed, so it is possible that by the time this thesis is completed, more feasible candidates are already available. In that case, it is wise to use them. The main emphasis is to choose commercial components that are off-the-shelf available. Also, the use of evaluation boards in the design is favorable, since the implementation period must be kept as short as possible.

The most critical component of the system is the power amplifier, due to its high linearity requirement. But, the up-conversion mixer will impose the design most, since the output power of the mixer has a certain upper limit which might be too low. Therefore, the design of the frequency converter will begin with the choice of the mixer and the choice of upper or lower sideband mixing. The performance of the mixer will probably force us to make some choices about the design.

After the mixer is chosen, the rest of the system is built starting from the microwave part of the converter and ending with the LO schematics. In the following sections, the process of the choosing of the components is described and illustrated along the way. In



some cases there are various choices for the best component. Thus, they are all presented and reviewed along the way.

### 6.3.1 Mixer

As stated in the introduction of this section, the mixer is the most influential component of the design — not the most critical though. The mixer is presumably a double balanced mixer, since this group of mixers has very good spurious rejection characteristics, good isolation between RF, IF and LO ports, and the compression point and third-order intermodulation characteristics are better than of other candidates [54]. For the mixer, there exists a number of good candidates in the commercially manufactured components, and actually, the most problematic design parameter was the input IF frequency of the ‘Otadigi’ DVB-T broadcast at 746 MHz.

Since the lower mixing sideband is the preferred one, the primary candidate for the mixer is the Hittite corporation model HMC219MS8 [55]. The data sheet of the HMC219MS8 is in the Appendices starting from page 95. The HMC219MS8 is a double-balanced mixer designed for frequency range of 4.5–9 GHz. In Table 6.1 the critical parameters of the HMC219MS8 are presented. It has a rather low IF port return loss, but it will be improved by the attenuator installed in front of the port. Also, it has a better linearity than the other candidate, which has the most weight in this design. The other possible candidate, the HMC168C8 [56] from Hittite, is also listed in Table 6.1.

**Table 6.1:** *Typical parameters for mixer candidates. Frequencies are in GHz and power levels in dBm.*

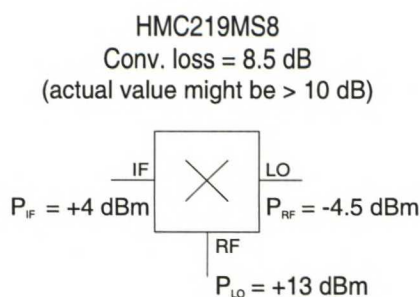
Model	LO & RF freq.	IF freq.	Conv. loss	$P_{LO}$	$P_{1dB,IN}$	$IP_{3,IN}$
HMC219MS8	4.5–9.0	DC–2.5	8.5 dB	+13	+10	+21
HMC168C8	4.5–8.0	DC–2.0	8.2 dB	+10	+10	+16

An estimate for the reasonable output power level for the mixer can be derived from Table 6.1. The IF port input power of +4 dBm is about 6 dB below the  $P_{1dB,IN}$ , which should enough. Therefore, the RF output power should be about -4.5 dBm ( $= P_{in} - \text{Conversion loss}$ ).

The IF port input power can be lower than the value above, and should be lowered if it is possible, but in any reason it cannot be higher than just derived. So, the rest of the design is completed in terms of the maximum usable power, and if possible, the power level is lowered. The first block of our design is illustrated in Figure 6.3.

From the choice of the mixer, design parameters for the local oscillator can be derived. The LO output power must be +13 dBm, for the mixer to perform as intended. An LO power of less than +13 dBm will result a decrease in performance: voltage standing wave rations (VSWR) of all three ports, frequency bandwidth, conversion gain and harmonic distortion will vary — most probably degenerate [57].

The frequency band of the LO can be either 4.979–5.129 GHz or 6.471–6.621 GHz, since the HMC219MS8 is capable of both of them.



**Figure 6.3:** Required IF and LO power levels for the maximum RF power level. Notice the mixer port definitions for up-conversion operation. The actual conversion loss might be higher than specified in the component data sheet (see Section 6.3.2).

### 6.3.2 Up-conversion Operation Specialities in Mixers

The operation notes for the HMC219MS8 are quite inadequate, e.g. it is vague which way the IF, LO and RF signals should be applied to the mixer for up-conversion. For down-conversion operation it seems that the operation is straight-forward [58]: apply LO signal to LO port and RF to RF port. The IF signal can be accessed from the IF port.

The problem arises from the fact that the up-conversion operation in the same operation note [58], which is actually for mixers HMC141/142 and HMC143/144, is not unambiguous: either the operation is similar to down-conversion mixing, or the LO and RF port signals must be interchanged. Apparently mixers, even the HMC219MS8, will work both ways, but the setup for best performance is not known — only way to be sure about this is to measure a purchased mixer or start lengthy correspondence with Hittite Microwave corp.

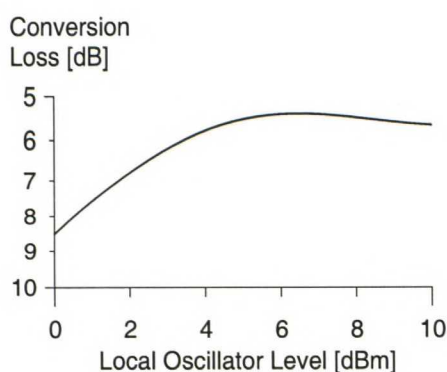
By comparing the data sheets of HMC141/142 [59] and HMC143/144 [60], it seems the mixer application note [58] mentioned in previous paragraph is bit more than vague. By comparing the data sheets, it seems that the HMC141/142 and HMC143/144 will work similarly even in up-conversion operation.

Therefore, it would be reasonable to assume that the HMC219MS8 should work as follows: for up-conversion operation with HMC219MS8, the ‘Otadigi’ UHF signal shall be fed to IF port. The LO signal must be applied to RF port, and the 5.8 GHz RF signal can be accessed from the LO port.

This switch of the LO and RF ports will probably cause a decrease in the mixer performance. The absolute maximum input power for the RF port is +13 dBm, which is the LO power level required for the performance indicated in the data sheet. Because we have to lower this RF port LO power by some decibels, the performance of the mixer will degenerate as indicated in the previous section (6.3.1). Also, the conversion loss will probably rise by 1–3 dB as shown in Figure 6.4.

Still, if we make a hopeful assumption that in the following sections of the design process the risen conversion loss can be compensated — e.g. with a higher amplifier gain — the design can continue with the assumed conversion loss of 8.5 dB. While the actual conversion loss, more correctly the conversion gain (usually a negative value) of up-conversion operation, could be even as high as 10 dB.





**Figure 6.4:** Typical conversion loss behavior with varying local oscillator power levels. A slight change from the optimum LO level will not change the loss that much, but change more than 3 dB will degenerate it considerably. (edited from [61]).

### 6.3.3 5.8 GHz ISM band filters and transmission lines

After the signal is up-converted, it shall be filtered with a narrow pass-band filter, and fed to the power amplifier block, which can be a few meters away. The selection of the 5.8 GHz ISM band filter is relatively easy, but the intriguing part in this block is the selection of an appropriate transmission line — since a semi-rigid cable might be too lossy.

For the 5.8 GHz ISM band, and pass-band width of 150 MHz, there are a number of choices from which to select the filter. Here two of them are introduced. The primary candidate is the Q Microwave Inc. ‘5.8 GHz Basestation Filter’ [44]. It is in all a good filter, the center frequency  $f_c$  can be chosen within 5.7–5.85 GHz, and the insertion loss IL is 1.7 dB. The pass-band ripple is about 0.1 dB. The only hinderance is the pass-band width of 100 MHz, which will not cover the whole ISM band. The data sheet of the ‘5.8 GHz Basestation Filter’ is in the Appendices of this thesis (onwards from page 95).

If a more customizable filter is required, the Lark Engineering Co. model 3B combline filter series [46] might be worth a more thorough inspection. For the ‘Lark 3B’, a custom made (special type) filter is a required, since the relative 3 dB bandwidth requirement is 2.5%.

In Table 6.2, the characteristics for the filters are presented. For the ‘Lark 3B’, the following design parameters were used: center frequency  $f_c$  of 5800 MHz, 2.5% relative 3 dB bandwidth (a 150 MHz passband) and six (6) sections. The rejection is derived for the  $\pm 250$  MHz from the center frequency of the filter.

**Table 6.2:** Parameters of 5.8 GHz filter candidates

Model	$f_c$	Passband	IL	Rejection
Q $\mu$ wave 5.8 GHz BS	5800 MHz	100 MHz	1.7 dB	50 dBc
Lark 3B (spec.)	5800 MHz	150 MHz (2.5% of $f_c$ )	2.6 dB	46 dBc

For the transmission line, there are practically three different choices: a low-cost coaxial cable, a high-cost low-loss coaxial cable, and a standard waveguide. These three different choices are now compared and the installation location of each choice is discussed.

The Huber&Suhner K 02252 D-64, double screened coaxial cable [62], can be used as an exemplar for the low-cost coaxial cable. It has an outer diameter of 3 mm, and the maximum operating frequency is 6 GHz. It has a nominal attenuation of 2.539 dB / m at 6.0 GHz.

The Huber&Suhner SF 106PE - SUCOFLEX 100, the flexible high performance microwave cable [63], is a good example of a low-loss coaxial cable. It is widely used in laboratory installations, and has good transmission characteristics — which directly translates into the cost of the cable. The ‘SF 106 PE’ has an outer diameter of 7.9 mm and the nominal attenuation is 0.41 dB / m at 6.0 GHz.

The standard waveguide for the 5.8 GHz ISM band is designated as ‘WR-159’. Its operation range is 4.9-7.05 GHz, the cut-off frequency for the TE<sub>10</sub> mode is 3.711 GHz and inner dimensions of the waveguide are:  $a_0 = 40.386$  mm,  $b_0 = 20.193$  mm. The attenuation at 5.7 GHz is 0.0421 dB / m (4.21 dB / 100 m) [64].

The comparison of these three different transmission lines is presented in Table 6.3. For the comparison the line attenuations are calculated for transmission line length of 10 m.

**Table 6.3:** Comparison of three different types of transmission line candidates for possible use at 5.8 GHz

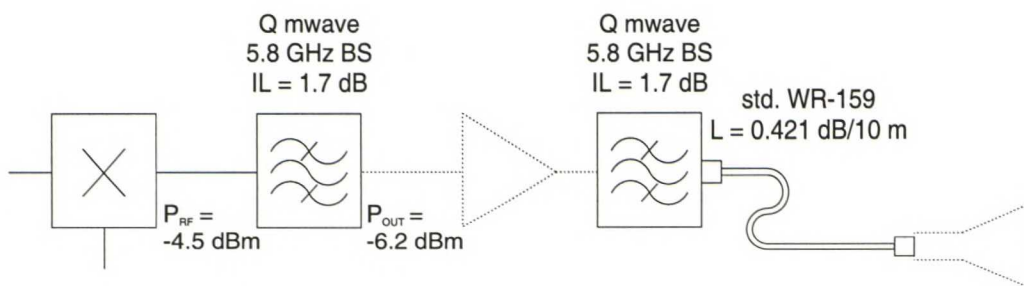
Type	Model	Nom. attenuation	Attenuation @ 10 m
‘low-cost’ coaxial line	K 02252 D-64	2.539 dB / m	25.39 dB
‘low-loss’ coaxial line	SF 106PE	0.41 dB / m	4.1 dB
standard waveguide	WR-159	4.21 dB / 100 m	0.421 dB

The ‘low-cost’ coaxial line, K 02242 D-64, has clearly a too high attenuation for these line lengths. The SF 106PE, the ‘low-loss’ coaxial cable, might be usable in the frequency converter system if losses of 4.1 dB can be tolerated in the system design. In any case, it must be installed in front of the power amplifier block in order not to lose any ‘precious’ output power of the power amplifier.

The best choice is the standard waveguide. The WR-159 has only ca. 0.5 dB of attenuation with line length of 10 m — actually, it is below the uncertainty of the system design so far. The waveguide can, and should, be installed between the last bandpass filter and the antenna. The horn antenna can be directly installed to the waveguide without any sort of adapter. The disadvantage of a waveguide is that the design is quite static and quite costly to be altered — waveguide sections cost quite a lot.

The WR-159 waveguide and microwave filters of the schematic are presented in Figure 6.5. The same ISM band filter is used to filter spurious emissions generated in the amplification process.





**Figure 6.5:** Schematic of ISM filter and the transmission line parts in the frequency converter design. The maximum output power of the up-conversion mixer is estimated to be  $-4.5$  dBm (see Section 6.3.1).

### 6.3.4 Power Amplifier

The input power level for the amplifier block is  $-6.2$  dBm, as derived in Section 6.3.3. Since the power level requirement at the antenna port is  $20$  dBm (Section 6.1) and the filter and the transmission line will attenuate the signal ca.  $2.1$  dB, the power amplifier output power requirement is  $22.1$  dBm. These two values can be used in the selection of candidate components. Also, the chosen linearization method, back-off, must be taken into account when choosing the amplifier.

After a brief review of commercial medium-power amplifiers capable of about  $20$  dBm of output power with reasonable back-off, it is certain that this design will require a driver amplifier in front of the power amplifier. Thus, at first the power amplifier is chosen, then suitable candidates for the driver amplifier are presented. Given the output power requirement of  $22.1$  dBm, with some reasonable back-off of about  $6$  dB, there are not many candidates available.

The primary candidate is the Hittite Microwave corporation HMC408LP3, a  $1$  watt power amplifier designed for frequency range  $5.1$ – $5.9$  GHz [65]. It has a gain of  $20$  dB, and at the derived input power level of  $2.1$  dBm the gain is in the more linear region of the amplifier, derived input  $1$  dB compression point is about  $23$  dBm. Also, it has a rather high output third order intercept point ( $IP_3$ ) of  $43$  dBm. The rest of parameters for the primary candidate are presented in Table 6.4. The published data sheet of the HMC408LP3 is in the Appendices starting from page 95.

Also, the next best candidate, the HMC406MS8G [66] also manufactured by Hittite Microwave corporation, is displayed there. Parameters are given for the frequency range of  $5.7$ – $5.9$  GHz, but the total operational frequency range is larger than that for both amplifiers.

It is common nowadays to use a low-noise amplifier as a driver amplifier, since it will provide enough amplification and does not deteriorate the signal due to its excellent noise characteristics. A problem might arise from the fact that LNAs are designed to amplify very low level signals, therefore it might not be possible to find an LNA that would not saturate at the required input power level of  $-6.2$  dBm. If the gain of the LNA is high enough, it is possible to lower the IF input power of the up-conversion mixer, and thus move further away from the saturation point.

**Table 6.4:** *Power amplifier candidates for the frequency converter*

Model	Gain	Output $IP_3$	Output $P_{1dB}$	Noise figure
HMC408LP3	20 dB	30 dBm	43 dBm	6 dB
HMC406MS8G	17 dB	27 dBm	38 dBm	6 dB

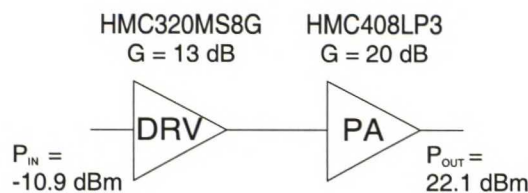
Requirements for the driver amplifier, i.e. LNA, are as follows: the input power level is expected to be at -6.2 dBm. The power amplifier requires a input power level of 2.1 dBm. So, a gain of about 8.4 dB is required. The input 1 dB compression point of the LNA must be well above -6.2 dBm, for the LNA to be in the linear region. In Table 6.5, candidates for the driver amplifier are presented.

**Table 6.5:** *List of driver amplifier candidates for the frequency converter*

Model	Gain	$P_{in}(P_{out} = 2.1 \text{ dBm})$	Output $P_{1dB}$	Input $IP_3$
HMC320MS8G	13 dB	-10.9 dBm	12 dBm	10 dBm
MAX2649	17 dB	-14.9 dBm	-9.6 dBm	0 dBm
HMC318MS8G	9 dB	-6.9 dBm	2 dBm	4 dBm

The primary candidate is the HMC320MS8G [67] from the Hittite Microwave corporation. The published data sheet of the HMC320MS8G is in the Appendices starting from page 95. The HMC320MS8G should be able to produce the required 2.1 dBm of output power, and still be some 10 dB away from the 1 dB compression point (i.e. well in the linear amplification region). The amplifier block schematic is shown in Figure 6.6.

Next best choices are the MAX2649 [68] from the Maxim-IC, and the HMC318MS8G [69] also from the Hittite Microwave corporation. Problem with these two is that either of them can not produce enough output power, without going into saturation — they are just introduced here to show the narrow selection that we have to work with.

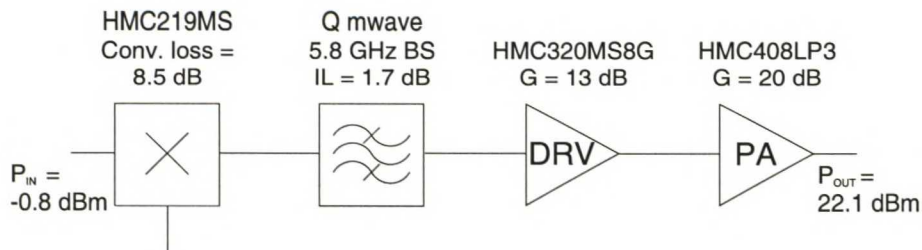


**Figure 6.6:** *Schematic and power level requirements for the amplifier block. The high gain of the driver amplifier has made it possible to lower the power level requirement for the preceding blocks. The required mixer RF output power can be lowered from -6.2 dBm to -10.9 dBm.*

Since the gain of the driver amplifier HMC320MS8G is 13 dB, the input power must



be lowered to -10.9 dBm, which directly translates into the up-conversion mixer IF input power. The updated illustration for the design process is presented in Figure 6.7. The required mixer IF input power can be lowered from +4 dBm to -0.8 dBm, which should lower the distortion of the OFDM signal in the mixing process.



**Figure 6.7:** Updated schematic and power level requirements of the high-frequency section of the frequency converter. The higher than expected gain of the driver amplifier allowed the power level requirement to be lowered ca. 5 dB.

### 6.3.5 UHF block

In previous section, we derived the required IF input power for the up-conversion mixer is -0.8 dBm. In the antenna port of the ‘Otadigi’ transmitter, the power level is 46 dBm (40 W). The directional coupler must withstand that much input power, but after the sample of the signal is taken the power level should be well below 1 W.

There are many ways of deriving component values, but in this work it is based on the fact that in order to get an optimal tuning range for a step attenuator, the attenuation shall be half of the maximum value. Then, after calculating the insertion loss of the UHF filter, the coupling value for the directional coupler and the required attenuation for a fixed precision attenuator are derived. In Table 6.6, the chosen components are presented — certainly there are number of other as-good-as components, but differences are not that significant. The schematic of the UHF block is illustrated in Figure 6.7

**Table 6.6:** List of chosen components for the UHF block

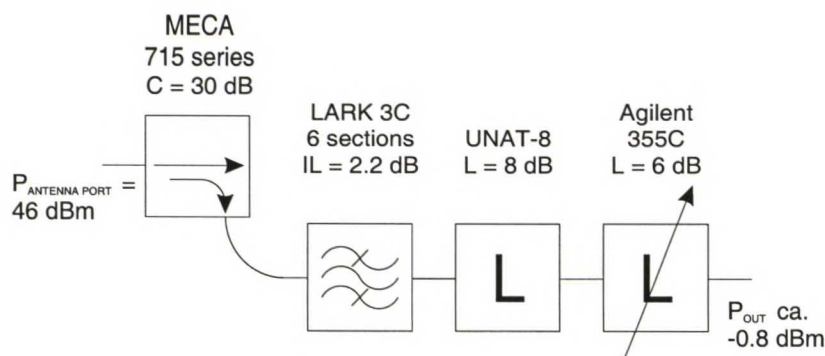
Component	Model	Manufacturer	Parameter
Directional Coupler	715-30-0.900	MECA Elec.	C = 30 dB
UHF filter	3C	Lark eng.	IL = 2.2 dB
Fixed attenuator	UNAT-8	Mini-Circuits	L = 8 dB
Step attenuator	355C	Agilent	L = 6 dB

The MECA Electronics, Inc. model 715-30-0.900 [70] was chosen for the directional coupler. It has a coupling factor  $C$  of 30 dB — in case of a redesign, the coupling factor can be selected from values of 6, 10, 20, 30 and 40 dB. The 715 series can withstand input power of 500 W, so it should well handle the 40 W of the ‘Otadigi’ transmitter.

The UHF filter can be selected from the Lark engineering models [46], from which the 3C series cavity filter should perform adequately. For a six (6) section filter with a center frequency of 746 MHz and a 10 MHz pass-band (1.34% relative width), the insertion loss is calculated to be ca. 2.2 dB. The calculated average input power that the filter can withstand is ca. 20 W.

The Agilent Technologies Inc. has a good selection of step attenuators. For the frequency converter a simple manual step attenuator with range of 0–12 dB is a good choice. The Agilent 355C [71] covers the wanted range in 1 dB steps, and has an average power handling capability of 0.5 W. To calculate the required attenuation of the fixed attenuator, the step attenuator is set to the attenuation of 6 dB.

The required attenuation of the fixed attenuator is calculated to be 8.6 dB. At this stage of the design, the 0.6 dB can be omitted — i.e. any little mismatch, or uncertainty in datasheet, somewhere will cause 0.6 dB of excess signal attenuation — so a 8 dB precision attenuator will be sufficient. Mini-Circuits is producing a good line of N-type connectorized precision attenuators, from which the UNAT-8 [72] has the wanted attenuation of 8 dB (with  $\pm 0.3$  dB uncertainty). It should withstand average input power of 0.5 W, which is sufficient.



**Figure 6.8:** Schematic of the frequency converter UHF block. Both the fixed and the step attenuator are required to be able to optimally adjust the signal power.

### 6.3.6 Antenna

In Section 5.2 we derived that the horn antenna must have beam-width of  $5^\circ$  in E-plane (vertical) and  $60^\circ$  in H-plane (horizontal). It was estimated that a horn antenna with those beam-widths would result an antenna gain of 20 dB. The horn antenna is directly implemented at the end of the waveguide section as described in Section 6.3.3.

The process of designing horn antenna with specific radiation patterns is discussed in [73]. It is pretty straight-forward task, with certain amount of trial and error cycles in order to design a physically realizable antenna. There are two dimensions per plane that are derived for wanted radiation patterns:  $b$  is the aperture width and  $l_e$  is the slant length of the flare for the E-plane, and  $a$  and  $l_b$  are in the H-plane, respectively.

Here the antenna is designed for the center frequency of the 5.8 GHz ISM band, therefore the wavelength  $\lambda \approx 0.052 \text{ m}$ . As specified in Section 5.2, antenna beam widths



$\theta_E$  and  $\theta_H$  are 3 dB beam widths: 3 dB (0.5) in relative power level corresponds to ca. 0.7 in relative field strength. This approximation is reasonable, since the design diagrams in [73] are quite coarse and good amount of imprecise pen, ruler and calculator work is required to derive wanted antenna dimensions.

By using an additional variable called maximum phase deviation in wavelengths,  $s$  in the E-plane and  $t$  in the H-plane, it is possible to derive the following equations for horn antenna dimensions and various values of  $s$  and  $t$ . Real number coefficients in the right side of equations are derived from diagrams in [73]:

$$b \approx \lambda \sin(\theta_E/2) \cdot \begin{cases} 0.444 & s = 1/8 \\ 0.472 & s = 1/4 \\ 1.321 & s = 1/2 \end{cases} \quad (6.1)$$

$$l_e = \frac{b^2}{8\lambda s} \quad (6.2)$$

$$a \approx \lambda \sin(\theta_H/2) \cdot \begin{cases} 0.6045 & t = 1/8 \\ 0.6436 & t = 1/4 \\ 0.784 & t = 1/2 \\ 1.321 & t = 3/4 \end{cases} \quad (6.3)$$

$$l_h = \frac{a^2}{8\lambda t} \quad (6.4)$$

As derived earlier  $\theta_E$  and  $\theta_H$  are  $5^\circ$  and  $60^\circ$ , respectively. The wavelength  $\lambda$  is 0.052 m. Using these values, two other diagrams in [73] and Equations 6.1–6.4, it is possible to evaluate  $b$ ,  $l_e$ ,  $a$  and  $l_h$ . This is summarized in Table 6.7.

**Table 6.7:** Possible dimensions of the pyramidal horn antenna for various phase deviations  $s$  and  $t$

$s$	$b$	$l_e$
1/8	0.529 m	5.388 m
1/4	0.563 m	3.043 m
1/2	1.575 m	11.9 m
$t$	$a$	$l_h$
1/8	0.063 m	0.076 m
1/4	0.669 m	0.043 m
1/2	0.082 m	0.032 m
3/4	0.137 m	0.060 m

To be able to physically realize the horn antenna from calculated values for dimensions, the following relation shall be satisfied [73]:

$$(a - a_0)^2 \left[ \left( \frac{l_h}{a} \right)^2 - \frac{1}{4} \right] = (b - b_0)^2 \left[ \left( \frac{l_e}{b} \right)^2 - \frac{1}{4} \right] \quad (6.5)$$

Dimensions of the WR-159 waveguide are  $a_0 = 40.386$  mm and  $b_0 = 20.193$  mm. Using calculated values in Table 6.7, values for left and right side of the Equation 6.5 can be evaluated. This process is summarized in Table 6.8.

**Table 6.8:** *Verification of possible dimensions of the pyramidal horn antenna*

$b_0$	$b$	$l_e$	right side of the Equation 6.5
0.020193 m	0.529 m	5.388 m	26.793
	0.563 m	3.043 m	8.534
	1.575 m	11.9 m	137.397
$a_0$	$a$	$l_h$	left side of the Equation 6.5
0.040386 m	0.063 m	0.076 m	0.000612
	0.669 m	0.043 m	0.000116
	0.082 m	0.032 m	-0.000163
	0.137 m	0.060 m	-0.000534

As seen from Table 6.8, none of the values on the left and right sides of the Equation 6.5 are even close to each other — and the negative values on the evaluation of the left side are peculiar. Thus, it is proven that the pyramidal horn antenna can not be constructed. Therefore, an alternative designs shall be examined. One solution might be a compound horn where E- and H-plane flares are constructed in cascade — in which case restrictions of Equation 6.5 can be ignored. The other solution could be simple E-plane sectoral horn, which is now evaluated briefly.

In Table 6.7 we have already calculated the dimensions for the E-plane sectoral horn antenna from the universal radiation patterns in [73]. An antenna aperture width  $b = 0.56$ m and a slant length  $l_e = 3.04$  m should create the wanted beam width of  $5^\circ$ .

From [52] we can derive estimates for the total flare angle  $2\psi_e \approx 15^\circ$  and the length of the antenna  $\rho_1 \approx 45\lambda = 2.34$ m along the center line of the waveguide. From these values, the aperture length  $b$  of 0.575 m can be calculated, which also confirms that values derived from diagrams in [73] are accurate enough.

The uncertainty in the design of the E-plane sectoral horn antenna is the radiation pattern shape in the H-plane. Since in either of the cited books there is not any sort of calculation for a TE<sub>10</sub>-mode aperture distribution in free space (only infinite ground-plane geometries were evaluated), the radiation pattern in the H-plane is unknown — but with practical reasoning it can be deduced that the H-plane beam width cannot be narrower than in the pyramidal horn antenna. Therefore, the gain of the sectoral antenna design will certainly be lower than 20 dB and the whole frequency converter will not perform sufficiently.

In all, if any sort of horn antenna — sectoral, pyramidal or compound — is designed for wavelength of 0.052 m and beam widths of  $5^\circ$  and  $60^\circ$ , the physical dimensions of the antenna will become too impractical. Maybe the only choice is to use an antenna array to reduce the dimensions of the antenna, maybe a slot-antenna array would be a good



choice. This would probably lead to a custom made antenna, manufactured in a company that is specialized in antenna design.

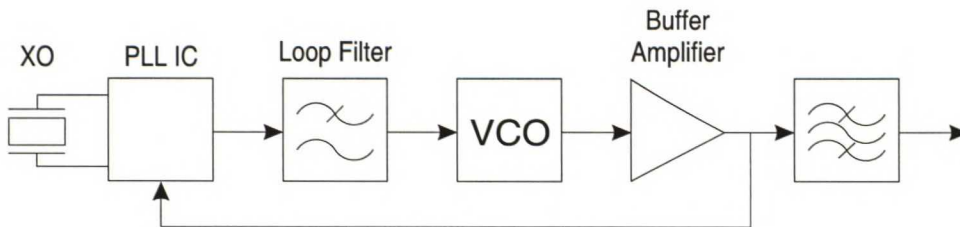
### 6.3.7 Local Oscillator

Even though the requirements for the LO are not of the most critical ones in the frequency converter design, the design and manufacturing of the phase-locked voltage-controlled oscillator (VCO) might prove to require the most work. Since the IF frequency (in UHF band) is not commonly used in conjunction with the 5.8 GHz ISM band, it is possible that no off-the-shelf component exists for the LO circuit. In that case, a more complex and time consuming design shall be adopted.

In this thesis, only a brief discussion is made about the design process of a phase-locked VCO circuit, since the amount of effort required to design the whole circuit is well beyond the scope of this thesis — the VCO circuit is just a one tiny part of the whole system.

A typical synthesized oscillator circuit consist of a VCO, a phase-locked loop (PLL) IC, a frequency reference (e.g. crystal oscillator) and a loop filter (a low-pass filter) [74]. Basically, the PLL circuit functions as follows: a sample of the RF signal is taken, pre-scaled and divided in a programmable divider. The stable reference oscillator, usually some sort of an XO, is also divided in order to provide wanted frequency steps in the LO output. Scaled RF and reference signals are compared in a phase-comparator, and from the result a driving signal to the VCO is derived. After some period of time, depending on the design of the loop filter, the VCO frequency will settle to a frequency derivable from division ratios and the reference frequency.

In order to fulfill the high output power requirement of the LO, a buffer amplifier is required after the VCO. In numerous commercial VCOs there is an integrated buffer amplifier, but the output power may still be too low to fully operate the mixer. Also, an output filter is implemented after the buffer amplifier to filter spurious responses from the LO signal before feeding the signal to the mixer, this will further reduce the output power — and further the need for buffer amplifier. The block diagram of the phase-locked VCO circuit designed for the frequency converter is presented in Figure 6.9.



**Figure 6.9:** Schematics for the local oscillator of the frequency converter. A phase-locked VCO will provide a stabile low phase-noise signal. The buffer amplifier circuit will amplify the signal to required output power of +13 dBm.

In Section 6.3.1, the mixer design was concluded with the following requirements for the local oscillator (LO). The LO frequency should be within 6.471–6.621 GHz, but

if no other choice exists, the lower mixing sideband (4.979–5.129 GHz) should also be attainable with the chosen mixer HMC219MS8. A tunable LO would be an advantage, since there is no knowledge what kind of transmissions there exists on the 5.8 GHz ISM band. The output power of +13 dBm is required for the mixer to perform as planned. The list of components from which the LO can be built is presented in Table 6.9 and the illustration of the fundamental design is shown in Figure 6.10. The individual components are introduced below.

As far as the author of this thesis has been able to deduce, there is only one commercial PLL circuit that is capable of comparing RF signals at frequencies over 6 GHz, the Analog Devices ADF4107 [75]. The ADF4107 has a bandwidth of 7 GHz, an RF input sensitivity is  $-5 - +5$  dBm, and the reference frequency can from 20 MHz to 250 MHz. It will provide a VCO tuning voltage of 0–5 V due to used charge pump technique, which will require an active loop filter circuit in order to drive a VCO requiring a wider tuning range (e.g. 0–10 V).

The reference signal of 20–250 MHz for the PLL circuit can be attained from a crystal oscillator. For required stability it is believed that basic crystal oscillator chip is sufficient, no temperature control or oven is required in the XO.

For the VCO, the Hittite HMC466LP4 [76] is a viable choice. It has tunable frequency range of 6.1–6.72 GHz while the tuning voltage range varied 0–10 V. The 6.471–6.621 GHz frequency range is attained with a tuning voltage of 4–7 V. It has an output power of +4.5 dBm, which requires substantial amplification to ensure the LO output power requirement +13 dBm.

The loop filter must be an active circuit, since the VCO tuning range is wider than the PLL can produce. The design of the loop filter will influence settling time and phase-noise characteristics of the RF signal. Low phase-noise levels should be preferred in the design, especially within the DVB-T signal bandwidth and close to the LO carrier, to prevent the deterioration of the OFDM signal.

The buffer amplifier can be implemented using the Hittite HMC392 [77]. It is designed as a low noise amplifier for 3.5–7.0 GHz, but it can be used as an LO driver, i.e. a buffer amplifier, for mixers. It has gain of 15.5 dB, which is little bit too high considering our requirements, so maybe a precision attenuator is required to lower the driver output power. The output power 1 dB compression point is about 13 to 16 dBm, but it should not cause the constant LO signal from deteriorating or disrupting too much.

The sampling of the VCO signal can be implemented with a directional coupler. The output power of the buffer amplifier is about 19 dBm and the sample level must be with  $-5 - +5$  dBm, so a coupling factor of 20 dB is required. The MECA Electronics, Inc. model 780-20-6.000 [70], a miniature directional coupler, should fulfill this requirement.

Before the LO signal is fed to the mixer, it shall be filtered to prevent spurious responses from deteriorating the mixing process. The filter must have a center frequency of 6.546 GHz and a pass-band bandwidth of 150 MHz (2.3% relative width). The 2.3% relative bandwidth might require a special filter. If it can be afforded, the Lark Engineer model 3B [46] could be a suitable component. With given requirements and a very sharp transition band, a ten (10) section filter should work, but has an insertion loss of ca. 4.5 dB.

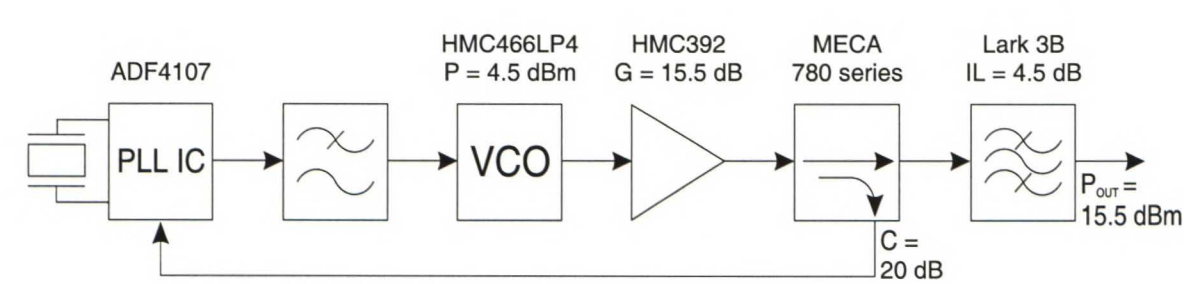
If an attenuator is required to lower the LO output power, it should be installed



between the LO output filter and the mixer LO port. Besides the wanted attenuation, an attenuator will also improve the matching on the mixer LO port, which is never a drawback.

**Table 6.9:** *List of chosen components for the construction of the LO*

Component	Model	Manufacturer	Parameters
PLL	ADF4107	Analog Devices	freq. range 0–7 GHz
VCO	HMC466LP4	Hittite	P = +4.5 dBm (6.1–6.72 GHz)
Buffer amplifier	HMC392	Hittite	G = 15.5 dBm
Directional coupler	780-20-6.000	MECA Elec.	C = 20 dB
LO filter	Lark 3B	Lark eng.	IL = 4.5 dB



**Figure 6.10:** *Chosen RF components for the local oscillator construct. Model for the reference oscillator and the exact design of the loop filter can be finalized when the construction of the LO begins.*

# Chapter 7

## Measuring the Performance of a DVB-T System

Before implementing a transmitter, its performance must be verified against some set of parameters. These parameters can be either in form of national broadcasting regulations, telecommunication standards or, simply, component specifications devised by the designer.

To verify the performance of a DVB-T system, the possible measurements can be divided into two parts. First, a single component or section of the DVB-T transmitter can be measured. Second, the overall performance (e.g. transmit power or reception area) can be measured for the built transmitter.

In the following sections, a short introduction about possible verification measurements for the frequency converter is given. For a good general description of possible measurements to verify the performance of a DVB system, ETSI has published guidelines for different measurements [78].

### 7.1 Linearity Measurements

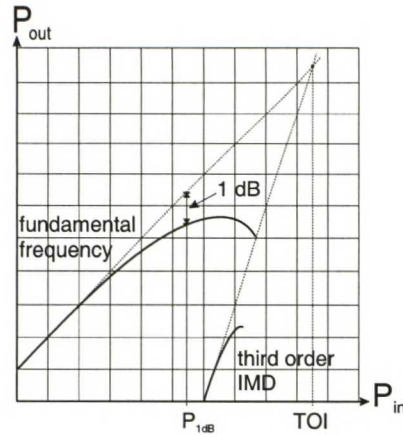
One of the basic measurements for an RF device is the scattering parameter (or S-parameter) measurement. This set of parameters is measured using a vector network analyzer (VNA) in order to get both the amplitude response and the phase response of the device, for given operation (bias) point. Usually, for a two-port device, the full S-parameter set (i.e.  $\mathbf{S}_{11}$ ,  $\mathbf{S}_{21}$ ,  $\mathbf{S}_{12}$  and  $\mathbf{S}_{22}$ ) is measured.

To attain a measure of the linearity for a device, the  $\mathbf{S}_{21}$  parameter (the input-output-port response) is of interest. This parameter can be measured while sweeping the input power  $P_{in}$ . The gain  $G$  of the device is the amplitude  $|\mathbf{S}_{21}|$ , from which the input-output power response  $P_{out}(P_{in})$ , and also the 1 dB compression point  $P_{1dB}$  can be calculated. Also, the phase response for swept input power  $P_{in}$  can be attained from the  $\mathbf{S}_{21}$  parameter. The input-output power response  $P_{out}(P_{in})$  and the 1 dB compression point  $P_{1dB}$  are illustrated in Figure 7.1.

The two-tone test is a basic measurement to evaluate non-linearities in a device. The idea of the two-tone test is to input two carrier signals, of equal or unequal power level, on close frequencies  $f_1$  and  $f_2$  into the device. Non-linearities in the device cause mixing



of these two signals. On the output of the device a spectrum can be measured. From the spectrum, frequencies  $2f_1 - f_2$  and  $2f_2 - f_1$  are the most interesting, since these are third order intermodulation distortion (IMD) signals produced by non-linearities in the device. By comparing levels of a third order IMD component with the input signal, a third order intercept point (TOI) can be extrapolated when power levels of input signals are varied [79]. This result illustrated in Figure 7.1. The TOI is widely used as the measure for the linearity of a device: higher the TOI, the higher is the linearity of the device.



**Figure 7.1:** *Illustration of results of two basic RF measurements. The 1 dB compression point  $P_{1dB}$  of a device can be measured using a single tone. The third order intercept point TOI requires two tones and the result must be extrapolated. (edited from [79])*

The problem with the two-tone test is that it gives a good measure of non-linearities in a device under simple signal conditions. To be able to measure the non-linear behavior of a device when a modern multi-tone modulation is used, a different set of measurements is needed. These measurements are: Adjacent Channel Power Ratio (ACPR), Noise Power Ratio (NPR), Multi-tone Intermodulation Ratio (M-IMR) and Shoulder Attenuation. The first three of these are discussed in [21], and the last is described in [78]. A brief examination of all of these is now conducted.

The Adjacent Channel Power Ratio (ACPR) measurement concept is illustrated in Figure 7.2. The ACPR is a measure for how much does the signal spread to a adjacent channel while amplified. The ACPR is defined as the ratio between power in the signal bandwidth  $B_1$  and power in bandwidth  $B_2$ , which is at defined offset  $f_o$  from the signal channels center frequency  $f_c$  [21].

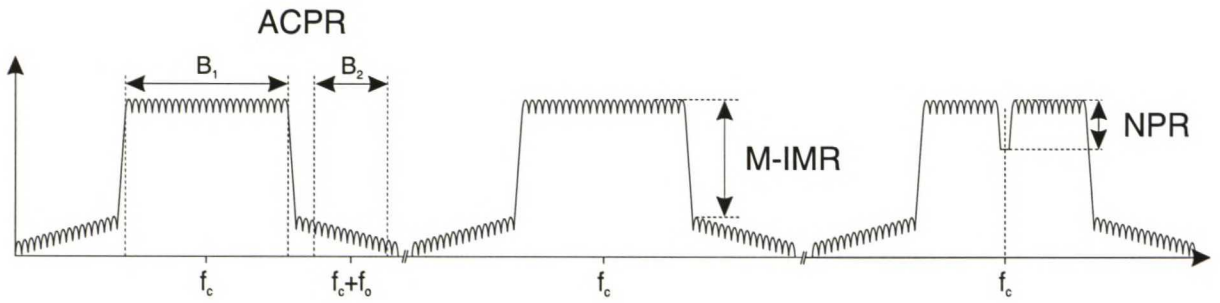
The ACPR concept is a well devised, when the requirement is towards the protection of other transmissions in the vicinity of the designated system is the primary concern. There is also a number of spectrum masks defined in the DVB-T standard [1] to control spurious transmissions of a DVB-T broadcast.

The concept of a Multi-tone Intermodulation Ratio (M-IMR) measurement is illustrated in Figure 7.2. The M-IMR is a measure of distortion caused by the non-linear amplification in a multi-carrier signal. The M-IMR is defined as a ratio between the wanted signal power and the intermodulation distortion just outside of the wanted signal

band [21].

The M-IMR measurement serves as a good indicator of the linearity of an amplifier, and also as the indicator of the system performance in all. Results from the measurement can be compared against specified spectrum masks, in the DVB-T specification [1] or in Figure 2.10. Or, simply compare the spectrum before and after the amplification in order to measure the risen level of the intermodulation distortion.

The idea of the Noise Power Ratio concept is to measure the unwanted in-channel distortion in the multi-tone signal, when it is amplified. The measurement can be achieved by attenuating a part of the multi-tone spectrum by using a notch filter, and then measuring the ‘filled-in’ noise in the notch after the amplification. This measurement concept is illustrated in Figure 7.2. The NPR is defined as the ratio between the measured noise power spectral density of the white noise in the center of the notch and the noise power spectral density measured without the notch filter [21].



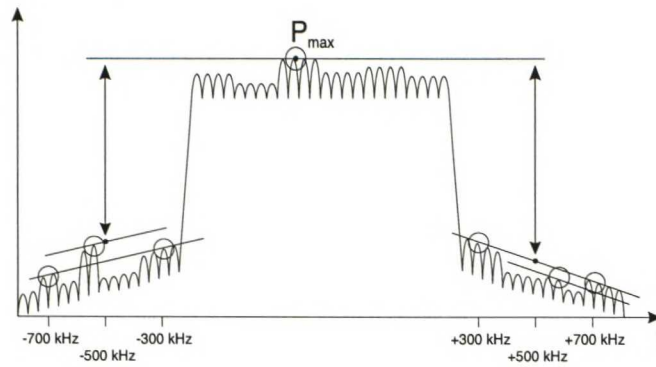
**Figure 7.2:** Concepts of the Adjacent Channel Power Ratio (ACPR), the Multitone Intermodulation Ratio (M-IMR), and the Noise Power Ratio (NPR) measurement. (edited from [21])

The Shoulder Attenuation measurement is used to characterize the linearity of an OFDM signal after it passes through a device. Comparing to the M-IMR, the attenuation is derived from values of more than one point in the spectrum. To derive the value of shoulder attenuation, the following procedure is described in [78] and is illustrated in Figure 7.3:

1. Make a note of the maximum power level  $P_{max}$  of the OFDM spectrum, using a resolution bandwidth at ca. ten (10) times the carrier spacing.
2. Place straight lines connecting the measured power levels at the offsets of 300 kHz and 700 kHz from the lower and upper edge of the OFDM signal. Draw additional lines parallel to these, so that the highest power level within the respective range lies on the line.
3. Subtract the power level value of the center of the line (at offset of 500 kHz from the upper and lower edge of the OFDM signal) from the maximum power level  $P_{max}$ , and use the worst case value as the measure of the shoulder attenuation.



By comparing the NPR concept with others introduced in this section, it is easy to see that it requires more specialized measurement system than the three others. For the ACPR, M-IMR and Shoulder Attenuation measurements, only a basic spectrum analyzer is required. Also, in the DVB-T specification there is no such value that could be compared with results given by the NPR measurement. In that sense, it seems that the NPR is the least useful concept while trying to measure the performance of a DVB-T transmitter.



**Figure 7.3:** *Concept of the Shoulder Attenuation measurement. Power levels are measured at offsets of 300 kHz and 700 kHz from the upper and lower edges of the OFDM signal. Comparing these to the power level between offsets, the shoulder attenuation can be then derived.*

## 7.2 Phase Noise Measurements

As noted in Section 2.5.3, the phase noise of a local oscillator (LO) is also a critical factor in the system performance. To measure the phase noise of a LO, there are different possibilities:

A basic spectrum analyzer can be used to measure the phase noise of a LO. The problem is that the spectrum analyzer has its own noisy LO, so a low phase noise LO cannot be measured this way. The phase noise level of the measured LO must be over 10 dB higher than of the spectrum analyzer [80]. Also, spectrum analyzer is designed to measure signal power not noise power, so the measured values must be corrected, which is nowadays handled by the spectrum analyzer itself [81], [82].

To measure a low phase noise LO, the amplitude modulation and carrier wave of the signal must be eliminated [80]. A delayed LO signal sampled with a 3 dB coupler setup will fulfill these requirements. The problem with the delay line measurement is that the required length of the delay line is usually too long to be practically realized. An alternative measurement setup to eliminate the carrier wave is called phase comparison, or dual oscillator method, measurement [80].

If a highly accurate, wide frequency range and short measurement time is required, a specialized phase noise measurement device should be considered (e.g. the Agilent E5500 models [83]).

The measured phase noise can be then compared with the required mask (Table 2.5 in Section 2.5.1). For a OFDM signal, the multiples of the sub-carrier spacing (1.116 kHz) are of great concern and especially these frequencies should be measured in addition to the wide frequency range phase noise performance [78].

### 7.3 System Level Measurements

To verify the performance of the whole broadcasting system, a different set of measurements can be made. Some of these measurements are similar to the multi-tone measurements made for a single component, but others result a measure of a system level performance. To acquire a full range of system level measurements to be performed, ETSI has published guidelines [78] for a verification of a DVB-T broadcast.

The multi-tone measurements described in Section 7.1, especially the ACPR, the M-IMR, and the shoulder attenuation measurement, can be used to verify the performance of a DVB-T broadcasting system. The spectrum at the input of the antenna can be compared against the specified spectrum mask (Figure 2.10 in Section 2.5.3), and also a more thorough measurement of spurious signals can be performed to the output signal spectrum. Comparing to the measurement of a single component, the system level measurement is even easier to make, since the multi-carrier signal is created in the system itself and no external signal generator is required.

For a transmitter, the output power can be measured by using a power meter. This result can be compared against broadcasting regulations, e.g. for 5 GHz ISM band the maximum EIRP is 25 mW. If an envelope analyzer, or fast diode sensor is available, the OFDM signal envelope power, or crest factor can be measured, respectively.

After the output spectrum and the output power level of the DVB-T transmitter is verified, it is possible to install the transmitter to the designated transmission point. This broadens available measurement choices. In the field, the received signal strength, or power level, can be measured as the receiver is transferred along a chosen path. That way the true reception area and log-distance path loss exponent  $n$  can be derived.

By using a DVB-T test receiver, it might be possible to derive the bit error rate (BER) for the whole broadcast system. To directly measure the BER of the broadcasting system, the whole input bit stream must be known. Then the received decoded bit stream is compared to this input stream, and the BER value can be calculated as the carrier-to-noise ratio (C/N) is varied.

To measure BER, in a much lower pace, a known constant bit combination that could be detected from the received broadcast, is required. In the DVB-T standard, there is no definition of a such constant bit combination useful for this purpose [9]. But, it seems that it is possible for the broadcaster to implement this kind of bit combination to the DVB-T transmission, by sacrificing some of the payload bit stream to implement a constant measurement stream. Also, it seems that it is possible to measure an indication of an error in the decoding process in the inner coder or the outer coder. By comparing this value and the throughput of the coder, an approximate of BER can be derived.



## Chapter 8

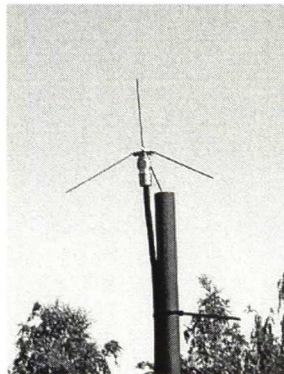
# Otadigi Reception Measurement

As pointed out in Chapter 5.1, the location of the ‘Otadigi’ DVB-T transmitter is not the best possible. Therefore, reception in Otaniemi area might not be as good as it could be. This would, in worst case, rule out the implementation of the relay-transmitter design of the frequency converter.

To evaluate this possibility, a small measurement campaign was devised to measure the ‘Otadigi’ DVB-T signal near the main measurement hall of the High Voltage Institute (marked as a square in Figure 5.1). The measurement was conducted with the following setup:

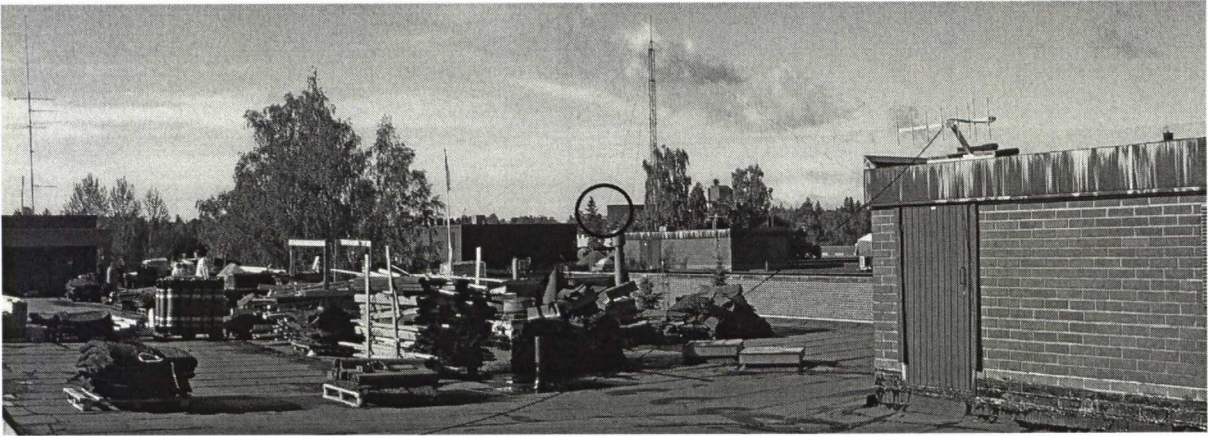
A quarter wave-length ( $\lambda \approx 40$  cm) monopole antenna was installed on top of the I-wing of the department of Electrical and Communications Engineering. The rooftop has a height of ca. 17 meters. The ‘Otadigi’ uses vertical polarization [37].

The antenna, shown in Figure 8.1, was at the height of about 1.5 meters from the roof. It was built from a female N-type RF connector. The antenna arm was quarter of a wave-length long (ca. 10 cm) and the ground-plane arms were one third of a wave-length (ca. 13 cm). An ideal monopole antenna above ground plane has a gain  $G$  of 5.15 dB [23], but this construction probably will not have as high gain as the ideal antenna — no verification measurement to ensure this was made, since there was no available shielded measurement space of required dimensions. The support structure of the antenna was constructed from a rigid plastic tube and some wooden boards.



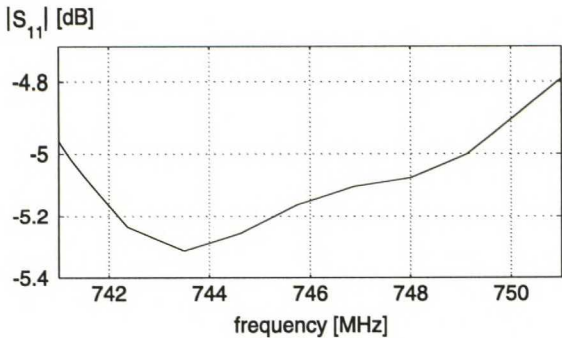
**Figure 8.1:**  $\lambda/4$  monopole antenna used in the ‘Otadigi’ DVB-T signal measurement.

The ‘Otadigi’ transmit antenna is barely visible behind all the buildings and trees, as shown in Figure 8.2. This suggests that the received signal would be degraded due to effects of multi-path propagation.



**Figure 8.2:** View from the measurement antenna towards the Ekono building where the ‘Otadigi’ transmitter is located. The ‘Otadigi’ antenna can be seen with bare eyes from the rooftop, but is circled in this figure. As can be noticed, the rooftop is currently under repair, and the repair equipment will certainly harm the reception of the UHF signal.

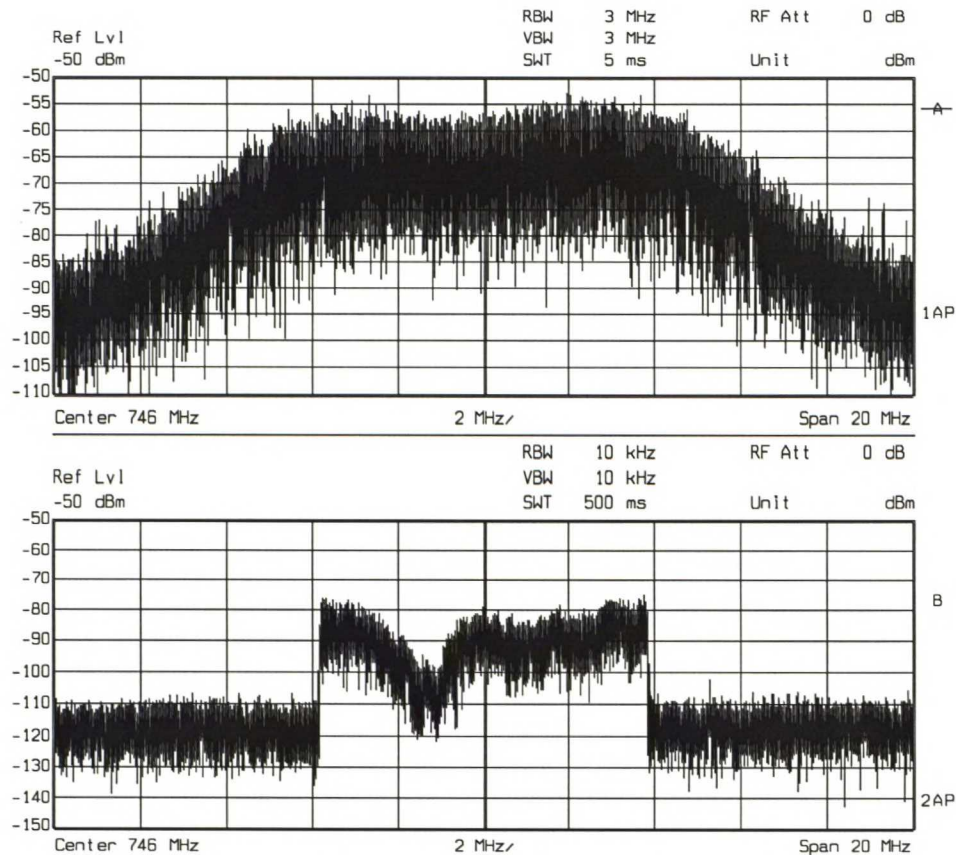
Signal was transferred to a spectrum analyzer in a room two floors down by using a semi-rigid coaxial cable (Acome Hypercell HPL50-1/4 F, M2930Z [84]). Total cable length was approximately 17 meters. Transmission losses of this cable were measured using a calibrated vector network analyzer (Hewlett Packard 8753D) and a short circuited termination on the antenna end of the cable. The short circuited termination can be approximated as an ideal and therefore the RF signal will fully reflect ( $|S_{11}| \approx 0$  dB). The transmission cable acts as an attenuator, thus, improving the matching. Therefore, cable losses are the half of the difference between 0 dB and the measured reflection coefficient  $|S_{11}|$  in Figure 8.3. A cable loss of 2.5 dB can be derived from results.



**Figure 8.3:** Results of the loss measurement for the transmission cable. Antenna port of the cable was terminated with a short circuit. Thus, cable losses of 2.5 dB can be derived from this VNA measurement.



The spectrum of the ‘Otadigi’ DVB-T signal was measured with a Rohde & Schwarz FSEA spectrum analyzer. The result is presented in Figure 8.4. From these wide resolution band width measurement (the upper section of the Figure), a signal power level of about -60 dBm can be derived, since the antenna gain was approximately 5 dB and cable losses were 2.5 dB. Also, The signal suffers from multi-path propagation effects, as seen from the lower section of the Figure 8.4. There are also distinct indications of a frequency selective fading, which is a phenomena related to the multi-path propagation environment. During the measurement, the region of maximum fading shifted a bit in both, frequency and power level, axes — maybe the workers repairing the rooftop caused the changing propagation environment.



**Figure 8.4:** Results of the ‘Otadigi’ DVB-T signal measurement. The location was at the top of the Department of Electrical and Communications Engineering. Cable losses were about 2.5 dB, and antenna gain was about 5 dB. Notice the different measurement settings on both spectrums. The distinct effect of multi-path propagation can be seen on the lower picture.

This result can be compared to a commonly used signal propagation model, the Hata model, mentioned in Section 4.6. The Hata model provides a median path loss in suburban

area, which is derived from the urban median path loss as follows [24]:

$$L_{50}(\text{urban})(\text{in dB}) = 69.55 + 26.16 \log f - 13.82 \log h_t - a(h_r) \\ + (44.9 - 6.55 \log h_t) \log d, \quad (8.1)$$

where  $f$  is the frequency (in MHz),  $h_t$  is the transmitter antenna height (in meters),  $h_r$  is the receiver antenna height (in meters), and  $d$  is the distance between the transmitter and the receiver (in km). The Hata model is valid for following parameter range:  $f = 150 - 1500$  MHz,  $h_t = 30 - 200$  m, and  $h_r = 1 - 10$  m. Also, the distance  $d$  should be over 1 km in order for the Hata model to compare closely with the Okumura curves. The antenna correction factor  $a(h_r)$  for small to medium sized cities is:

$$a(h_r) = (1.1 \log f - 0.7)h_r - (1.56 \log f - 0.8) \text{ dB} \quad (8.2)$$

To obtain the suburban median path loss from the urban path loss, the Hata model shall be modified as follows:

$$L_{50}(\text{suburban})(\text{in dB}) = L_{50}(\text{urban}) - 2 [\log(f/28)]^2 - 5.4 \quad (8.3)$$

These equations can now be evaluated for the measurement setup. The distance  $d$  from the ‘Otadigi’ transmitter to the measurement antenna was about 1.2 km. If the ground level variations are neglected (see the surface contour in Figure 5.2), the receiver height  $h_r \approx 10$  m. Also, the transmitter height will only be  $h_t \approx 25$  m. Thus, some of the parameters are slightly outside the valid range of the model, but if the model behaves smoothly, this should not cause too much uncertainty in the calculations. The calculated median path loss in the suburban environment  $L_{50}(\text{suburban})$  is ca. 98 dB.

A short derivation for received power  $P_r$  can be made: the ‘Otadigi’ transmitter antenna input port power  $P_t$  is 40 W (46 dBm). The transmit antenna is a dipole antenna, thus ideally has a gain  $G_t$  of 2.15 dB [23]. Since the receiver antenna gain  $G_r$  has been reduced from the measurement results,  $G_r = 0$  dB. Therefore, the received power  $P_r$  can be evaluated as follows:

$$P_r = P_t + G_t - L_{50}(\text{suburban}) + G_r \\ = 46 \text{ dBm} + 2.15 \text{ dB} - 98 \text{ dB} + 0 \text{ dB} \\ = -50 \text{ dBm}$$

This calculated power level of -50 dBm, from the Hata model, is 10 dB higher than the measured power level in Figure 8.4.

The Hata model only provides a median path loss value. It can be recalled from the log-distance path loss model, in Section 4.7, that the various different locations on the same distance from the transmitter can be accounted with a log-normal shadowing parameter  $X_\sigma$ . The remaining 10 dB of attenuation between the measured and the Hata model can be partially, at least about 3–6 dB [85], [86], accounted with this shadowing parameter.

This rather small residual deviation between the model and the measurement can be related to the validity range of the model — and the values derived measurement setup were near the limits of the valid range of the model.



Since the signal is deteriorated, due to multi-path propagational effects, there is only little basis to build a relay transmitter type of the frequency converter this far from the ‘Otadigi’ transmitter. The received signal might be better on top of the main measurement hall of the High Voltage Institute. But, as seen in Figure 8.2, the main building of the HUT will obscure the line-of-sight path, if the antenna is moved further westward — more to the right. Even though the antenna would be at a higher altitude, the loss of direct signal path between ‘Otadigi’ and frequency converter antennas could degrade the signal even further. At least, effects of multi-path propagation would be much stronger.

Therefore, the chimney of the Espoo Vesi power plant might be the best installation point for the relay type frequency converter. Actually, the Otaniemi water tower would also be the best choice for the relay-transmitter, if it would be permitted to be installed there.

# Chapter 9

## Conclusions

A practical design for the experimental frequency converter to serve as a basis for further studies in mobile DVB-T reception was introduced. The proposed directional coupler – mixer – power amplifier design should perform well in this kind of situation.

The link budget was calculated by gathering information from some of the more recent results in well-known publications, and the design parameters for the test transmitter were then derived. The 10 W EIRP transmitter design devised should be sufficient to cover the major part of the Otaniemi cape area. By reviewing current capabilities of commercial manufactured off-the-shelf components in the 5.8 GHz range, a block level design of the frequency converter was presented, while some single blocks still require some further work in detail. It is certain that an experimental transmitter can be constructed — and it is possible that even better components are present when the implementation begins.

For the future work, the following hindrances ought to be resolved:

- In 5.8 GHz ISM band, the maximum transmit power is ca. 14 dBm EIRP, and to cover the whole Otaniemi area an output power of 40 dBm is required. Therefore, some effort to acquire a license from the local Communications Regulatory Authority is required.
- The best location for the experimental frequency converter, the Otaniemi water tower, is the other end point of the antenna measurement range used by VTT Radio Technology, which they protect from nearby radio interference. So, some effort to cooperate with VTT shall be made, to allow even ‘every now and then’ tests to be run from the Otaniemi water tower. Also, a practical way to transfer the signal from the ‘Otadigi’ transmitter to the top of the Otaniemi water tower shall be devised. The relay type converter would possibly work in a short spanned link like in this situation, or losses of UHF transmission cabling between the current ‘Otadigi’ location and the water tower can be tolerated, with some minor design changes.
- A horn antenna was proven to be too impractical in physical dimensions when realizing required beam widths. Therefore, some other kind of antenna design must be completed. A slot-antenna array of some sort might work.



# Bibliography

- [1] *Digital Video Broadcasting (DVB); Framing structure, channel coding and modulation for digital terrestrial television*, European Telecommunications Standards Institute (ETSI), January 2001, European Standard (Telecommunications series) EN 300 744, v1.4.1.
- [2] J. Henriksson, "DVB-X," *DVB Scene*, no. 5, p. 7, March 2003, a quarterly magazine of the DVB Project, URL: <http://www.dvb.org/>.
- [3] *IEEE Std 802.11a-1999, Part 11: Wireless LAN Medium Access Control (MAC) and Physical Layer (PHY) specifications - High-speed Physical Layer in the 5 GHz Band*, LAN/MAN Standards Committee of the IEEE Computer Society, 1999, Supplement to IEEE Std 802.11-1999, editor: Hitoshi Takanashi.
- [4] M. Johnson, "HiperLAN/2 - The Broadband Radio Transmission Technology Operating in the 5 GHz Frequency Band," HiperLAN/2 Global Forum, URL: <http://www.hiperlan2.com/>, White Paper, 1999, version 1.0.
- [5] G. Durgin, T. S. Rappaport, and H. Xu, "Measurements and models for radio path loss and penetration loss in and around homes and trees at 5.85 GHz," *IEEE Transactions on Communications*, vol. 46, no. 11, pp. 1484–1496, November 1998.
- [6] X. Zhao, J. Kivinen, P. Vainikainen, and K. Skog, "Propagation characteristics for wideband outdoor mobile communications at 5.3 GHz," *IEEE Journal on Selected Areas in Communications*, vol. 20, no. 3, pp. 507–514, April 2002.
- [7] "OtaDigi: Finnish digital television experimenting project," March 2003, WWW-pages, URL: <http://www.otadigi.net/index.html>, are mainly in Finnish, but there is an English section.
- [8] V.-H. Kilpiä and P. Eskelinen, "An experimental frequency converter for DVB-T transmitter tests," to be presented at The European Conference on Wireless Technology (ECWT), October 9–10, 2003, has been accepted and is submitted to be published in the proceedings.
- [9] P. Dambacher, *Digital Terrestrial Television Broadcasting - Designs, Systems and Operation*. Springer-Verlag, 1998, translated by Horst E. von Renouard, BA, MIL, BDÜ.
- [10] J. Vermasvuori, "Digi-TV:n lähetystekniikkaa," *Sähkö & Tele*, no. 5, pp. 23–28, 2002.

- [11] Y. Wu, "Performance comparison of ATSC 8-VSB and DVB-T COFDM transmission systems for digital television terrestrial broadcasting," *IEEE Transactions on Consumer Electronics*, vol. 45, no. 3, pp. 916–924, August 1999.
- [12] R. Burow *et al.*, "On the performance of the DVB-T system in mobile environments," in *Proceedings of IEEE Global Telecommunications Conference, GLOBECOM 98*, vol. 4, November 1998, pp. 2198–2204.
- [13] I. Gaspard, "Mobile reception of the terrestrial DVB-system," in *Proceedings of the 49th IEEE Vehicular Technology Conference*, vol. 1, May 1999, pp. 151–155.
- [14] B. Franca *et al.*, "DTV report on COFDM and 8-VSB performance, FCC/OET 99-2," Federal Communications Commission, Office of Engineering and Technology, Tech. Rep., September 1999.
- [15] J. C. McKinney and R. Hopkins, "Guide to the use of the ATSC Digital Television Standard, Doc. A/54," Advanced Television Systems Committee (ATSC), Technical Guide, October 1995.
- [16] B. Fox, "Digital TV Rollout," *IEEE Spectrum*, vol. 38, no. 2, pp. 65–67, February 2001.
- [17] P. Schmidt, "ISDB-T - Digital terrestrial broadcasting in Japan," *News from Rohde & Schwarz*, no. 177, pp. 32–36, 2003, (2003/I).
- [18] "Transmission Systems for Digital Terrestrial Broadcasting – From Hi-Vision to Mobile Multimedia," NHK (Japan Broadcasting Company) Science & Technical Research Laboratories, URL: <http://www.nhk.or.jp/strl/open99/de-2/index.html>, WWW-page, 1999, visited on March, 2003.
- [19] *Digital Video Broadcasting (DVB); Implementation guidelines for DVB terrestrial services; Transmission aspects*, European Telecommunications Standards Institute (ETSI), December 1997, Tech. Rep. TR 101 190, v1.1.1.
- [20] *Digital Video Broadcasting (DVB); OFDM modulation for microwave digital terrestrial television*, European Telecommunications Standards Institute (ETSI), September 2000, European Standard (Telecommunications series) EN 301 701, v1.1.1.
- [21] P. B. Kenington, *High-Linearity RF Amplifier Design*. Artech House, Inc., 2000.
- [22] C. Heinemann, "Compact exciter for digital terrestrial TV," *News from Rohde & Schwarz*, no. 177, pp. 40–41, 2003, (2003/I).
- [23] A. Räisänen and A. Lehto, *Radiotekniikka*, 8th ed. Otatieto Oy, 1993.
- [24] T. S. Rappaport, *Wireless Communications - Principles & Practice*. Prentice Hall PTR, 1996.
- [25] H. L. Bertoni, *Radio Propagation for Modern Wireless Systems*. Prentice Hall PTR, 2000.



- [26] I. Lindell, *Radioaaltojen eteneminen*, 4th ed. Otatieto Oy, 1985.
- [27] O. Landron, M. J. Feuerstein, and T. S. Rappaport, "A comparison of theoretical and empirical reflection coefficients for typical exterior wall surfaces in a mobile radio environment," *IEEE Transactions on Antennas and Propagation*, vol. 44, no. 3, pp. 341–351, March 1996.
- [28] O. Klemola and A. Lehto, *Tutkatekniikka*, 2nd ed. Otatieto Oy, 1998.
- [29] B. Sklar, "Rayleigh Fading Channels in Mobile Digital Communication Systems – Part I: Characterization," *IEEE Communications Magazine*, vol. 35, no. 7, pp. 90–100, July 1997.
- [30] H. Masui, T. Kobayashi, and M. Akaike, "Microwave path-loss modeling in urban line-of-sight environments," *IEEE Journal on Selected Areas in Communications*, vol. 20, no. 6, pp. 1151–1155, August 2002.
- [31] *Propagation data and prediction methods for the planning of short-range outdoor radiocommunication systems and radio local area networks in the frequency range 300 MHz to 100 GHz*, International Telecommunications Union Radiocommunication Section ITU-R, 2001, Recommendation ITU-R P.1411-1.
- [32] T. Schwengler and M. Gilbert, "Propagation models at 5.8 GHz - path loss & building penetration," *Radio and Wireless Conference, RAWCON 2000*, pp. 119–124, 2000.
- [33] J. Kivinen, T. O. Korhonen, P. Aikio, R. Gruber, P. Vainikainen, and S.-G. Häggman, "Wideband radio channel measurement system at 2 GHz," *IEEE Transactions on Instrumentation and Measurement*, vol. 48, no. 1, pp. 39–44, February 1999.
- [34] J. Kivinen, "Development of wideband radio channel measurement and modeling techniques for future radio systems," Thesis for the degree of Doctor of Technology, Helsinki University of Technology, Espoo, 2001.
- [35] K. Sakawa *et al.*, "Microwave path-loss characteristics in an urban area with base station antenna on top of a tall building," *International Zurich Seminar on Broadband Communications*, pp. 31–1 – 31–4, February 2002.
- [36] VTT Information Technology, "VTT:lle lupa digi-TV-koelähetystoimintaan," Press release, July 2002, the text is in Finnish.
- [37] "Correspondence between Ville Ollikainen (Senior Research Scientist in VTT Information Technology) and Ville-Hermanni Kilpiä," 2003, correspondence was conducted via e-mail and telephone.
- [38] "Conversation between Pertti Luukkonen (Master Workman, Utilization at Espoon Vesi) and Ville-Hermanni Kilpiä," May 2003, conversation was conducted via telephone.

- [39] "Correspondence between Jari Ahonen (Surveyor at Land Surveying unit, city of Espoo) and Ville-Hermanni Kilpiä," April 2003, correspondence was conducted via e-mail.
- [40] *Broadband Radio Access Networks (BRAN); HIPERLAN Type 2; Physical (PHY) layer*, European Telecommunications Standards Institute (ETSI), December 2001, Tech. Spec. TS 101 475, v1.3.1.
- [41] "HIPERLAN/2," European Telecommunications Standards Institute (ETSI), URL: <http://portal.etsi.org/bran/kta/hiperlan/hiperlan2tech.asp>, Technical Overview, 2003, page updated: 2003-05-22 08:53:06.
- [42] "Radiocommunications: Frequency Allocation Table 3400 MHz – 31,000 GHz," Finnish Communications Regulatory Authority, URL: <http://www.ficora.fi/>, Frequency Allocation Table, March 2003.
- [43] *MAX2648, 5GHz to 6GHz Low-Noise Amplifier in 6-Pin UCSP*, Maxim Integrated Products, Inc., URL: <http://www.maxim-ic.com/>, January 2001, doc # 19-1894, revision 0.
- [44] *5.8 GHz Basestation Filter*, Q Microwave, Inc., April 2003, URL: [http://www.qmicrowave.com/5.8GHz\\_Product\\_Line.pdf](http://www.qmicrowave.com/5.8GHz_Product_Line.pdf).
- [45] *HMC218MS8, GaAs MMIC Double-Balanced Mixer, 4.5 - 6 GHz*, Hittite Microwave Corp., URL: <http://www.hittite.com/>, v01.0300.
- [46] *RF & Microwave Filters Catalog*, Lark Engineering Comp., URL: <http://www.larkengineering.com/>, 2002.
- [47] J. D. Kraus, *Radio astronomy*, 2nd ed. Cygnus-Quasar Books, 1986.
- [48] *Universal Mobile Telecommunications System (UMTS); Selection procedures for the choice of radio transmission technologies of the UMTS*, European Telecommunications Standards Institute (ETSI), April 1998, Tech. Rep. TR 101 112, v3.2.0.
- [49] T. Taga, "Analysis for mean effective gain of mobile antennas in land mobile radio environments," *IEEE Transactions on Vehicular Technology*, vol. 39, no. 2, pp. 117–131, May 1990.
- [50] K. Kalliola *et al.*, "Angular power distribution and mean effective gain of mobile antenna in different propagation environments," *IEEE Transactions on Vehicular Technology*, vol. 51, no. 5, pp. 823–838, September 2002.
- [51] R. Seppänen, S. Tiihonen, *et al.*, *MAOL-taulukot*, 2nd ed. Kustannusosakeyhtiö Otava, 1991, editor: Riitta Happonen.
- [52] C. A. Balanis, *Antenna Theory - Analysis and Design*. Harper & Row, Publishers, Inc., 1982.



- [53] "Conversation between Pertti Strömmer (Project Manager at Espoon Sähkö Oyj) and Ville-Hermanni Kilpiä," May 2003, conversation was conducted via telephone.
- [54] L. E. Larson, Ed., *RF and Microwave Circuit Design for Wireless Communication*. Artech House, 1996.
- [55] *HMC219MS8, GaAs MMIC SMT Double-Balanced Mixer, 4.5 - 9 GHz*, Hittite Microwave Corp., URL: <http://www.hittite.com/>, v01.0801.
- [56] *HMC168C8, GaAs MMIC SMT Double-Balanced Mixer, 4.5 - 8 GHz*, Hittite Microwave Corp., URL: <http://www.hittite.com/>, v01.0801.
- [57] *Introducing Hittite GaAs MMIC Mixers*, Hittite Microwave Corp., URL: <http://www.hittite.com/>, February 2000, application Note.
- [58] *HMC141/142 Mixer Operation Note*, Hittite Microwave Corp., URL: <http://www.hittite.com/>, February 2000, v01.05.00.
- [59] *HMC141 / HMC142, GaAs MMIC Double-Balanced Mixer, 6 - 18 GHz*, Hittite Microwave Corp., URL: <http://www.hittite.com/>, v01.0801.
- [60] *HMC143 / HMC144, GaAs MMIC Double-Balanced Mixer, 5 - 20 GHz*, Hittite Microwave Corp., URL: <http://www.hittite.com/>, v01.0801.
- [61] *How to select a mixer*, Mini-Circuits Corp., September 1999, Application Note.
- [62] *K 02252 D-64 - Double screened coaxial cable*, Huber+Suhner AG, URL: <http://www.hubersuhner.com>, Document: TEMP\_PDB\_23005576.PDF, Issued: 25.6.2002 16:01.
- [63] *SF 106PE - SUCOFLEX 100, the flexible, high performance microwave cable*, Huber+Suhner AG, URL: <http://www.hubersuhner.com>, Document: TEMP\_PDB\_22511150.PDF, Issued: 29.4.2003 08:43.
- [64] *Rectangular Waveguide Reference Specifications*, Gabriel electronics, Inc., URL: <http://www.gabrielnet.com/>.
- [65] *HMC408LP3, GaAs InGaP HBT MMIC 1 Watt Power Amplifier, 5.1 - 5.9 GHz*, Hittite Microwave Corp., URL: <http://www.hittite.com/>, v01.0702.
- [66] *HMC406MS8G, GaAs InGaP HBT MMIC Power Amplifier, 5.0 - 6.0 GHz*, Hittite Microwave Corp., URL: <http://www.hittite.com/>, v02.1202.
- [67] *HMC320MS8G, GaAs MMIC Low Noise Amplifier, 5.0 - 6.0 GHz*, Hittite Microwave Corp., URL: <http://www.hittite.com/>, v00.0900.
- [68] *MAX2649, 5GHz Low-Noise Amplifier with Shutdown*, Maxim Integrated Products, Inc., URL: <http://www.maxim-ic.com/>, July 2002, doc # 19-2492, revision 0.
- [69] *HMC318MS8G, GaAs MMIC Low Noise Amplifier with AGC, 5.0 - 6.0 GHz*, Hittite Microwave Corp., URL: <http://www.hittite.com/>, v00.0900.

- [70] *Signal Control Product Catalog*, MECA Electronics, Inc., URL: <http://www.e-meca.com/>, Catalog dated: 12/03/02.
- [71] *Agilent 355C/D, VHF Attenuators dc to 1 GHz*, Agilent Technologies, Inc., URL: <http://www.agilent.com/>, June 2001, Data Sheet 5952-0922.
- [72] *UNAT-SERIES N-Type Fixed Attenuators, DC to 6000 MHz*, Mini-Circuits Corp., URL: <http://www.minicircuits.com/>, REV. A M82480 ED-10269 UNAT-SERIES URJ/LC/CP 020801.
- [73] H. Jasik, Ed., *Antenna Engineering Handbook*, 1st ed. McGraw-Hill Book Company, Inc., 1961.
- [74] *VCO Designer's Handbook 2001*, Mini-Circuits Corp., Division of Scientific Components, 13 Neptune Avenue, Brooklyn, NY 11235.
- [75] *ADF4107, PLL Frequency Synthesizer*, Analog Devices, Inc., URL: <http://www.analog.com/>, May 2003, REV. 0.
- [76] *HMC466LP4, MMIC VCO w/ Buffer Amplifier, 6.1 - 6.72 GHz*, Hittite Microwave Corp., URL: <http://www.hittite.com/>, v00.0503.
- [77] *HMC392, GaAs MMIC Low Noise Amplifier, 3.5 - 7.0 GHz*, Hittite Microwave Corp., URL: <http://www.hittite.com/>, v00.1002.
- [78] *Digital Video Broadcasting (DVB); Measurement guidelines for DVB systems*, European Telecommunications Standards Institute (ETSI), May 2001, Tech. Rep. TR 101 290, v1.2.1.
- [79] A. Lehto and A. Räisänen, *Mikroaaltomittaustekniikka*, 4th ed. Otatieto Oy, 1999.
- [80] J. Säily, "Vähäkohinaiset paikallisoskilaattoriratkaisut millimetri- ja alimillimetriaaltoalueelle (Low-Noise Local Oscillator Configurations for Millimeter and Submillimeter Wavelengths)," Master's thesis, Helsinki University of Technology, December 1997.
- [81] B. Peterson, *Spectrum Analysis Basics*, Agilent Technologies, Inc., 2000, Application Note 150 (5952-0292).
- [82] J. Wolf, *Phase Noise Measurements with Spectrum Analyzers of the FSE family*, Rohde & Schwarz, October 1995, Application Note 1EPAN 16E.
- [83] *Agilent E5500 Series: Phase Noise Measurement Solution*, Agilent Technologies, Inc., 2000, Product Overview 5965-7590E.
- [84] *HYPERCELL 2002 - Cables and accessories for radiocommunication networks*, Acome, division radio videocommunication, URL: <http://www.acome.com/>, (ref: DRDV 12/2001 133 An).



- [85] R. D. Stevens and I. J. Dilworth, "Mobile radio shadowing loss variability and co-channel signal correlation at 452 MHz," *IEEE Electronics Letters*, vol. 32, no. 1, pp. 16–17, January 1996.
- [86] S. Aguirre, K. C. Allen, and M. G. Laflin, "Signal strength measurements at 915 MHz and 1920 MHz in an outdoor microcell environment," in *1st International Conference on Universal Personal Communications (ICUPC '92)*, 29 Sep - 1 Oct 1992, pp. 01.04/1–01.04/7.

# Appendices

Hittite Microwave corp. HMC219MS8	data sheet
Hittite Microwave corp. HMC408LP3	data sheet
Hittite Microwave corp. HMC320MS8G	data sheet
Q Microwave Inc. '5.8 GHz Basestation Filter'	data sheet



# HMC219MS8

## GaAs MMIC SMT DOUBLE-BALANCED MIXER, 4.5 - 9 GHz

### Typical Applications

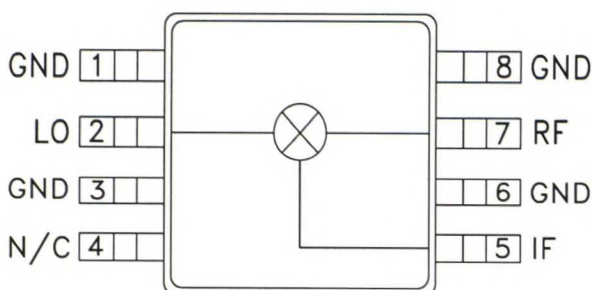
The HMC219MS8 is ideal for:

- UNII & HiperLAN
- ISM
- Microwave Radios

### Features

- Ultra Small Package: MSOP8
- Conversion Loss: 8.5 dB
- LO / RF Isolation: 25 dB

### Functional Diagram



### General Description

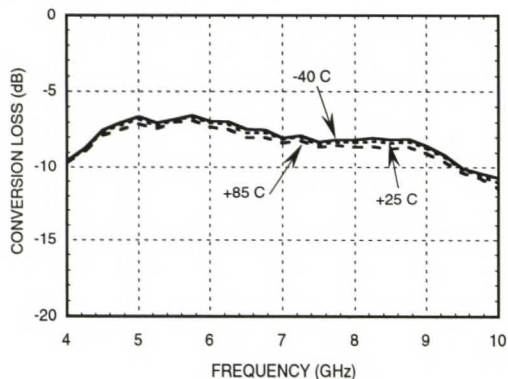
The HMC219MS8 is an ultra miniature double-balanced mixer in an 8 lead plastic surface mount package (MSOP). This passive MMIC mixer is constructed of GaAs Schottky diodes and novel planar transformer baluns on the chip. The device can be used as an upconverter, downconverter, bi-phase (de)modulator, or phase comparator. The consistent MMIC performance will improve system operation and assure regulatory compliance.

### Electrical Specifications, $T_A = +25^\circ\text{C}$ , As a Function of LO Drive

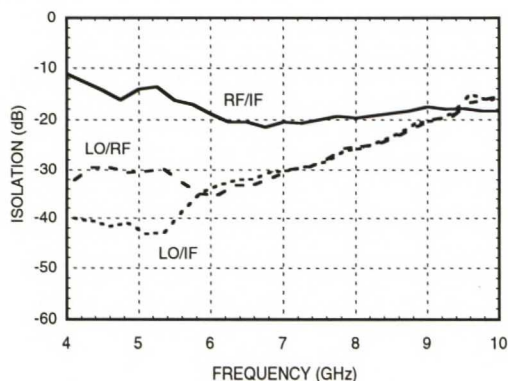
Parameter	LO = +13 dBm IF = 100 MHz			LO = +11 dBm IF = 100 MHz			Units
	Min.	Typ.	Max.	Min.	Typ.	Max.	
Frequency Range, RF & LO	4.5 - 9.0			4.5 - 8.6			GHz
Frequency Range, IF	DC - 2.5			DC - 2.5			GHz
Conversion Loss		8.5	10		8.5	10	dB
Noise Figure (SSB)		8.5	10		8.5	10	dB
LO to RF Isolation	17	25		20	25		dB
LO to IF Isolation	17	25		20	25		dB
IP3 (Input)	15	21		15	21		dBm
1 dB Gain Compression (Input)	7	10		5	8		dBm

## GaAs MMIC SMT DOUBLE-BALANCED MIXER, 4.5 - 9 GHz

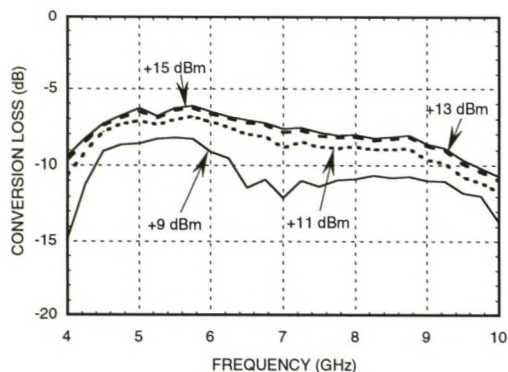
**Conversion Loss vs Temperature @ LO = +13 dBm**



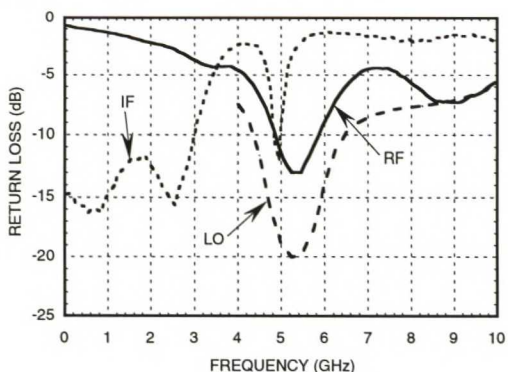
**Isolation @ LO = +13 dBm**



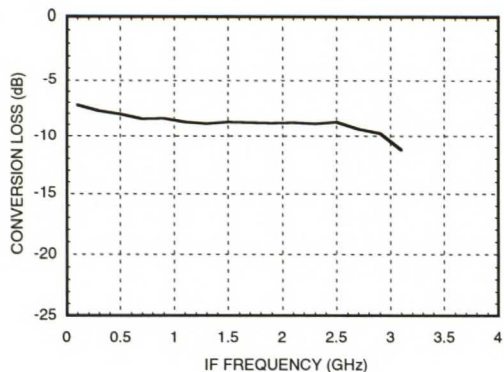
**Conversion Loss vs. LO Drive**



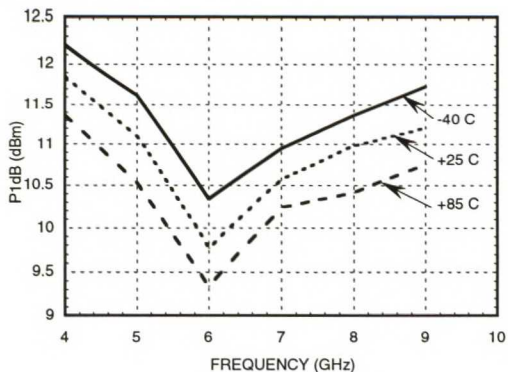
**Return Loss @ LO = +13 dBm**



**IF Bandwidth @ LO = +13 dBm**



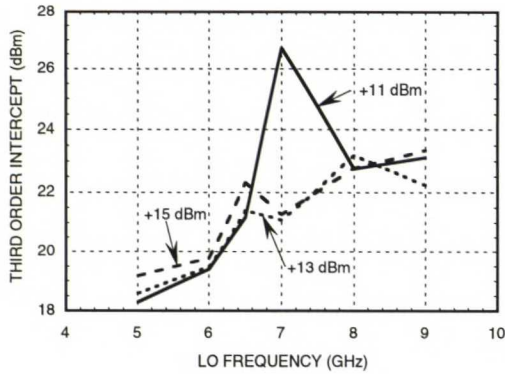
**P1dB vs. Temperature LO = +13 dBm**



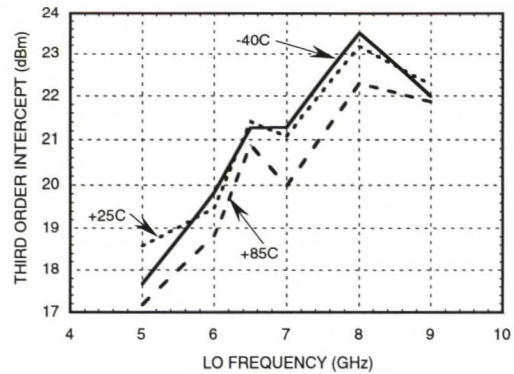


## GaAs MMIC SMT DOUBLE-BALANCED MIXER, 4.5 - 9 GHz

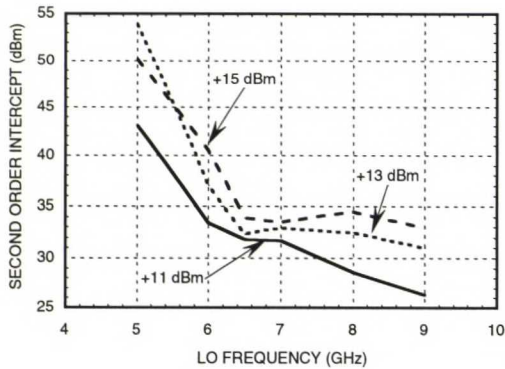
**Input IP3 vs. LO Drive**



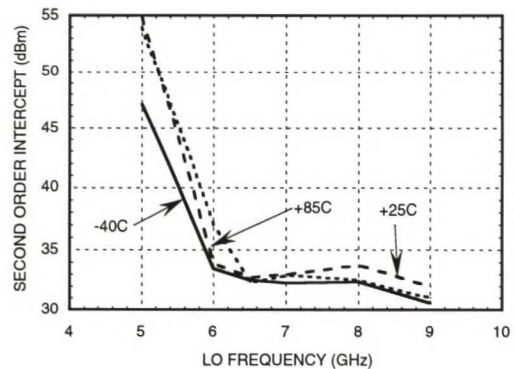
**Input IP3 vs. Temperature @ LO = +13 dBm**



**Input IP2 vs. Drive**



**Input IP2 vs. Temperature @ LO = +13 dBm**



**MxN Spurious Outputs**

mRF	nLO				
	0	1	2	3	4
0	xx	12.2	22.3	20.7	33.9
1	13.2	0	36.9	36.7	49.5
2	79.8	53.7	47.7	55.4	68.1
3	>105	>105	78.1	65.5	83.1
4	>105	>105	>105	98.1	87.1

RF = 6 GHz @ -10 dBm  
LO = 6.1 GHz @ +13 dBm  
All values in dBc below the IF power level (-1RF + 1LO).

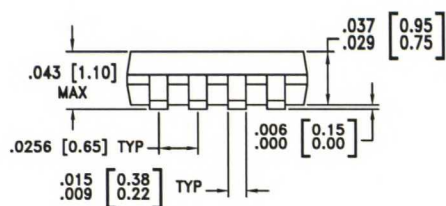
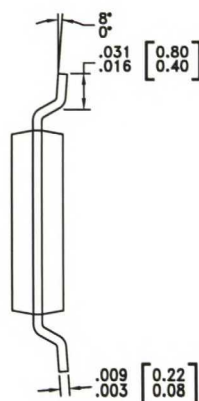
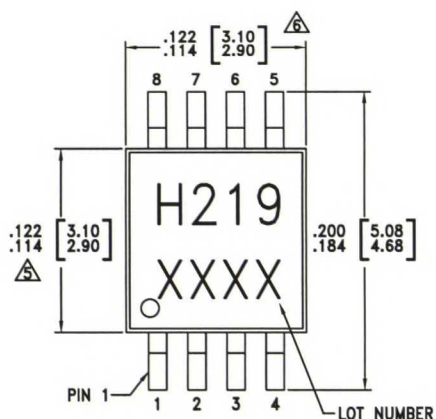
**Harmonics of LO**

LO Freq. (GHz)	nLO Spur at RF Port			
	1	2	3	4
4.0	33	29	39	54
5.0	31	23	34	47
6.0	35	21	40	55
7.0	31	26	53	xx
8.0	27	32	54	xx
9.0	21	43	xx	xx

LO = +13 dBm  
Values in dBc below input LO level measured at the RF port.

**GaAs MMIC SMT DOUBLE-BALANCED MIXER, 4.5 - 9 GHz**
**Absolute Maximum Ratings**

RF / IF Input	+13 dBm
LO Drive	+27 dBm
Storage Temperature	-65 to +150 °C
Operating Temperature	-40 to +85 °C

**Outline Drawing**

**NOTES:**

1. PACKAGE BODY MATERIAL: LOW STRESS INJECTION MOLDED PLASTIC SILICA AND SILICON IMPREGNATED.
2. LEADFRAME MATERIAL: COPPER ALLOY
3. LEADFRAME PLATING: Sn/Pb SOLDER
4. DIMENSIONS ARE IN INCHES [MILLIMETERS].
- △ DIMENSION DOES NOT INCLUDE MOLDFLASH OF 0.15mm PER SIDE.
- △ DIMENSION DOES NOT INCLUDE MOLDFLASH OF 0.25mm PER SIDE.
7. ALL GROUND LEADS MUST BE SOLDERED TO PCB RF GROUND.



# HMC408LP3

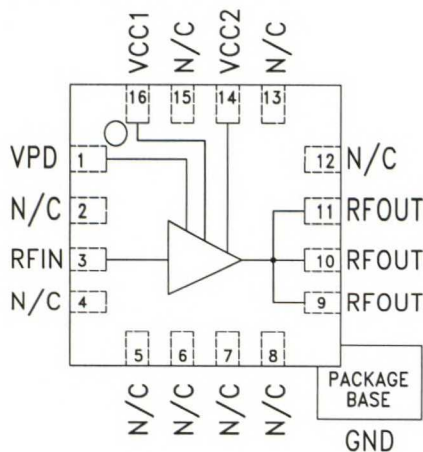
## GaAs InGaP HBT MMIC 1 WATT POWER AMPLIFIER, 5.1 - 5.9 GHz

### Typical Applications

The HMC408LP3 is ideal for:

- 802.11a & HiperLAN WLAN
- UNII & Pt-Pt / Multi-Pt. Radios
- Access Point Radios

### Functional Diagram



TOP VIEW

### Features

- Gain: 20 dB
- Saturated Power: +32.5 dBm @ 27% PAE
- Single Supply Voltage: +5.0 V
- Power Down Capability
- 3x3 mm Leadless SMT Package

### General Description

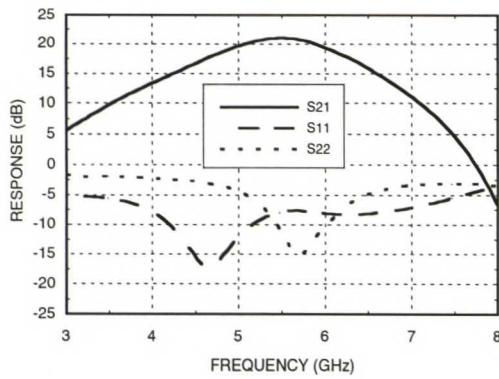
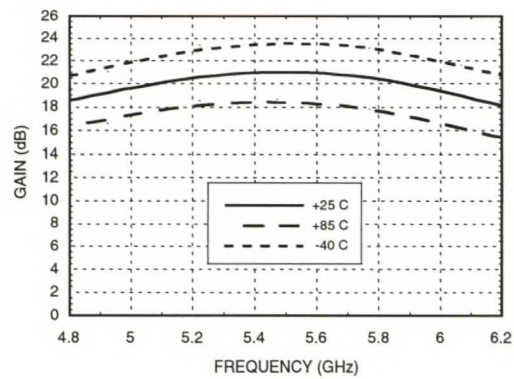
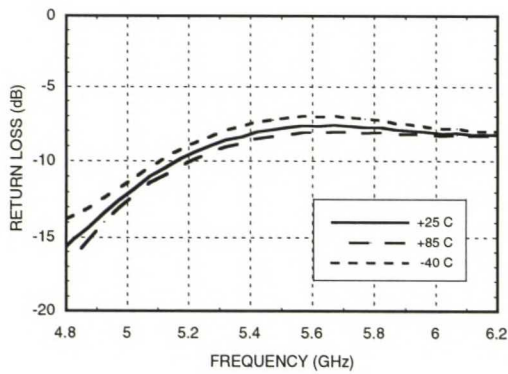
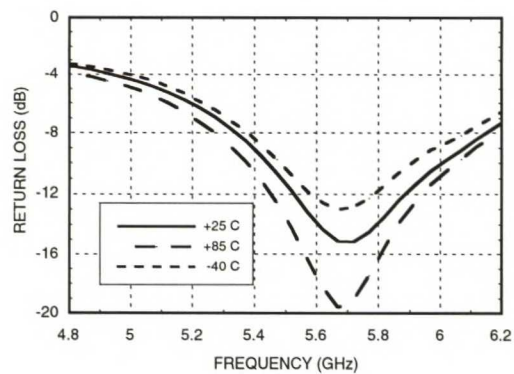
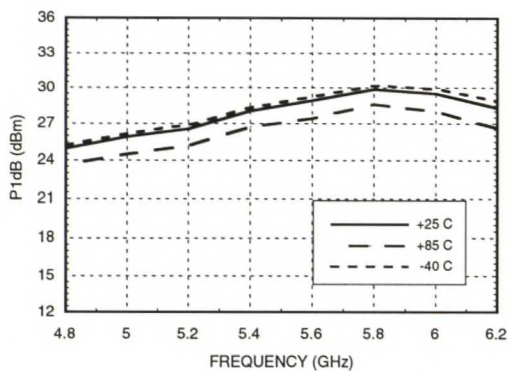
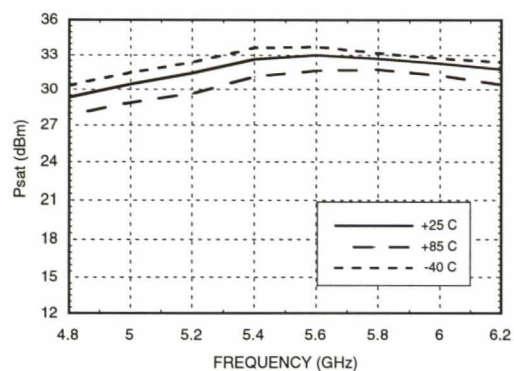
The HMC408LP3 is a 5.1 - 5.9 GHz high efficiency GaAs InGaP Heterojunction Bipolar Transistor (HBT) Power Amplifier MMIC which offers +30 dBm P1dB. The amplifier provides 20 dB of gain, +32.5 dBm of saturated power, and 27% PAE from a +5.0V supply voltage. The input is internally matched to 50 Ohms while the output requires a minimum of external components. Vpd can be used for full power down or RF output power/current control. The amplifier is packaged in a low cost, 3x3 mm leadless surface mount package with an exposed base for improved RF and thermal performance.

### Electrical Specifications, $T_A = +25^\circ\text{C}$ , $V_s = 5\text{V}$ , $V_{pd} = 5\text{V}$

Parameter	Min.	Typ.	Max.	Min.	Typ.	Max.	Units
Frequency Range	5.7 - 5.9			5.1 - 5.9			GHz
Gain	17	20		17	20		dB
Gain Variation Over Temperature		0.045	0.055		0.045	0.055	dB/°C
Input Return Loss		8			8		dB
Output Return Loss*		14			6		dB
Output Power for 1 dB Compression (P1dB)	27	30		24	27		dBm
		27			23		
Saturated Output Power (Psat)		32.5			31		dBm
Output Third Order Intercept (IP3)	40	43		36	39		dBm
Harmonics, Pout= 30 dBm, F= 5.8 GHz	2 fo	-50			-50		dBc
		-90			-90		
Noise Figure		6			6		dB
Supply Current (Icq)	Vpd= 0V/5V		0.002 / 750			0.002 / 750	mA
Control Current (Ipd)	Vpd= 5V		14			14	mA
Switching Speed	tOn, tOff		50			50	ns

\* Output match optimized for 5.7 - 5.9 GHz operation. See Application Circuit herein.

For price, delivery, and to place orders, please contact Hittite Microwave Corporation:  
12 Elizabeth Drive, Chelmsford, MA 01824 Phone: 978-250-3343 Fax: 978-250-3373  
Order Online at [www.hittite.com](http://www.hittite.com)

**GaAs InGaP HBT MMIC 1 WATT  
 POWER AMPLIFIER, 5.1 - 5.9 GHz**
**Broadband Gain & Return Loss**

**Gain vs. Temperature**

**Input Return Loss vs. Temperature**

**Output Return Loss vs. Temperature\***

**P1dB vs. Temperature**

**Psat vs. Temperature**


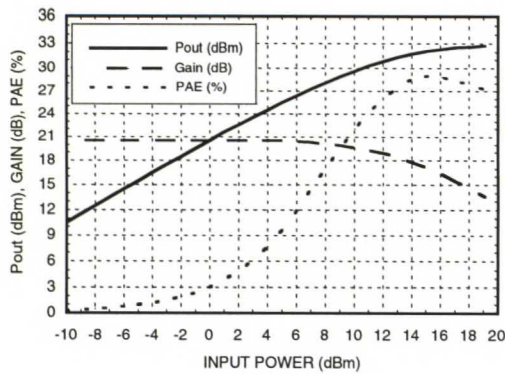
\* Output match optimized for 5.7 - 5.9 GHz.

For price, delivery, and to place orders, please contact Hittite Microwave Corporation:  
 12 Elizabeth Drive, Chelmsford, MA 01824 Phone: 978-250-3343 Fax: 978-250-3373  
 Order Online at [www.hittite.com](http://www.hittite.com)

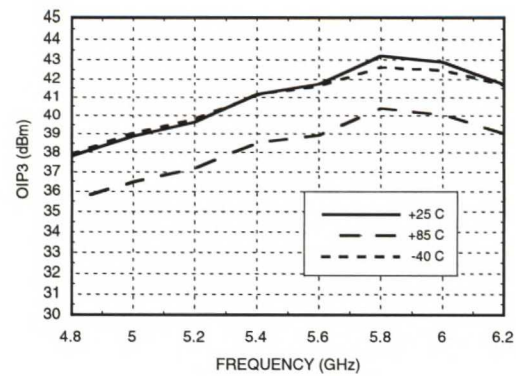


## GaAs InGaP HBT MMIC 1 WATT POWER AMPLIFIER, 5.1 - 5.9 GHz

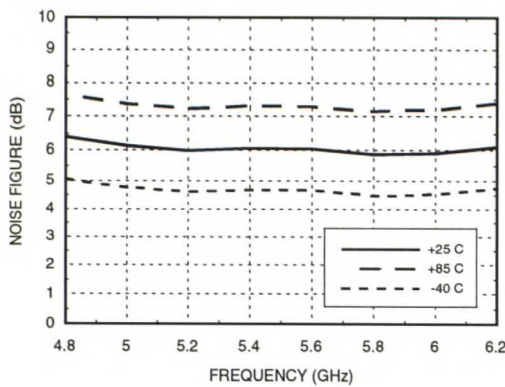
**Power Compression @ 5.8 GHz**



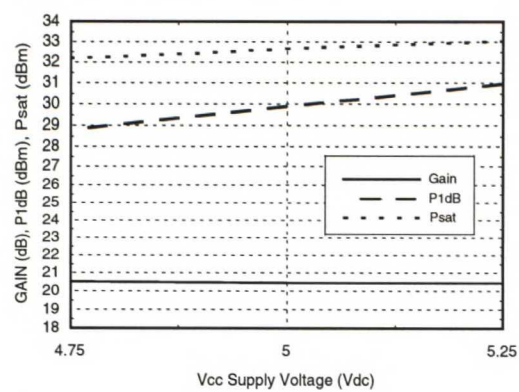
**Output IP3 vs. Temperature**



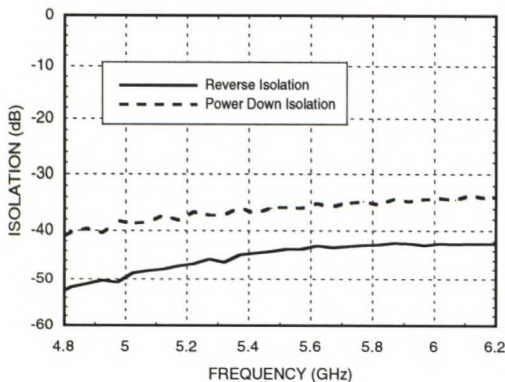
**Noise Figure vs. Temperature**



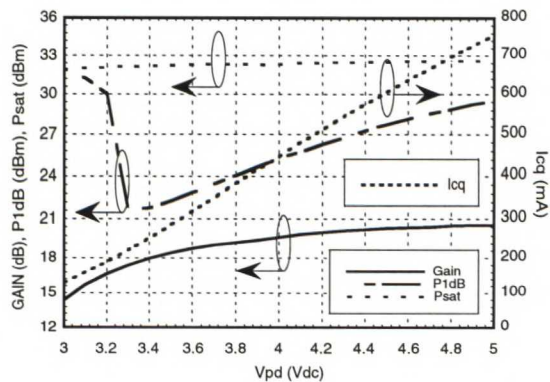
**Gain & Power vs.  
Supply Voltage @ 5.8 GHz**



**Reverse Isolation vs. Temperature**



**Gain, Power & Quiescent  
Supply Current vs. Vpd @ 5.8 GHz**



## GaAs InGaP HBT MMIC 1 WATT POWER AMPLIFIER, 5.1 - 5.9 GHz

### Absolute Maximum Ratings

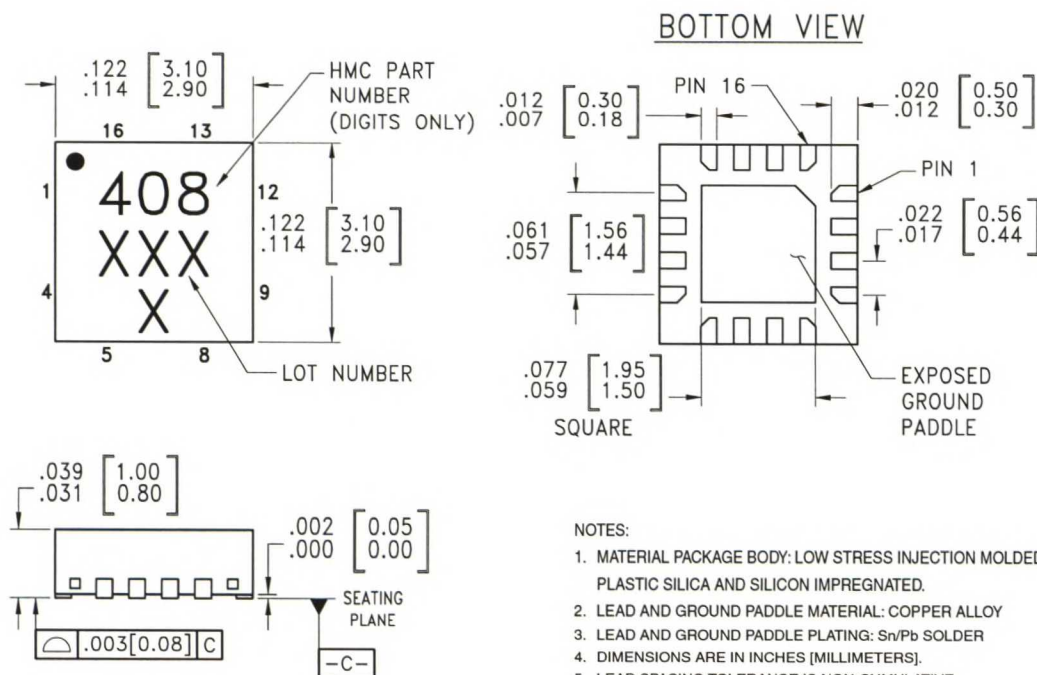
Supply Voltage (Vcc)	+5.5 Vdc
Control Voltage (Vpd)	+5.5 Vdc
Input Power (RFIn)	+20 dBm
Channel Temperature	150 °C
Continuous P <sub>diss</sub> (T= 85 °C) (derate 72.5 mW/°C above 85 °C)	4.71 W
Storage Temperature	-65 to +150 °C
Operating Temperature	-40 to +85 °C

### Typical Supply Current vs. V<sub>s</sub>= V<sub>cc1</sub> + V<sub>cc2</sub>

V <sub>s</sub> (V)	I <sub>cq</sub> (mA)
4.75	725
5.0	750
5.25	780

Note: Amplifier will operate over full voltage range shown above

### Outline Drawing



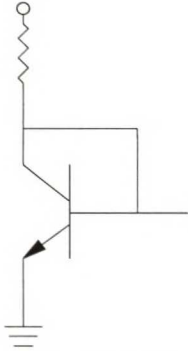

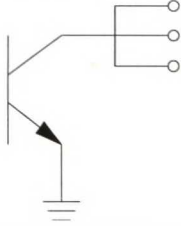
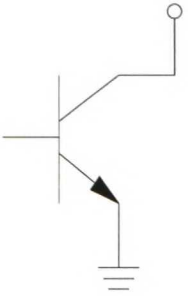

#### NOTES:

1. MATERIAL PACKAGE BODY: LOW STRESS INJECTION MOLDED PLASTIC SILICA AND SILICON IMPREGNATED.
2. LEAD AND GROUND PADDLE MATERIAL: COPPER ALLOY
3. LEAD AND GROUND PADDLE PLATING: Sn/Pb SOLDER
4. DIMENSIONS ARE IN INCHES [MILLIMETERS].
5. LEAD SPACING TOLERANCE IS NON-CUMULATIVE
6. PAD BURR LENGTH SHALL BE 0.15mm MAXIMUM.  
PAD BURR HEIGHT SHALL BE 0.05mm MAXIMUM.
7. PACKAGE WARP SHALL NOT EXCEED 0.05mm.
8. ALL GROUND LEADS AND GROUND PADDLE MUST BE SOLDERED TO PCB RF GROUND.



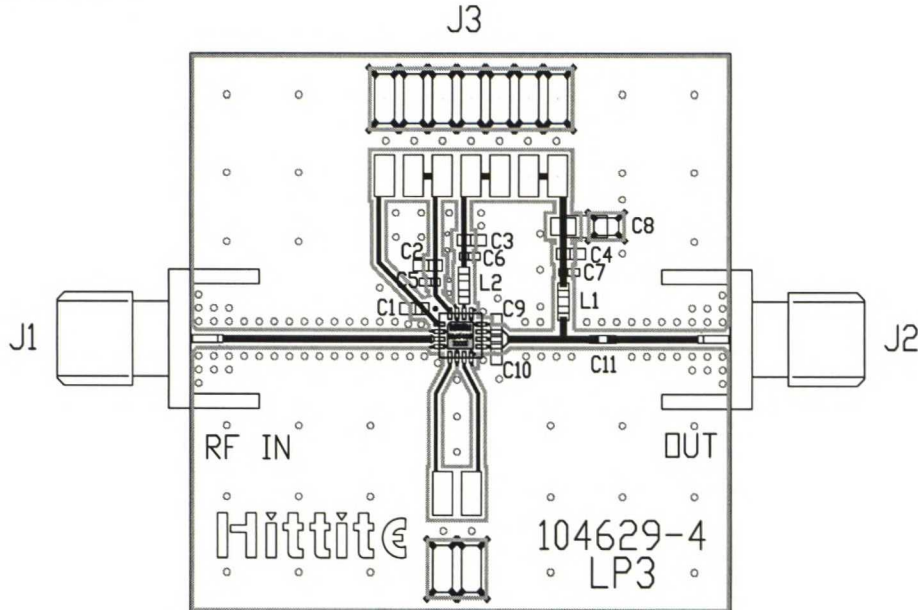
## *GaAs InGaP HBT MMIC 1 WATT POWER AMPLIFIER, 5.1 - 5.9 GHz*

### Pin Descriptions

Pin Number	Function	Description	Interface Schematic
1	Vpd	Power control pin. For maximum power, this pin should be connected to 5.0V. A higher voltage is not recommended. For lower idle current, this voltage can be reduced.	
2, 4, 5 - 8, 12, 13, 15	N/C	No Connection	
3	RF IN	This pin AC coupled and matched to 50 Ohms from 5.1 - 5.9 GHz.	
9, 10, 11	RF OUT	RF output and DC bias for the output stage.	
14	Vcc2	Power supply voltage for the second amplifier stage. External bypass capacitors and pull up choke are required as shown in the application schematic.	
16	Vcc1	Power supply voltage for the first amplifier stage. External bypass capacitors are required as shown in the application schematic.	
	GND	Ground: Backside of package has exposed metal ground slug that must be connected to ground thru a short path. Vias under the device are required.	

**GaAs InGaP HBT MMIC 1 WATT  
POWER AMPLIFIER, 5.1 - 5.9 GHz**

**Evaluation PCB**



**List of Material**

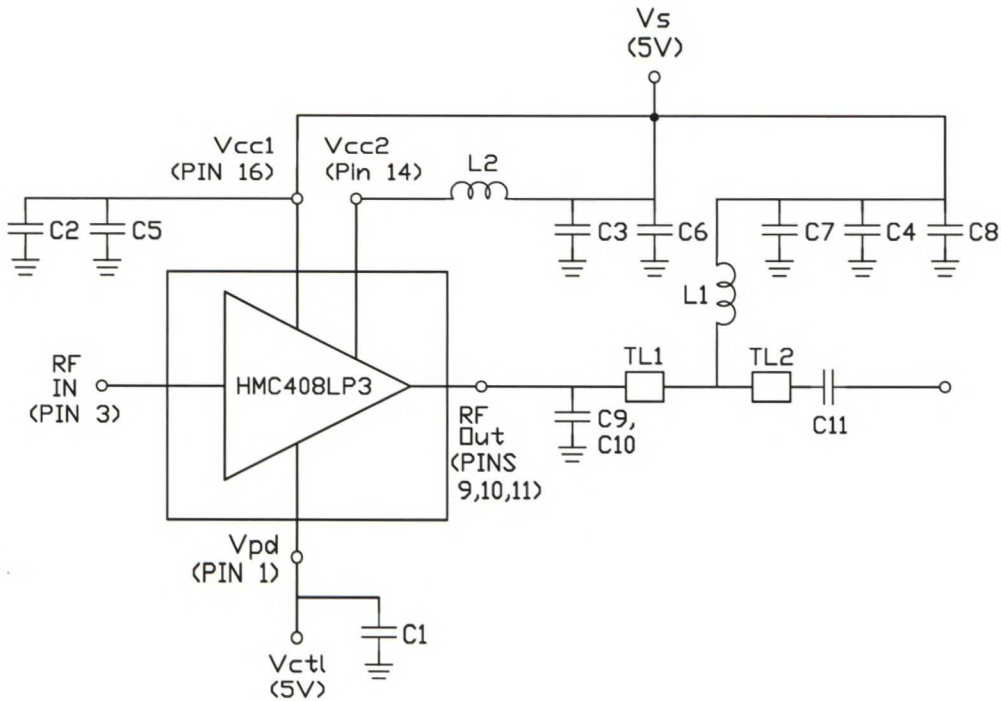
Item	Description
J1 - J2	PC Mount SMA RF Connector
J3	2 mm DC Header
C1 - C4	1,000 pF Capacitor, 0603 Pkg.
C5 - C7	100 pF Capacitor, 0402 Pkg.
C8	2.2 $\mu$ F Tantalum Capacitor
C9 - C10	0.5 pF Capacitor, 0603 Pkg.
C11	10 pF Capacitor, 0402 Pkg.
L1 - L2	1.6 nH Inductor, 0603 Pkg.
U1	HMC408LP3 Amplifier
PCB*	104629 Eval Board
* Circuit Board Material: Rogers 4350	

The circuit board used in the final application should use RF circuit design techniques. Signal lines should have 50 ohm impedance while the package ground leads and exposed paddle should be connected directly to the ground plane similar to that shown. A sufficient number of VIA holes should be used to connect the top and bottom ground planes. The evaluation board should be mounted to an appropriate heat sink. The evaluation circuit board shown is available from Hittite upon request.



## GaAs InGaP HBT MMIC 1 WATT POWER AMPLIFIER, 5.1 - 5.9 GHz

### Application Circuit



Recommended Component Values	
L1, L2	1.6 nH
C1 - C4	1,000 pF
C5 - C7	100 pF
C8	2.2 $\mu$ F
C9 - C10	0.5 pF

	TL1	TL2
Impedance	50 Ohm	50 Ohm
Length	0.200"	0.100"

Note 1: C9, C10 should be located < 0.020" from pins 9, 10, & 11.

Note 2: Application circuit values shown are optimized for 5.7 - 5.9 GHz operation.

Contact our Applications Engineers for optimization of output match for other frequencies.

For price, delivery, and to place orders, please contact Hittite Microwave Corporation:  
12 Elizabeth Drive, Chelmsford, MA 01824 Phone: 978-250-3343 Fax: 978-250-3373  
Order Online at [www.hittite.com](http://www.hittite.com)



v01.0702

## HMC408LP3

***GaAs InGaP HBT MMIC 1 WATT  
POWER AMPLIFIER, 5.1 - 5.9 GHz***

***Notes:***

8

AMPLIFIERS - SMT



# HMC320MS8G

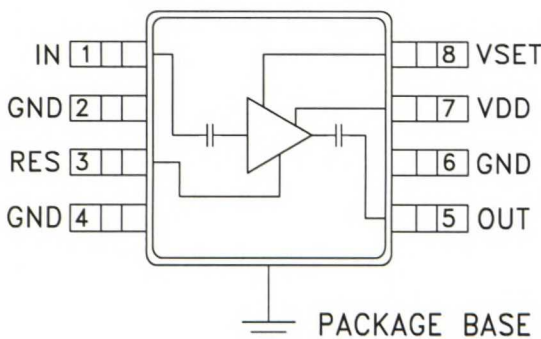
## GaAs MMIC LOW NOISE AMPLIFIER , 5.0 - 6.0 GHz

### Typical Applications

The HMC320MS8G is ideal for:

- UNII
- HiperLAN

### Functional Diagram



### Features

Selectable Functionality:  
LNA, Driver, or LO Buffer Amp  
Adjustable Input IP3 Up to +10 dBm  
+3V Operation  
Ultra Small 8 Lead MSOP:  
14.8 mm<sup>2</sup> x 1mm High

### General Description

The HMC320MS8G is a low cost C-band fixed gain Low Noise Amplifier (LNA). The HMC320MS8G operates using a single positive supply that can be set between +3V and +5V. With +3V bias, the LNA provides a noise figure of 2.5dB, 12dB gain and better than 10dB return loss across the UNII band. The HMC320MS8G also features adaptive biasing that allows the user to select the optimal P1dB performance for their system using an external set resistor on the "RES" pin. P1dB performance can be set between a range of +1 dBm to +13dBm. The low cost LNA uses an 8-leaded MSOP ground base surface mount plastic package, which occupies less than 14.8mm<sup>2</sup>.

### Electrical Specifications, $T_A = +25^\circ\text{C}$ , $V_{DD} = +3V$

Parameter	Low Power* (VSET = 0V, Idd = 7 mA)			Medium Power* (VSET = 3V, Idd = 25 mA)			High Power* (VSET = 3V, Idd = 40 mA)			Units
	Min.	Typ.	Max.	Min.	Typ.	Max.	Min.	Typ.	Max.	
Frequency Range	5 - 6			5 - 6			5 - 6			GHz
Gain	8	10	16	8	12	16	9	13	16	dB
Gain Variation over Temperature		0.025	0.035		0.025	0.035		0.025	0.035	dB/°C
Gain Flatness		±0.5			±1.0			±1.5		dB
Noise Figure		2.7	3.8		2.5	3.8		2.6	3.8	dB
Input Return Loss	4	10		4	10		4	10		dB
Output Return Loss	7	13		10	18		10	20		dB
Output Power for 1 dB Compression (P1dB)	-4	-1		6	9		9	12		dBm
Input Third Order Intercept Point (IIP3)	-3	1		4	8		6	10		dBm
Supply Current (Idd)		7			25			40		mA

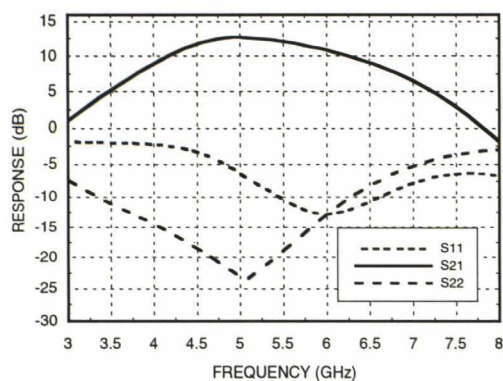
\*  $R_{BIAS}$  resistor value sets current. See adaptive biasing application note.

For price, delivery, and to place orders, please contact Hittite Microwave Corporation:  
12 Elizabeth Drive, Chelmsford, MA 01824 Phone: 978-250-3343 Fax: 978-250-3373  
Order Online at [www.hittite.com](http://www.hittite.com)

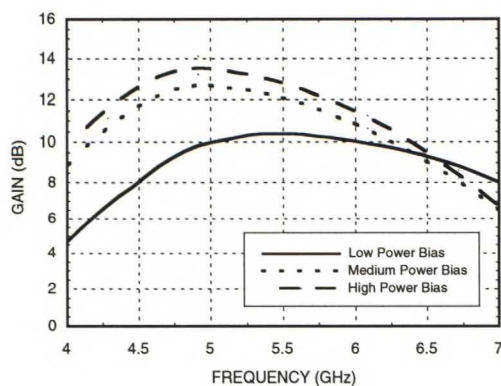
# HMC320MS8G

## GaAs MMIC LOW NOISE AMPLIFIER, 5.0 - 6.0 GHz

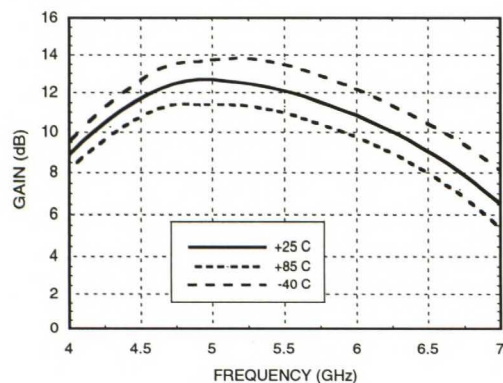
### Broadband Gain & Return Loss Medium Power Bias



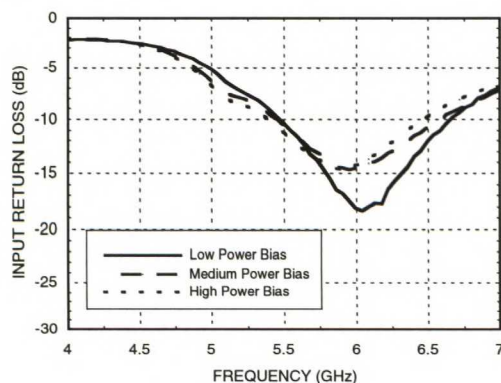
### Gain @ Three Bias Conditions



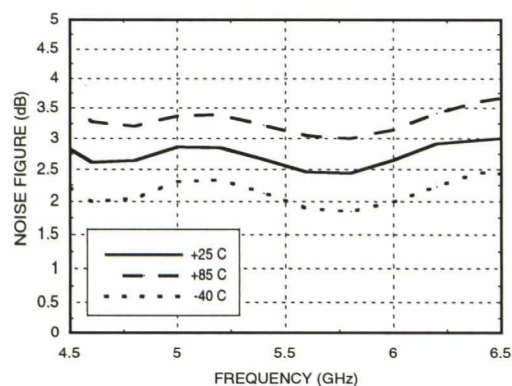
### Gain vs. Temperature Medium Power Bias



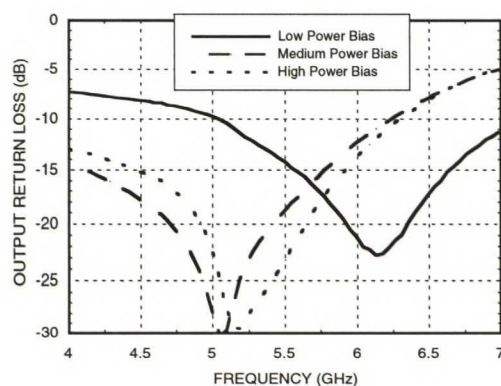
### Input Return Loss @ Three Bias Conditions



### Noise Figure vs. Temperature Medium Power Bias



### Output Return Loss @ Three Bias Conditions





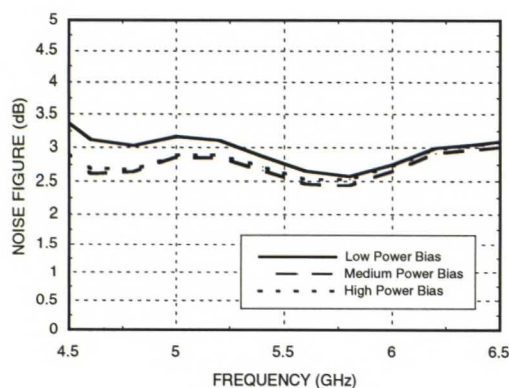


v00.0900

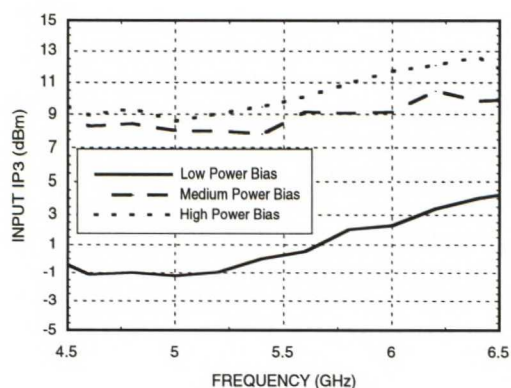
# HMC320MS8G

## GaAs MMIC LOW NOISE AMPLIFIER, 5.0 - 6.0 GHz

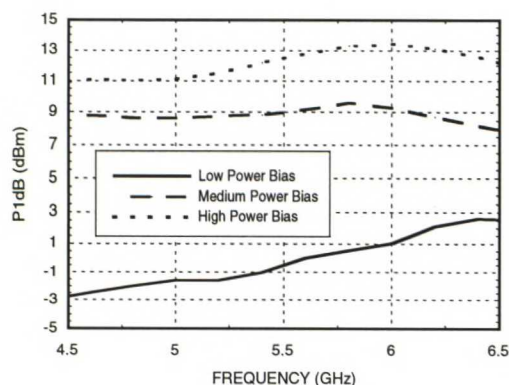
Noise Figure  
@ Three Bias Conditions



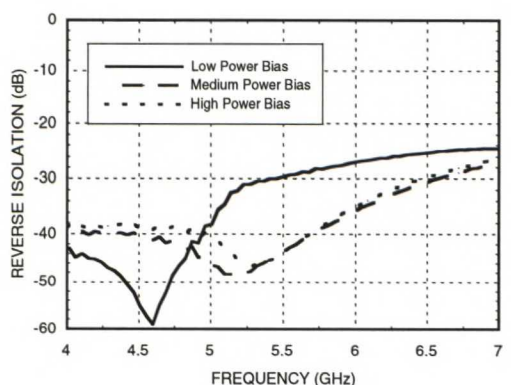
Input IP3 @ Three Bias Conditions



Output 1dB Compression  
@ Three Bias Conditions



Reverse Isolation  
@ Three Bias Conditions



### Adaptive Biasing

#### Optimizing P1dB Performance

The bias level may be changed to adjust the P1dB and return loss performance. The table below contains the HMC320MS8G RF performance as a function of various VSET and RBIAS settings. It will be necessary for the VSET voltage source to provide 100uA of current to the amplifier. The Idd and Vdd quiescent performance will not change as a function of changing the VSET voltage.

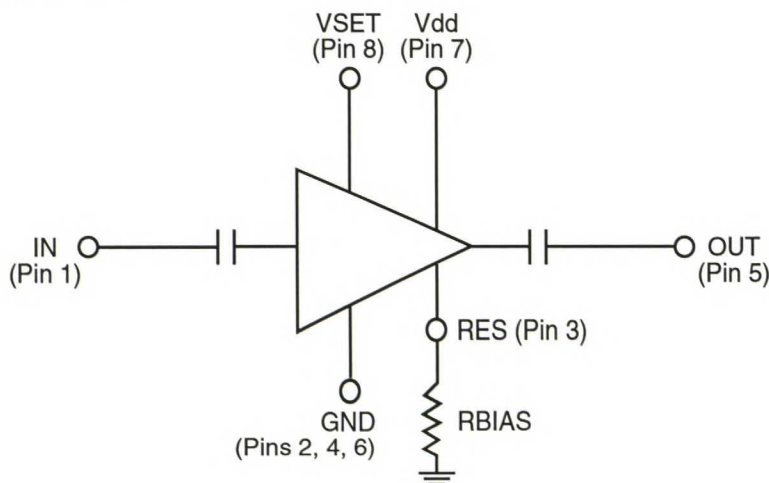
#### RF Performance at 5.8 GHz (Vdd = +3V)

VSET (VDC)	RBIAS Resistor Between Pin 3 and GND (Ohms)	Idd (mA)	Output P1dB (dBm)	Output Return Loss (dB)
0	174	7	1.0	16.0
3	23	25	9.0	12.0
3	7	40	13.0	15.0
3	GND (No Resistor)	60	14.0	15.0

#### Applying the adaptive biasing

A dynamically controlled bias can be implemented with this design. A typical application will include sensing an RF signal level and then adjusting the VSET. The bias adjustment can be accomplished by either analog or digital means, after the RF signal has been detected and translated to a DC voltage using external power detection circuitry.

#### Schematic





**HMC320MS8G**  
**GaAs MMIC LOW NOISE**  
**AMPLIFIER , 5.0 - 6.0 GHz**

**Absolute Maximum Ratings**

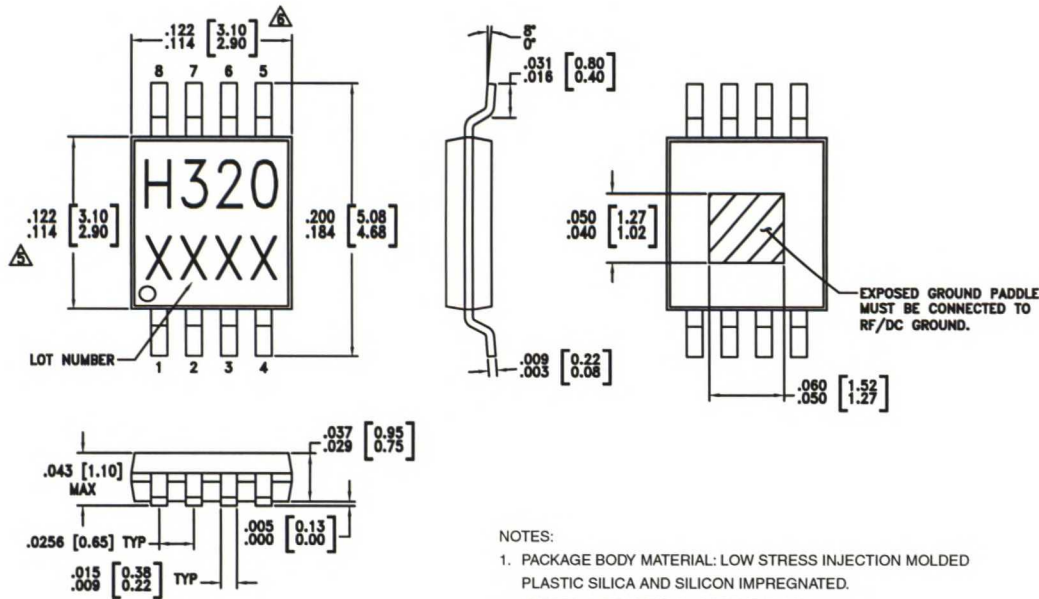
Supply Voltage (Vdd)	+7.0 Vdc
VSET	0V to Vdd
Input Power	+5 dBm
Channel Temperature (Tc)	175°C
Continuous P <sub>diss</sub> (Ta = 85°C) (derate 2.98 mW/°C above 85°C)	268 mW
Storage Temperature	-65 to +150°C
Operating Temperature	-40 to +85°C

**Truth Table**

VSET	Operating Current I <sub>dd</sub>	Operating State	Resistor R <sub>bias</sub>
0V	7 mA	Low Power	174 Ohm
3V	25 mA	Medium Power	23 Ohm
3V	40 mA	High Power	7 Ohm

Set external bias resistor (R<sub>BIAS</sub>) to achieve desired operating current, 0 < R<sub>BIAS</sub> < 200 Ohm.

**Outline Drawing**

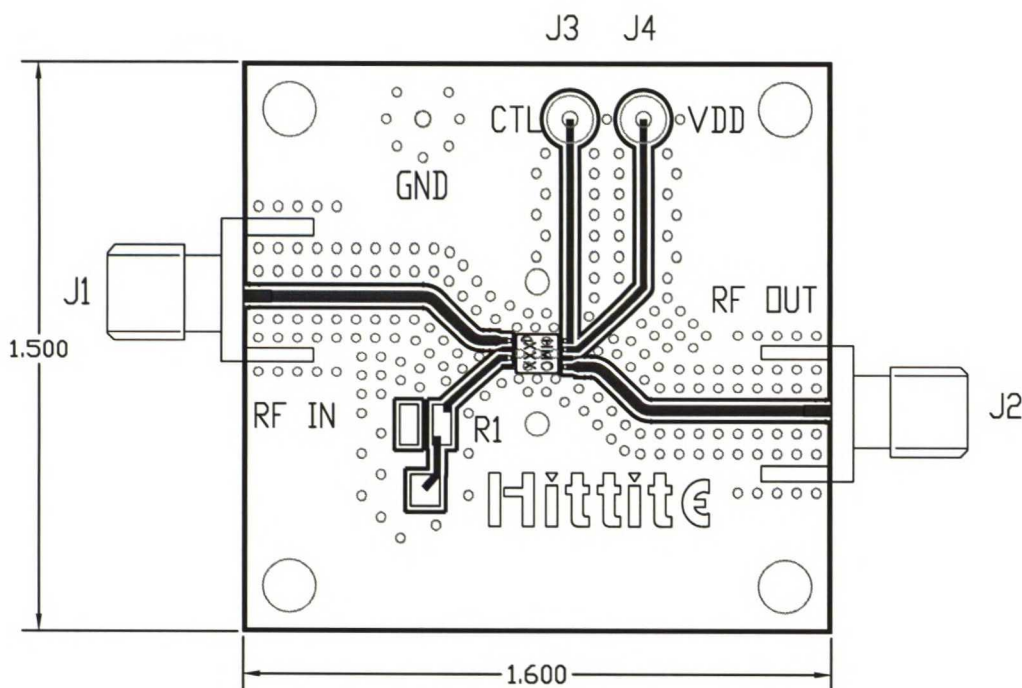


- NOTES:
1. PACKAGE BODY MATERIAL: LOW STRESS INJECTION MOLDED PLASTIC SILICA AND SILICON IMPREGNATED.
  2. LEADFRAME MATERIAL: COPPER ALLOY
  3. LEADFRAME PLATING: Sn/Pb SOLDER
  4. DIMENSIONS ARE IN INCHES [MILLIMETERS].
  5. DIMENSION DOES NOT INCLUDE MOLDFLASH OF 0.15mm PER SIDE.
  6. DIMENSION DOES NOT INCLUDE MOLDFLASH OF 0.25mm PER SIDE.
  7. ALL GROUND LEADS AND GROUND PADDLE MUST BE SOLDERED TO PCB RF GROUND.

# HMC320MS8G

**GaAs MMIC LOW NOISE  
AMPLIFIER , 5.0 - 6.0 GHz**

## Evaluation PCB

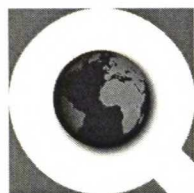


## List of Material

Item	Description
J1, J2	PC Mount SMA Connector
J3, J4	DC Pins
R1	200 Ohm Potentiometer
U1	HMC320MS8G Amplifier
PCB*	Evaluation PCB 1.6" x 1.5"
*Circuit Board Material: Rogers 4350	

The circuit board used in the final application should use RF circuit design techniques. Signal lines should have 50 ohm impedance while the package ground leads and exposed paddle should be connected directly to the ground plane similar to that shown. A sufficient number of via holes should be used to connect the top and bottom ground planes. The evaluation circuit board shown is available from Hittite upon request.





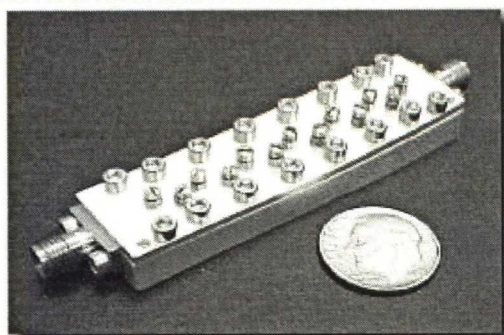
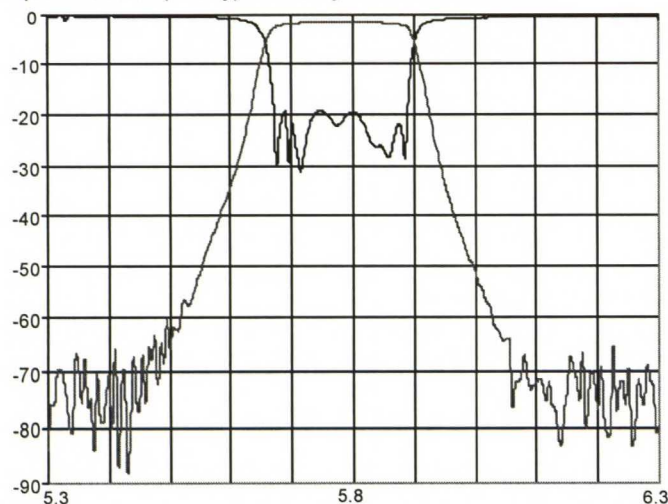
# Q Microwave

## THE FAST FILTER COMPANY

### 5.8 GHz FILTER PRODUCT LINE

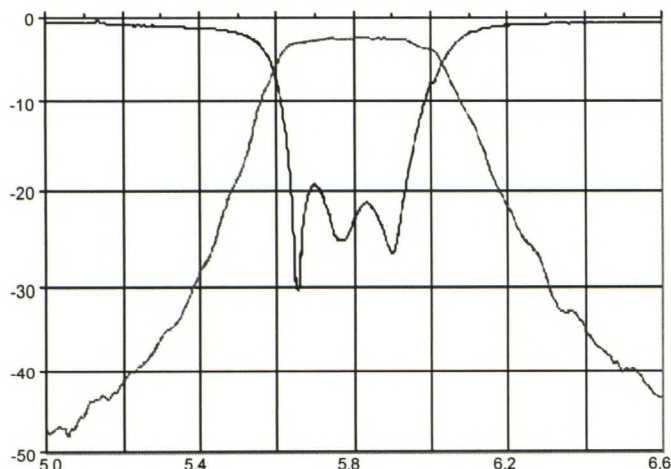
**Q Microwave, Inc.**, the FAST filter company, announces the launch of its 5.8 GHz Filter Product Line in response to demand by wireless LAN and other ISM band system designers. Current products include our streamlined basestation filter and our Surface Mount filter. For information on these and other 5.8 GHz filter products, contact us by phone at 619-258-7322, fax 619-258-7516, sales@qmicrowave.com, or visit us online at [www.qmicrowave.com](http://www.qmicrowave.com).

**5.8 GHz Basestation Filter** achieves excellent loss and rejection performance in a streamlined package. At only 0.4 inch high, it is compatible with typical rack-mounted board designs. Electrically, the filter provides 1.5 dB of insertion loss over a 100 MHz passband and 50 dBc of rejection at a 500 MHz bandwidth. Prices are as low as US\$30 in quantities with prototype delivery in 4 to 8 weeks ARO.



Parameter	Capability
Center Frequency (Fc)	5.7-5.85 GHz
Passband	100 MHz
Insertion Loss	1.7 dB max in passband
VSWR	1.5:1 max in passband
Fine-Grain Ripple	0.1 dB max in passband
Rejection 50 dBc	Lower: Fc-250 MHz Upper: Fc+250 MHz to 26 GHz
Power	45 dBm
Input / Output	SMA, pins, or surface mount
Outline	2.5 x 0.66 x 0.4 inches

**5.8 GHz SMT Filter** provides great performance in low cost SMT packaging. At a mere 0.2 inch high, it is easily integrated into even the most challenging configurations. Electrically, it nominally provides 2.5 dB of insertion loss over a 100 MHz passband and 20 dBc of rejection at an 800 MHz bandwidth out to 14 GHz. Pricing is as low as US\$15 in quantities with prototype delivery in 2 to 4 weeks ARO.



Parameter	Capability
Center Frequency (Fc)	5.7-5.85 GHz
Passband	100 MHz
Insertion Loss	3.0 dB max in passband
VSWR	1.5:1 max in passband
Rejection 20 dBc	Fc +/- 400 MHz Typically held out to 14 GHz.
Power	30 dBm
Input / Output	SMT
Outline	0.81 x 0.545 x 0.2 inches